PETROLOGY AND GEOCHEMISTRY OF THE TELUK RAMUNIA VOLCANICS, SOUTHEASTERN JOHOR, PENINSULAR MALAYSIA; IMPLICATION FOR MIDDLE TRIASSIC TECTONIC

MUHAMMAD HATTA BIN ROSELEE

FACULTY OF SCIENCE

UNIVERSITY MALAYA

KUALA LUMPUR

2014

PETROLOGY AND GEOCHEMISTRY OF THE TELUK RAMUNIA VOLCANICS, SOUTHEASTERN JOHOR, PENINSULAR MALAYSIA; IMPLICATION FOR MIDDLE TRIASSIC TECTONIC

MUHAMMAD HATTA BIN ROSELEE

DISSERTATION SUBMITTED IN FULFILLMENT OF THE REQUIREMENT FOR THE DEGREE OF MASTER OF SCIENCE

DEPARTMENT OF GEOLOGY

FACULTY OF SCIENCE

UNIVERSITY MALAYA

KUALA LUMPUR

2014

Penghargaan

Syukur Alhamdulillah pada Allah S.W.T dengan berkat izinnya aku telah berjaya menyiapkan tesis ini. Pertama sekali aku ingin mengucapkan terima kasih terhingga kepada Prof. Dr. Azman Abd Ghani selaku penyelia tesis yang banyak memberi dorongan dan memberi idea sehingga tesisku selesai.

Kepada kedua insan yang bernama Aminah Binti Rashid dan Roselee Bin Mohamed. Mereka adalah kedua ibu-bapa yang senantiasa menyokongku untuk menyiapkan tesis ini. Jasa mereka terhadap mereka terlalu banyak sehingga aku tidak mampu membalasnya. Mereka ini adalah pencetusku untuk menjadi seorang insan yang berguna.

Kepada kedua-dua kekandaku iaitu Allahyarham Kamarul Hadi Roselee dan Norashikin Binti Roselee, terima kasih kepada dua insan ini yang telah banyak menyumbang dari segi kewangan serta memberi semangat kepadaku untuk menyiapkan tesis ini. Tidak lupa juga kepada kakak ipar dan abang ipar yang bernama Irdawati binti Lokman dan Nik Fazul Fazlee yang juga turut membantuku dari segi kewangan. Hanya ucapan terima kasih yang aku dapat berikan buat masa ini.

Ainur Najihah bt Kamarul Hadi, Iman Khadijah bt Kamarul Hadi, Nik Aqil b. Nik Fazul Fazlee, Nik Alia bt Nik Fazul Fazlee dan juga Nik Aqif b. Fazul Fazlee, mereka sentiasa membuat aku terhibur dengan gelagat dan permainan mereka. Segala penat dan lelah terasa terus hilang apabila mereka berada di depan mata. Mereka ini ada anak-anak buah yang aku sangat sayangi.

Terima kasih juga kepada rakan seperjuangan BILIK 321 Farid, Hafifi, Long, Nyein Azlan, Wong serta Liyana yang sentiasa memberi dorongan untuk menyelesaikan tesis ini.

Akhir sekali kepada tunangku Nurshamira binti Suhaimi yang telah banyak memberi dorongan dan membantu menyediakan format tesisku. Terima kasih.

Hatta 2014

ABSTRAK

Objektif utama kajian ini adalah untuk mengkaji petrologi, geokimia dan petrogenesis batuan volkanik dari tenggara Semenanjung Malaysia terutamanya di sekitaran Teluk Ramunia. Batu gunung berapi dari kawasan itu terletak di magmatisma jaluran timur yang didominasi oleh Batuan Jenis-I. Batu di kawasan kajian terdiri daripada rhyolit, traki-dasit dan diorite. Mereka menunjukkan sepadan batuan yang tidak teratur dimana ia menunjukkan penghabluran berlaku pada masa yang hampir sama. Analisis petrografi menunjukkan ciri-ciri batuan jenis-A dimana terdapat kewujudan biotite dan hornblend dicelah mineral lain dan juga tekstur inter-pertumbuhan. Analisis geokimia menunjukkan bahawa rhyolit berasal dari magma berbeza daripada traki-dasit dan diorit. Nilai Ga / Al dan HFSE (Zr + nb + Ce + Hf) untuk semua batuan dari kawasan kajian adalah lebih kurang sama dengan purata batuan Jenis A. Semua batuan menunjukkan indek alkali silica daripada metaluminous ke peralumina lemah berdasarkan nilai A/CNK. Semua batuan mempunyai nilai suhu ketepuan yang tinggi (826$\pm$ 5^{o}C) dan kandungan tinggi unsur-unsur bidang kekuatan yang tinggi (cth. Zr, Nb, Ce dan Hf) dimana kedua-duanya jelas menunjukkan magma berasal dari sumber yang kering atau lebit tepat perleburan pada tekanan rendah. Berdasarkan pengumuran zirkon U-Pb, umur riolit adalah kira-kira 238 + 2 Ma dimana semua batuan terbentuk adalah berkait rapat dengan proses subduksi kerak lautan Palaeo-Tethys kebawah kerak daratan Indochina (arka gunung berapi). Walau bagaimanapun kewujudan A-jenis memberi implikasi bahawa semua batuan menghablur semasa lanjutan kerak lautan disebabkan oleh balikan-kerak (slab-rollback). Basalt yang terbentuk daripada mantle akan menceroboh masuk ke bahagian bawah dan tengah kerak benua semasa lanjutan kerak. Haba yang tinggi daripada basalt akan menyumbang kepada perleburan separa pada

tekanan rendah dimana ia akan menghasilkan magma jenis – A. Kebarangkalian besar kewujudan batuan jenis- A juga wujud sepanjang Jalur Timur Semenajung Malaysia.

ABSTRACT

The main objective of this study is to investigate the petrology, geochemistry and petrogenesis of volcanic rocks from southeast Peninsular Malaysia mainly within Teluk Ramunia. The volcanic rocks from that area are located on the eastern belt magmatism dominated by I-type rocks. The rocks from study area are dominated by rhyolite, trachydacite and diorite and they show irregular contact which suggests contemporaneous crystallization. Petrographically, all rocks shows occurrence of microgranophyric, interstitial biotite and hornblende which is characteristic of the A-type rocks and sub-volcanic emplacement. Field and geochemical evidence shows that the rhyolite is derived from a different magmatic pulse than trachydacite and diorite. The value of Ga/A and HFSE (Zr+Nb+Ce+Hf) for all rocks from study area is comparable to the average A-type rocks. All rocks shows range from metaluminous to weakly peraluminous in term of their A/CNK value. All rocks from Ramunia yield high zircon saturation temperature value (826$\pm$ 5^{o}C) and high content of high field strength elements (e.x. Zr,Nb,Ce and Hf) which are clearly indicative of dry source derived or low pressure incongruent melting. Based on geochemical, petrographical and high saturation temperature and low pressure (~3.2kbar) calculated from thermometry shows that all Rock from Ramunia may plausibly derived from low pressure melting of granodiorite. Based on zircon U-Pb isotope age, rhyolite gave age about 238 $\pm$ 2 Ma which suggest that all rocks are related to subduction of the Palaeo-tethys ocean underneath Indochina (volcanic arc). However the occurrences A-type give implication that all rocks are formed during crustal extension due to oceanic slab rollback. The under-plated mantle derived basalt will intrude into the lower to middle crust and provide sufficient heat to melt the country rocks. The high heat yield by the mantle derived basalt will contribute to the low pressure incongruent melting of the middle

crust rocks (tonalite and granodiorite) which will formed the A-type magma and gradually crystallized to be Ramunia volcanics. It is high possible that there are more occurrence of the A-type rocks throughout Eastern belt province of Peninsular Malaysia.

TABLE OF CONTENTS

ABSTRAK i

ABSTRACT iii

TABLE OF CONTENTS v

LIST OF FIGURES vii

LIST OF PLATES ix

1.0 INTRODUCTION 1
- 1.1 General Introduction and background of Teluk Ramunia 1
- 1.2 Research Objective 3
- 1.3 Research Method / Methodology 4
  - 1.3.1 Reviewing Literature 4
  - 1.3.2 Fieldwork mapping and sampling 4
  - 1.3.3 Produce Detail Geological Map 5
  - 1.3.4 Preparing Samples 5
  - 1.3.5 Petrography Analysis 5
  - 1.3.6 Geochemical Analysis 6
- 1.4 Literature Review 6

2.0 REGIONAL GEOLOGY OF PENINSULAR MALAYSIA 8
- 2.1 Volcanism in Peninsular Malaysia 8
  - 2.1.1 Research History on volcanic rocks in Peninsular Malaysia 8
  - 2.1.2 Western Belt Volcanism 15
  - 2.1.3 Eastern Belt Volcanism 17
  - 2.1.4 Volcanic rocks in Pahang, North Terengganu and North Kelantan 18
  - 2.1.5 Volcanic rocks in central, eastern and southeastern of Johor 19
  - 2.1.6 Islands on the Southeastern Offshore of Johore 20
- 2.2 General Geology of Study Area. 21
- 2.3 Tectonic Implication (Palaeozoic to Mesozoic) 29

3.0 PETROGRAPHY ANALYSIS 33
- 3.1 Introduction 33
- 3.2 General Description 33
  - 3.2.1 Diorite 33
  - 3.2.2 Rhyolite 34
  - 3.2.3 Trachydacite 35
- 3.3 Photomicrograph of Diorite from study area 38
- 3.4 Photomicrograph Of Rhyolite From Study Area 39
- 3.5 Photomicrograph of trachydacite from study area 40
- 3.6 Discussion and Conclusion 41

4.0 GEOCHEMISTRY 44
- 4.1 Introduction 44
- 4.2 Analytical procedure 48
  - 4.2.1 X- ray fluorescence (XRF) 48

4.2.2 ICP-MS 48
4.3 Major Element Variations 49
4.4 Trace Element Variation. 54
4.5 Rare Earth Trace Elements 59
4.6 Rocks classification of rhyolite, trachydacite and diorite from Ramunia rocks. 62
4.7 Zircon, Apatite and Monazite Saturation Thermometry 70
4.8 Magma thermometry 70
4.9 Discussion On Saturation Temperature And Estimated Depth Of Melting Of A-Type Ramunia Source 71
4.10 Magmatic Evolution 74
4.11 Source rocks potential of the A-type rocks from study area 78
4.12 Integrated petrogenetic model in forming the A-type magma/rocks 82
4.13 Implication of the A-type magma on Peninsular Malaysia geotectonic during Anisian (Early Middle Triassic) 83

5.0 CONCLUSION 88
5.1 Introduction 88
5.2 Summary of conclusion on volcanism within Teluk Ramunia 88
5.3 New Finding 89
5.4 Future work suggestion. 89

REFERENCES 91

LIST OF FIGURES

Figure 1.1	Map shows the satellite image of whole Peninsular Malaysia and close up of the study area	2
Fiure 1.2	Geological map of Pengerang area southeastern of Peninsular Malaysia	7
Figure 2.1	Distribution of the volcanic rocks within Peninsular Malaysia	9
Figure 2.2	Distribution and relative age of volcanic rocks in Peninsular Malaysia (modified after Hutchison, 1973a)	14
Figure 2.3a	Photograph shows the thick soil overlying the volcanic rocks	21
Figure 2.3b	Photograph shows other part of the study area which also shows thick soil overlying the volcanic rocks	22
Figure 2.4a	Photograph the occurrence of pink rhyolite. It formed as massive homogenous body	22
Figure 2.4b	Photograph shows massive trachydacite with poor conchoidal texture. Note the trachydacite shows grey	23
Figure 2.4c	Photograph shows the rock contact between pink rhyolite and diorite	23
Figure 2.5	Photograph shows clear irregular contact shown by rhyolite and trachydacite	24
Figure 2.6	Photograph shows the elongated mafic phase which are mainly biotite and hornblende yield by diorite	24
Figure 2.7	Photograph shows the rocks from study area are been intrude by mafic dyke	25
Figure 2.8	Photograph shows the rocks shows porphyritic texture where the main phenocryst phase are plagioclase	25
Figure 2.9	Photograph shows occurrence of chilled margin shown by mafic dyke	27
Figure 2.10	Photograph shows the occurrence of faulting (left lateral strike slip?)	27
Figure 2.11	Photograph shows there are at least 3 sets of joint formed within the igneous rocks from study area	28
Figure 2.12	Four possible causes of delamination, convective instability, riting , plume erosion or continental collision	30
Figure 2.13	Cartoons showing the sequence of events leading to the delamination slab break-off	31
Figure 4.1	TAS volcanic classification (modified after Middlemost (1994)	50
Figure 4.2	Harker diagram for major element plot of igneous rock from Ramunia	51
Figure 4.3	K_2O vs SiO_2 diagram shows that most of the rocks from Ramunia are plot into High-K calc alkaline series	52

Figure 4.4a	Mol of Al2O3/(CaO+Na2O+K2O) against SiO2 After Shand (1943)	53
Figure 4.4b	Mol of Al2O3/(Na2O+K2O) against mol of Al2O3/(CaO+Na2O+K2O) after Shand (1943)	53
Figure 4.5	Diagram of FeOt/(FeOt + MgO) vs SiO2 adapted from Frost (2001)	54
Figure 4.6	Harker diagram plot of selected trace for igneous rock from Ramunia	57
Figure 4.7	Multi-elements spidergrams normalized to Primitive Mantle	58
Figure 4.8	Vector diagram Th/Bn versus Zr shows that Ramunia rocks are pointing toward AFC	59
Figure 4.9	REE normalized to chondrite for all rocks from Ramunia.	61
Figure 4.10	Discrimination diagrams after Whalen et al. (1987) on Ramunia rocks	63
Figure 4.11	Discrimination diagrams after Whalen et al. (1987) comparing of A-type Ramunia with I and S type granite	65
Figure 4.12a	Multi-elements spidergram comparison between A-type Ramunia with S-type and I-type granite	67
Figure 4.12b	Rare Earth Element spidergram comparison between A-type Ramunia with S-type and I-type granite	68
Figure 4.13	Discrimination diagrams of a) Nb – Y – 3Ga and b) Nb – Y – Ce	69
Figure 4.14	Zr concentration in ppm versus melt basicity index (M) after Watson and Harrison 1983	74
Figure 4.15	Diagram of Rb/Sr vs SiO2	75
Figure 4.16	Diagram of (a) Ba versus Eu/Eu*, Sr vs Eu/Eu* after Eby (1990)	76
Figure 4.17	Large ion lithophile element modelling for rhyolite, trachydacite and diorite from Ramunia	77
Figure 4.18	Spidergram of Ramunia volcanic and mafic dyke within study area	80
Figure 4.19	Tectonic discrimination diagram (after Pearce et al 1984)	84
Figure 4.20	Diagram of observed Bouguer gravity and calculated gravity for a model with no granite in the Central back	86
Figure 4.21a	Tectonic setting schematic diagram for volcanism from study area and volcanic rocks on the eastern belt	87
Figure 4.21b	Diagram illustrating the relation between Slab dip angle and asthenospheric flow force	87

LIST OF PLATE

Plate A1	Hand specimen of diorite taken from western part of Pit 3. The diorite shows medium to coarse grained.	38
Plate A2	Most of the euhedral plagioclase at the centre of photomicrograph shows zoning extinction.	38
Plate A3	Photomicrograph shows that 80% of the sample dominated by euhedral to subhedral plagioclase with interstitial of quartz	38
Plate A4	Photomicrograph view occurrence of prismatic hornblende in diorite sample	38
Plate A5	Micrograph shows occurrence of hornblende with biotite inclusion in sample MIX 4A	38
Plate A6	Secondary epidote and hornblende form a network surrounding anhedral to subhedral plagioclase.	38
Plate B1	Hand specimen of rhyolite taken from Pit 3 of Pejal quarry	38
Plate B2	Twinning plagioclase phenocryst surrounded by relatively finer grained K- feldspar, quartz and plagioclase	39
Plate B3	Micrograph of euhedral k-feldspar microphenocryst in rhyolite.	39
Plate B4	Presence of microgranophyric intergrowth texture in rhyolite	39
Plate B5	Clot in P3C which composed of numerous anhedral secondary epidote is common features in rhyolite	39
Plate B6	Photomicrograph of rhyolite shows another shape of microgranophyric texture in rhyolite	39
Plate C1	Hand specimen of rhyolite taken from Pit 3 of Pejal quarry	39
Plate C2	General view of sample P3J showing that rhyolite are composed of mainly K-feldspar and Quartz	40
Plate C3	K-feldspar shows euhedral shape and formed glomercryst or glomeroporphyritic texture in sample P3J	40
Plate C4	K-feldspar and quartz intergrowth forming microgranophyric texture in trachydacite	40
Plate C5	Photomicrograph shows the occurrences of secondary epidote inclusion in Plagioclase in P3K samples	40
Plate C6	Photomicrograph shows biotite formed as interstitial in trachydacite	40

1.0 INTRODUCTION

1.1 General Introduction and background of Teluk Ramunia

Teluk Ramunia and its adjacent area is famous for abundances of bauxite deposits (aluminium ore) since 1950 until now. First research study has been done by Grubb in his PhD research in 1962 which cover whole Pengerang district . Later in 1965, detailed geological investigation has been done by Geological Survey of Malaysia with compilation manuscript from Grubb research. There is no doubt that large amount of bauxite has only been found within Pengerang area. Bauxite has been economically mined since then.

This research is done on smaller area within Pengerang district because there has been lot of quarry activities within Teluk Ramunia area which give chances of more geological investigation within that area. This research focus more on petrology and geochemistry of the volcanic rock from that area.

Teluk Ramunia is situated within Kota Tinggi district which located at very most southeastern part of Johor State. The north and south boundaries lines of latitude 1^{O} 24'N and 1^{O} 21'N respectively, while to the east and west it is contained within lines of longitude 104^{O} 15' and 104^{O} 17' respectively (Figure 1.1).The volcanic rocks from the study area have special features compared to the volcanic rock from other area within south east Johore as weathering of these rock produce bauxite. The area (Teluk Ramunia) is one of the main bauxite producer in Malaysia since early ninetinth century. From 1998 to 2003, 600 000 tonne bauxite have been produce by the bauxite mined in the study area (JMG report 2003). The aim of this paper is to study the geochemical characteristis of volcanic rocks as well as the associate granitic rocks from Teluk Ramunia. Presently, the quarry where the research took place has been bought by the Malaysian local company from Singapore company because the rocks are mostly composed of volcanic rocks which absolutely not suitable for rock aggregate.

Figure 1.1: Figure shows the satellite image of whole Peninsular Malaysia. Mark 'A' shows the location of the Teluk Ramunia (upper). The satellite image shows close up of study area (below)

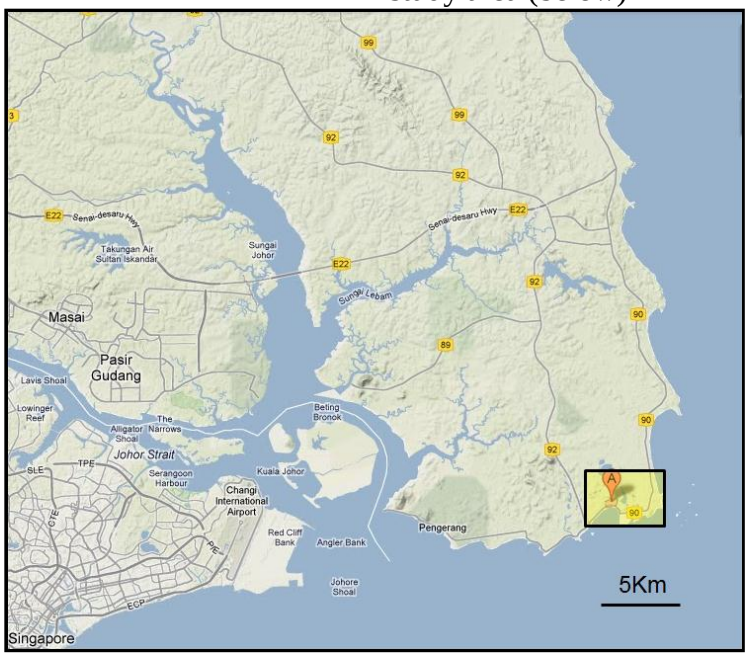

1.2 Research Objective

There is no detailed geochemistry study in previous research for igneous rocks from Teluk Ramunia. The study is only focussing on the distribution of the economic mineral mainly bauxite (Grubb 1968). The purpose of this study is to determine the petrology and petrogenesis of the igneous rocks from Teluk Ramunia. This study will include the aspects of field relationship, petrology analysis and geochemical. From these studies, the writer will have sufficient information to discuss about the petrogenesis of the rocks. It is also possible to determine the tectonic setting with the help of published rock age. Apart from that, geochemical data and relation between the minerals, texture and phenocryst assemblages can be used to determine the evolution of magma and its emplacement. Summaries of the objectives are :-

- To obtain more systematical information/datas regarding geology of Teluk Ramunia which include the field relation, petrology and geochemistry analysis.
- To discuss the magmatic evolution and their process in producing the volcanic and plutonic rocks.
- Propose the petrogenesis of the rocks based on the geochemistry analysis
- To make improvement to the geological map made by previous researcher.
- To predict the tectonic setting using the published tectonic discrimination diagrams and correlated it to the Permo-Triassic tectonic model.

1.3 Research Method / Methodology

1.3.1 Reviewing Literature

There are few methodologies that are crucial or important in order to make this research a successful project. By systematically order, first, the writer will do literature review as many as possible which is correlated with the research study. They included thesis, books, journals and memoirs. Any relevant information about the research area especially geological information will be used to help before going to field. This is very important because it can give the general ideas about geology of the study area before going to fieldwork. Literature review will be done throughout the thesis in order to obtain ideas or new ideas regarding research work.

1.3.2 Fieldwork mapping and sampling

Over 30 samples rocks samples consists of volcanic and plutonic were collected for this research. Most of the samples were taken from fresh outcrop within Quarry in surrounding Teluk Ramunia. Only non- weathered, unaltered and unmixing rock samples were used for geochemistry purposes. Location of each rock samples were marked by using GPS. All the geological features such as joint and shear or faults will be noted and will be added in the previous geological map done by Grubb (1968). This research covers detail on Teluk Ramunia part including Bukit Boping, Bukit Lontar, Bukit Wakap, Kampung Teluk Ramunia and adjacent areas. Rock samples will be collected during the mapping. All the samples will be mark on the base map and also in GPS. Each rock samples will be given specific name to make sure that the samples will not mix up.

1.3.3 Produce Detail Geological Map

A mapping has been done based on the geological features found within the research area. A detail geological map with appropriate scale will be produced by using GPS and GIS software. All geological information obtain from the study area will be input in this map.

1.3.4 Preparing Samples

The collected samples will be taken to lab for petrography and geochemistry analysis. Of all the samples, 30 rock samples of different rock type will be chosen for analysis. The chosen samples were made sure not weathered or it will affect the result especially geochemical analysis. Thin section will be made with standard thickness that is 30 micron meter will be made for petrography analysis. Besides that, same rock samples that had been made for thin section will be crushed into powder for geochemical analysis. Jaw crusher (rock crusher) will be use for crushing rocks into smaller size and Tema Mill will be used for milling process to make powder.

1.3.5 Petrography Analysis

Rocks are analysed petrographically by using petrology microscope in order to determine the rock constituents. Minerals and texture formed in rock is determined and will be discuss in detail in one chapter. Rock types type from the study area will be classify base on their general texture and mineral composition.

1.3.6 Geochemical Analysis

Geochemical analysis is done to determine the petrogenesis of the rock as as well as magma evolution in forming the rock. Other than that, geochemical data also can be used to backup petrography observation in determining rock type.

1.4 Literature Review

Petrology, petrography and geochemistry has been done by previous study on most part of Pengerang district. The study on geological aspect has been done by Grubb 1968 for his Phd research. His research was more emphasized on bauxite formation. There are two types of bauxite reported by high which are residual bauxite and transported bauxite however his research is lack of geochemistry approach. More detailed petrology and geochemistry of rock soil related which forming the bauxite has been done by Hutchison (1979). However there is no detailed petrology and geochemistry of igneous rock within Teluk Ramunia vicinity. Furthermore there are some intermediate plutonic found nearby Teluk Ramunia. The main rocks that found within Pengerang area were ranging from intermidiate to felsic type such as rhyolite, andesite, tuff, pegmatite and granite which associate with keratophyric dyke. The pegmatite formed as stock which intruded the granite at the eastern of Teluk Ramunia. Pegmatite is commonly known as late magmatic rock where the pegmatite was formed from the residual melt The volcanic rhyolite within Pengerang area has been dated and they were generally formed during Middle Triassic which are not very much different compared to the granite age. Study to determine the volcanic eruptions center has been done by Zainal (1984). He measured and statistically analyzed the clast sizes of agglomerates and input the clast contoured. The larger clast sizes will be proximal to the source of eruption foci and the smaller clast size will be distal from eruption foci. The geological map of the whole pengerang district is shown in Figure 1.

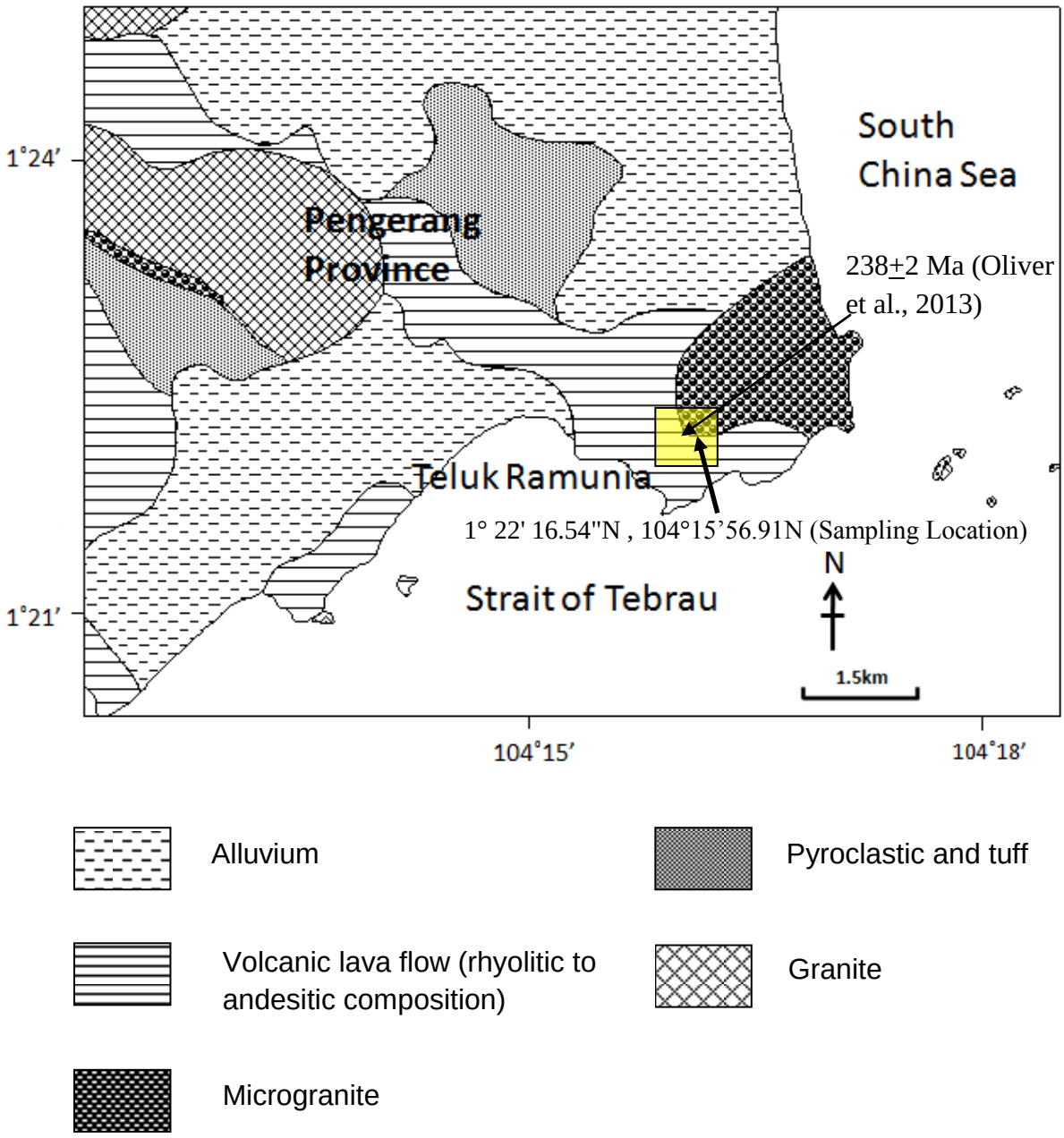

Figure 1.2: Geological map of Pengerang district. The area shaded (blue) in the box marked the location of the study area. Note the yellow box marked the occurrence of A-type volcnics

2.0 REGIONAL GEOLOGY OF PENINSULAR MALAYSIA

This chapter will summarize the occurrence and general description for all volcanic rocks throughout Peninsular Malaysia. Field characteristic in the study area will be discussed in detail at the end of this chapter. The major distribution of the volcanic rocks is shown in Map 1. Hutchison (1973a) has summarized the distribution and the relative age of the Peninsula Malaysia volcanic sequence (Figure 2.2).

2.1 Volcanism in Peninsular Malaysia

2.1.1 Research History on volcanic rocks in Peninsular Malaysia

The occurrences of the volcanic, pyroclastic and subvolcanic in Peninsular were first noted as Pahang Volcanic Series (Wilbourn, 1917; Scrivenor, 1931). The relative ages of their formation are assumed to be restricted from Carboniferous up to Triassic age (Scrivenor 1931). Richardson (1951) suggested that the termed Pahang Volcanic Series should be apply only to all volcanic rocks with known origin. However more field investigation shows that the volcanic rocks including lava, pyroclastics were found on more broad area rather than within Pahang state itself. Their occurrences spread from Kelantan on the north down to Terengganu, Negeri Sembilan (Fitch, 1952) and Johore (Grubb, 1965) toward the south. Therefore, the use of the term Pahang Volcanic Series have been disregard due to broad occurrences of volcanic rocks throughout out the Peninsular Malaysia.

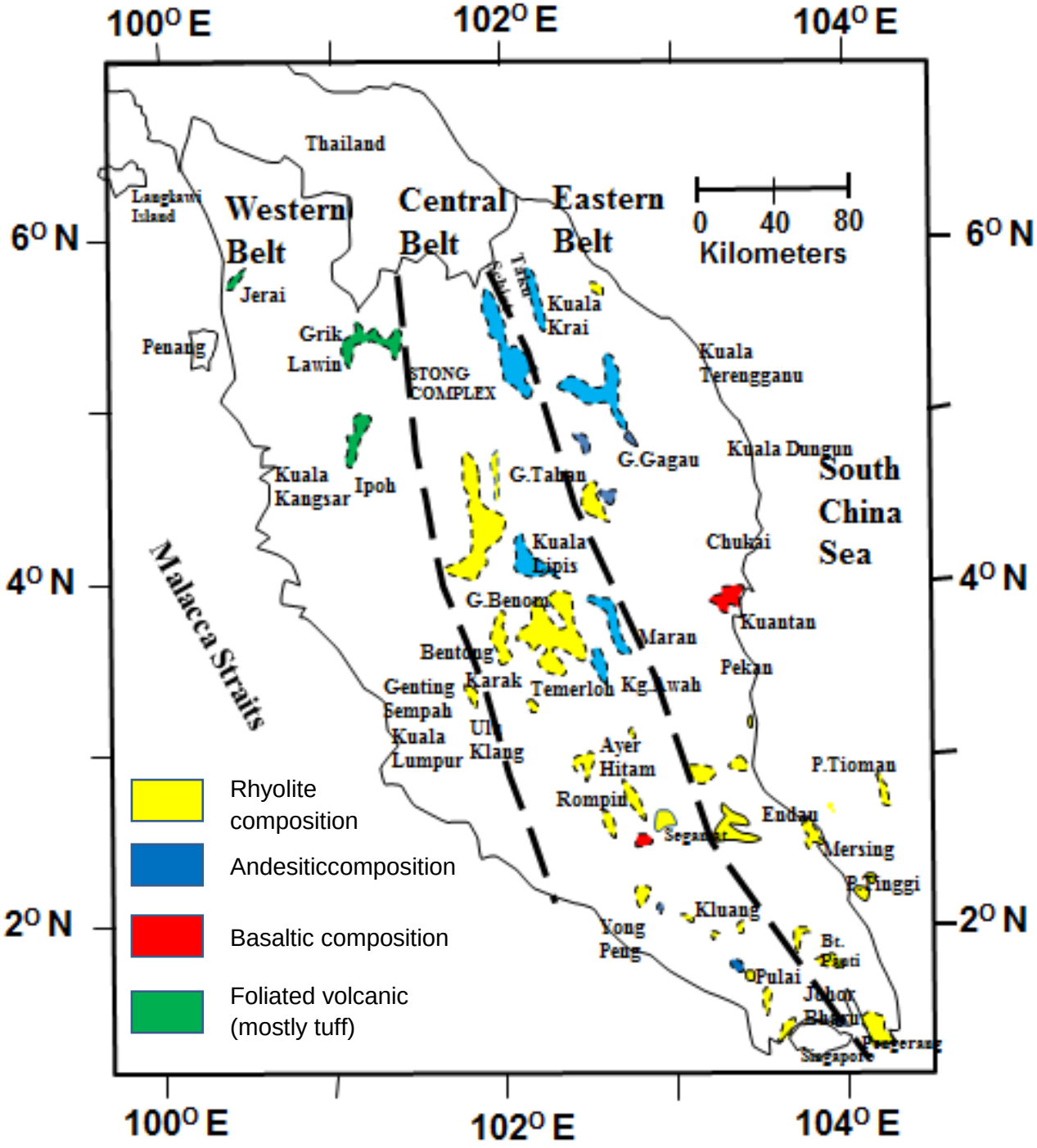

Figure 2.1: Distribution of the volcanic rocks within Peninsular Malaysia (modified after Hutchison, 1973a)

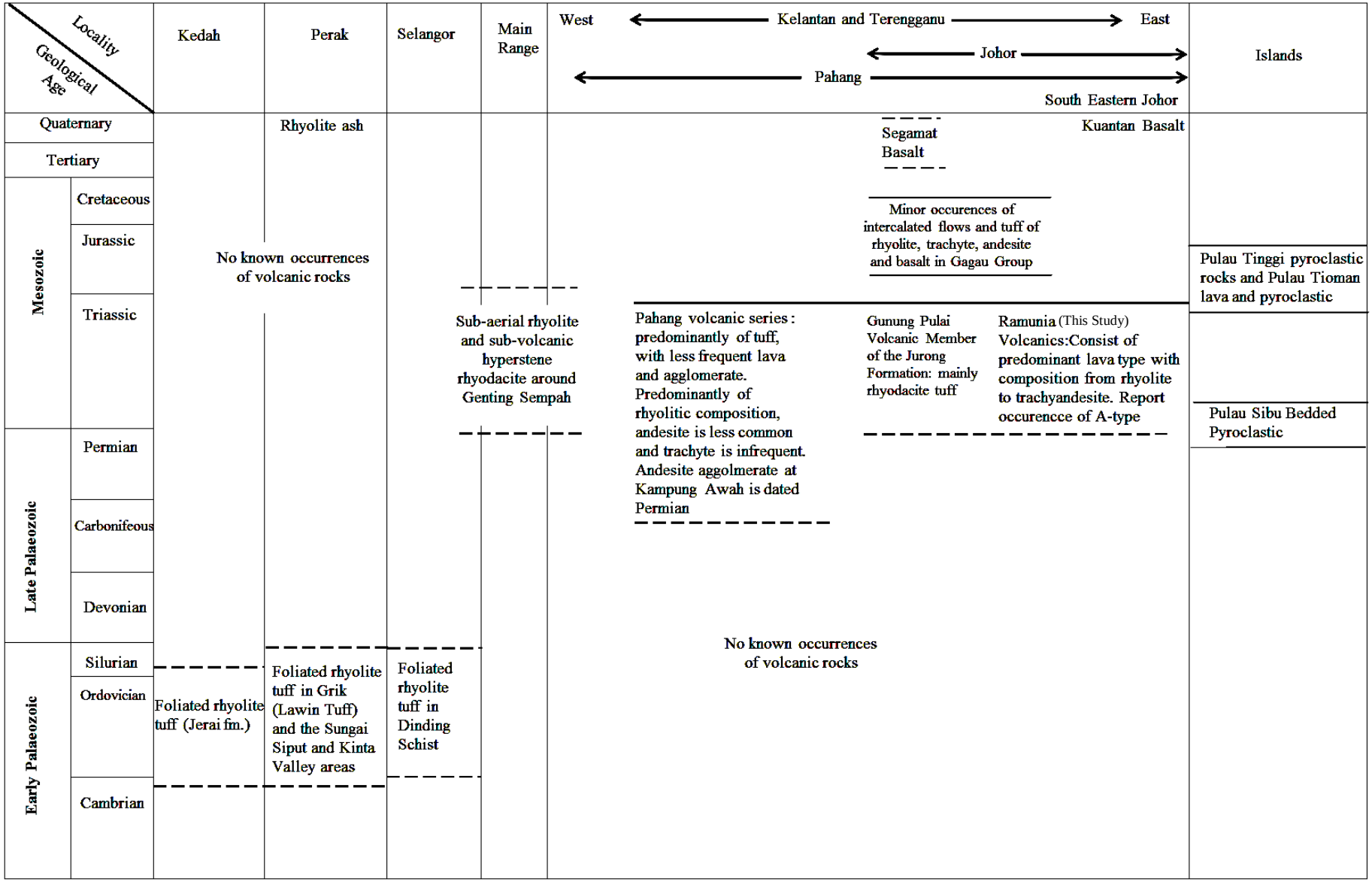

Figure 2.2: Distribution and relative age of volcanic rocks in Peninsular Malaysia (modified after Hutchison, 1973a)

The overall distribution of volcanic rocks are shown in Fieldwork occurrence and detailed petrographic description has been reviewed by Hutchison (1973a). The volcanic and pyroclastic rocks are described only according to localities that marked their occurrences. The geochemistry and isotopic age of the overall volcanic rocks within Peninsular Malaysia has been reviewed by (Ghani, 2009). Ghani (2009) has subdivided the volcanic rocks in Peninsular into 3 belts which are Western belt, Eastern Belt and Genting Sempah Complex.

2.1.2 Western Belt Volcanism

Volcanic rocks occur as scattered bodies of foliated rhyolitic flows and tuff which is conformable with metasediments and occur as interbedded with Ordovician rocks. For example there are occurrences of foliated rhyolite tuff in the Jerai Formation and foliated rhyolite in the Dinding Schist, Lawin Tuff and Genting Sempah volcanic rocks. The main rock type of Lawi tuff is foliated rhyolite and rhyodacitic tuff. All these volcanic rocks were interfoliated with Ordovician to Silurian meta quartzite and limestone of Baling Group. As for Dinding Schist in Kuala Lumpur, the main volcanic rock type is Meta- rhyolitic (Gobbet 1965a), There are clear occurrences of strong foliated of flow banded of the similar rock. At the northern part of the Western Belt, there is small occurrence of porphyry found in the Jerai Formation at Northeast of Gunung Jerai summit. The rock is conformable with the metasediments of the Jerai Formation. Bradford (1972) suggested that it may have been a tuff or volcanic rock and described t as quartz feldspatic hornfel. There are quite similar quartz porphyry with finer grained groundmass that occurs at Pulau Bunting which located on northwest of Gunong Jerai (Chung 1959).

This is somewhat similar to as Gunung Jerai Porphyry that is associated with metasediments that contained biotite, epidote, garnet, magnetite and andalusite.

Genting Sempah Volcanic is believed of both temporally and spatially related with the Main Range Granite (Haile et al., 1977). This volcanic complex consists of pyroclastic tuff, rhyolite and orthopyroxene bearing porphyry rhyodacite (Liew, 1977, 1983; Chakraborty, 1995). Detailed fieldwork studies show that rhyolite and orthopyroxene (hyperstene) rhyodacite predominates the Sempah Volcanic Complex where the (Chakraborty, 1995; Singh & Ghani, 2000). Zircon U-Pb age for orthopyroxene rhyodacite give the concordia at 219$\pm$5 Ma and 1550$\pm$300 Ma. The lower intercept is most likely to represent volcanic and sub-volcanic while the higher intercept represent the age of the basement rocks. However there are no occurrences of rocks with Pre-Cambrian age within the area or even in Peninsular Malaysia. Based on petrography characteristic, the hyperstene rhyodacite does not represent on single magma (magma mixing?) (Ghani, 2009). Detail study on geochemical behaviour on rhyolite and hyperstene rhyodacite has been done by Singh and Ghani, (2000) and Ghani, (2005). It is suggest that the magma that produced these both units are influenced by assimilation-fractional crystallization where the fractional crystallization are controlled by alkali feldspar, plagioclase and biotite. However the source rocks for these is yet determined. From the author observation on previous study on the orthopyroxene rhyodacite, the occurrences of glomeroporphyritic orthopyroxene (hyperstene) in rhyodacite give important implication in determining the source rock of the rhyodacite and rhyolite. Assumption can made that the magma was initially water under-saturated because orthopyroxene can be produced from partial melting with minimum liquidus temperature (~750^{O}C) at lower pressure (2Kbar) and water content (wt% H_2O < 5%) (Wood, 1973; Nany, 1983; Frost and Frost, 2007). So the author propose that that

rhyolite and Opx bearing rhyodacite are plausibly derived from previously dehydrated and dry granulite rock or charnockite at high temperature melting. This is because orthopyroxene in present in granulite and charnockite and the orthopyroxene can be possibly preserved in more evolved charnockite (~60%) because fractional crystallization is not so large in more evolved rock compared to the basic rock.

It must be note that high temperature is needed to melt the dry granulite or the charnockite. Based on gravity studies across Peninsular Malaysia, there is some evidence shows that Central belt of Peninsular Malaysia might has undergone crustal extension (Ryall et al 1982, Loke et al., 1983). The mechanism that can contribute to the extension of the lower crustal are slab-roll back (e.g Chung et al., 2005; Zhao et al. 2008), post-collision and rifting (Loiselle and Wones, 1979; Eby, 1992).

2.1.3 Eastern Belt Volcanism

Main occurrences of volcanic rocks on the eastern belt (Indochina Terrain) can be divided into 2 group based on their locality. The first group covered from eastern margin of Bentong Raub Suture Zone and several parts of Pahang (Central and North), north Terengganu and north Kelantan. The second group covers the central, south and southeastern of Johor which is located at southern part of Peninsular Malaysia.The occurrences of the volcanic rocks on the Eastern Belt or East of Main Range are believed to have age from Late Paleozoic to Early Mesozoic (see Hutchison 1973a). According to previous studies, the tuff is more common compared to the lava flow type

(Hutchison, 1973a). The compositions of the volcanic rocks on the eastern belt are from andesitic to acidic. Late Permian volcanic rocks consist of andesitic-acidic and Triassic

volcanic rocks mainly of acidic composition (Metcalfe et al., 1982). There is also occurrence of Cenozoic-Tertiary basalt (Kuantan basalt and Segamat Basalt) located on Eastern Belt which is absence on the Western Belt (Gobbett and Hutchison, 1973; Ghani, 2009).

2.1.4 Volcanic rocks in Pahang, North Terengganu and North Kelantan

In many of the area of the area, the volcanic rock show close association with the metasediments formation (Hutchison, 1973a). Based on field occurrence of volcanic associated with Middle Paleozoic metasediment and structural, Richardson (1950) has proposed a succession that volcanic rock of rhyolitic material are produced first from volcanoes and later material ranging from trachytic to andesitic were produced. On other part of Eastern Belt near Kuantan there are also similar volcanic occurrences of rhyolite and volcanic associated with Lower Carboniferous metasediments. Fitch (1952) suggested that the volcanic and pyroclastic rocks in the Kuantan area are submarine but was extruded near a shoreline.

Porphyry andesite and agglomeratic andesite (refer to Wong, 1960; Hutchison, 1973) were believed to be contemporaneous and they are found at a quarry in Kampung Awah (Wong, 1960; Chong and Yong, 1967). From geochemical classification, all analyzed rock samples from Kampung Awah fall in basaltic andesite, tephrite/basanite and basalt (Ghani, 2009). The volcanic andesitic shows an evidence of intrusion into the limestone prior to eruption.

Similar lava, pyroclastic and agglomerate type found in from North Terengganu to North Kelantan which most probably extension from the volcanic body from central Pahang. Volcanic rocks within this area have been subdivided into two groups which are 1) almost all andesitic composition and 2) predominant rhyolitic and trahytic

composition with subordinate of dacitic and andesitic component. Field occurrences and petrography of the volcanic rocks from North Terengganu to North Kelantan has been reviewed by Macdonald (1968). Petrographically, biotite shows variable textures and K-feldspar shows euhedral shape may implicate high temperature source rocks (e.g. Loiselle and Wones Li et al., 2011,)

Temangan ignimbrite are occur in the north Kelantan and in contact with shale and sandstone. It shows intrusive nature and generally formed as laterally and vertically homogenous massive body with minor flow texture. Temangan Ignimbrite appear to be related to Lebir Fault zone (e.x. Hutchison, 1973a ; Aw, 1967)

2.1.5 Volcanic rocks in central, eastern and southeastern of Johor

The main volcanic area for this group is in central, southeastern and eastern of Johor state. There are also occurrences of volcanic rocks found at the several islands on the east and southeastern offshore of Johor.

The occurrence of volcanic rocks within the central part of Johor has been described by Rajah (1967) and subdivided them into Sedili Volcanic and Chemendong Volcanic. Both Sedili and Chemendong consist of pyroclastic and lava flow type. The composition of lava type at Sedili volcanic is ranging from rhyolitic to rhyodacitic while restricted lava flow of andesitic to dacitic formed within tuff bodies. Ignimbrite, lithic tuff, agglomerate tuff, agglomerate and ash are the main pyroclastic in Sedili with approximately similar composition as the lava type.

Volcanic lava type that occur within Chemendong volcanic are rhyolite and rhyodacite with very minor occurrence of quartz-andesite. The occurrence of pyroclastic type are not as extensive as in Sedili volcanic. Rajah (1967) deduced that the Sedili and Chemedong are Triassic although some may be Permian or possibly Carboniferous.

South and Southeastern Johor

Studies on volcanic rock in south and southeast Johor mainland are mostly done by Grubb (1968). He described the volcanic rock within this area consist of chiefly lava flow and pyroclastic. These volcanic rocks are associated with graphitic and muscovite schist. The composition of lava and pyroclastic are ranging from intermediate to felsic. Grubb (1968) proposed that lava of andesitic composition extrude at initial stage of extrusive followed by intermediate and felsic flow and lastly by explosive pyroclastic deposition. Detail petrology and field observation has been described by Grubb (1968) and short summary will be given here. Volcanic rocks are the main igneous rocks that occur in southeastern of Johor within Pengerang district. 4 types of volcanic rocks of lava types that have been recognized, they are andesite, dark non banded rhyolite, banded porphyritic rhyolite and banded felsitic rhyolite (Grubb, 1968). According to Grubb (1968), andesite is the oldest volcanic sequence of volcanic and felsitic rhyolite is the youngest of lava flow type. The occurrence of pyroclastic is mostly consist of tuff. Grubb (1968) has subdivided the pyroclastic tuff into ashy tuff and agglomeratic tuff where the former is more common. On Nenas Island within Johor strait, there are also occurrence of pyroclastic ranging from rhyolitic to andesitic composition.

2.1.6 Islands on the Southeastern Offshore of Johore.

Tioman, Sibu and Tinggi island of southeast are dominated by felsic to intermediate lava and pyroclastic (Bean 1972; Ismail et al., 2003). Apparently volcanic rock of lava type on Tioman island has been metamorphosed to meta-rhyolite with some meta-trachyte and meta-andesite (Grubb 1972). The occurrence of tuff also is common and associated with the metamorphosed lava. Unlike Tioman island, Sibu and Tinggi island are totally consist of pyroclastic rocks with very little of lava flow type (Ghani,

2006). Field evidence shows that the Tinggi Island is distinct from Sibu Island in term of volcanic rock types. The size of the pyroclastic rock on Tinggi island are varies from mm to 5cm while pyroclastic on Sibu island shows ashy characteristic (Ghani, 2006). Detail field and petrographic has been discuss by Hutchison (1973) and Ghani (2009). Unpublished data for Ar-Ar wholerock dating shows that Tioman volcanic (~88.9 Ma) have close age with Tinggi Island (~85 Ma) while age of Sibu volcanic is much older than Tioman and Tinggi volcanic (~296Ma $\pm$ 0.96) (see page 198 in Ghani, 2009). Based on these ages, it is likely that only Sibu volcanic is related to the Permian-Triassic volcanic arc. It is clearly shows that Tioman/Tinggi and Sibu Island are formed within distinct tectonic environment.

2.2 General Geology of Study Area.

The study area located at southeastern part of Pengerang district and about 5km east of Sungai Rengit. Geological map of study area is shown in Figure 1.2. Most of the studies are carry out in a quarry which consist are mainly consists of rhyolite, dark colour trachydacite and diorite. All these rocks are overlain by soil/laterite with thickness of 10m – 15m thick (Figure 2.3a, 2.3b). These reddish – yellowish colour soils are known to be the source of the bauxite (Grubb, 1968).

Figure 2.3a: Photograph shows the thick soil overlying the volcanic rocks. The un-continuous yellow line marked the contact between soil and underlain rocks

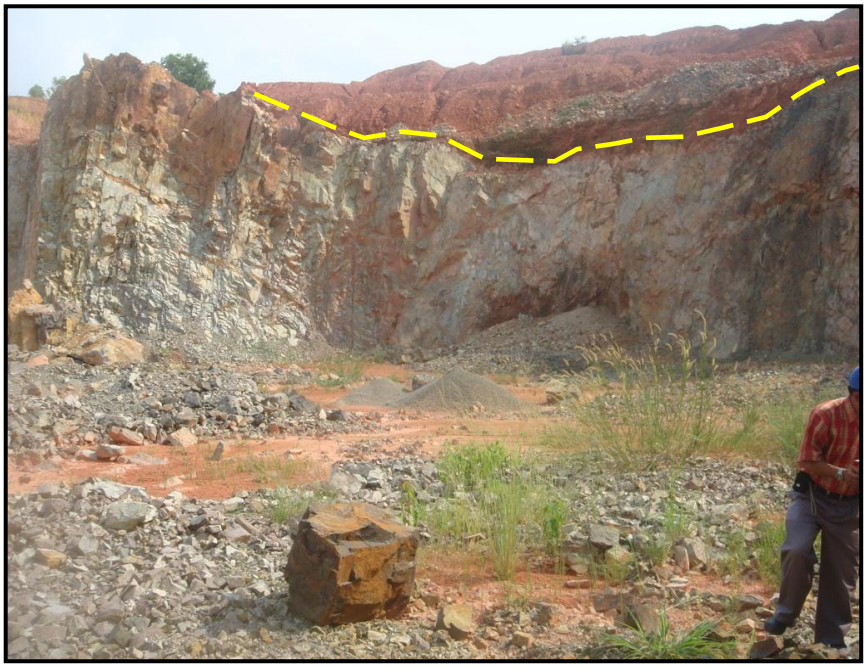

Figure 2.3b : Photograph shows other part of the study area which also shows thick soil overlying the volcanic rocks.

Figure 2.4a: Photograph the occurrence of pink rhyolite. It formed as massive homogenous body.

Figure 2.4b: Photograph shows massive trachydacite with poor conchoidal texture. Note the trachydacite shows grey colour.

Figure 2.4c : Photograph shows the rock contact between pink rhyolite and diorite. Note the elongated hornblend and biotite shown within diorite.

Figure 2.5: Photograph shows clear irregular contact shown by rhyolite (light colour) and trachydacite (dark colour)

Figure 2.5: Photograph shows the elongated mafic phase which are mainly biotite and hornblende yield by diorite.

Figure 2.6: Photograph shows the rocks from study area are been intrude by mafic dyke.

Figure 2.7: Photograph shows the rocks shows porphyritic texture where the main phenocryst phase are plagioclase (light colour) and clinopyroxene with minor olivine (dark colour).

On the eastern part of the Ramunia, there is intrusion of igneous body mainly of granitic composition where Grubb (1968) classify it as micro-granite. Within the study area, there is a quarry consist of 3 pits. These quarry consist of predominantly pink rhyolite and minor occurrence of trachydacite and diorite (Figure 3a,3b and 3c). Rhyolite is the main volcanic rocks in the study area followed by trachydacite and diorite. The writer classified it as pink rhyolite because of its very characteristic colou. The pink rhyolite and dark grey trachydacite are formed as massive igneous body and clearly shows irregular contact (Figure 4). There is no trace of banded or preferred orientation within the rhyolite and trachydacite. As for diorite, the appearance of long prismatic to sub-accicular mafic phase (hornblende and minor biotite) can be clearly seen in macroscopic scale (Figure 5). The relation between rhyolite, trachy-dacite and diorite are very clear. The diorite are high probably older that the volcanics because there is occurrences several diorite enclave in volcanic body. All rocks from study area type intruded by a series of younger doleritic dykes (Figure 6).The size of the dyke varies from centimeters up to meters and they shows porphyritic texture (Figure 7) and chilled margin is common on the margin of the smaller size dykes (Figure 8). Faults and joints are common within the igneous body. Some crushed rocks can be found along the large scale fault (Figure 9). There are 3 sets of joint can be found within the rocks (Figure 10). Some of the rhyolite rocks shows yellow colour due to weathering. Apart from the study area, there is also a quarry in Belungkur which located on the north-eastern from Teluk Ramunia where the main rocks are banded rhyolite and pyroclastic rocks (Shafik Izzuan 2011). Volcanic rocks from that area might be related to the volcanic rocks from study area.

Figure 2.8: Photograph shows occurrence of chilled margin shown by mafic dyke. Note the chilled margin occur in small dyke.

Figure 2.9: Photograph shows the occurrence of faulting (left lateral strike slip?). Note the crushed rocks produced due to the faulting.

Figure 2.10: Photograph shows there are at least 3 sets of joint formed within the igneous rocks from study area.

2.2 Tectonic Implication (Palaeozoic to Mesozoic)

Distribution and the age of the volcanic rocks obtained from previous studies the relative age of the volcanic rocks are ranging from Early Permian to late Triassic (Metcalfe, 2000b). Summary of volcanic rocks age is presented by Ghani (2009). Based on these ages the writer sub-divided them into 3 distinct major tectonic setting that lead to volcanism activity in Peninsular Malaysia. The first occurrences of volcanic rocks are related to the volcanic arc setting which occur during Early Permian to Middle Triassic. The volcanic rocks that formed during this time marked the periods of subduction of the Paleo-tethys oceaninc crust underneath the Indochina Block (East Malaya). The period of volcanic arc has ceased probably during the Late Triassic. During late Triassic, the volcanic arc subduction is ceased prior to the collision between Sibumasu Block (Westmalaya) and Indochina Block (East Malaya). At the end of the collision period the

crust will be uplifted then sink because of overburden (Jurrassic). It have been proven that the continental crust particularly below the central belt is thin (Ryall, 196x; Loke.). Several previous studies has interpreted that the thinning below the central belt is due to slab-break off which obviously may lead to crust thinning (Mustaffa Kamal and Ghani. 2003;Umor, 2009). However, slab delamination also may play part instead of slab-break-off. Either one of these two mechanisms will be triggered in time after collision has ceased (e.g. Whalen et al., 1996).

Slab break-off is also known as slab detachment. Slab-break-off will occur when subducted oceanic lithosphere is detached from the continental lithosphere during continental collision (Davies & Blanckenburg, 1995). The occurrence of slab break-off is due to decrease in the subduction rate that was damped by positive buoyancy of continental lithosphere introduced into the subduction zone (Davies & Blanckenburg, 1995; Gerya, 2004)

Slab delamination is the detachment of thickened lithospheric mantle from overlying crust during continental collision (Bird, 1978). In order delamination process to begin, some which lead to the break through mantle lithosphere must be developed first allowing asthenosphere to contact with the crust. According to Bird (1979), there are 4 possible cause of delamination which are convective instability, rifting, plume erosion and continental collision (Figure 11). Both of slab break-off and delamination of the subducting slab will lead to the rise of hot asthenospheric mantle through the lithospheric gap and causes a transitory thermal anomaly and caused partial melting of the lower crust. (Figure 12) (Bird 1979; Sinclair, 1997; van de Zadde and Wortle,2001; Rogers et al., 2002; Ferrari, 2004).

Either slab break-off or delamination event can lead to the magmatism activities from Jurassic up to Cretaceous time in Peninsular Malaysia. The igneous suites that

related to these post-collision events are mostly occur on the central belt of Peninsular Malaysia (e.x. (Mustaffa and Ghani, 2003; Rozi Umor, 2010).

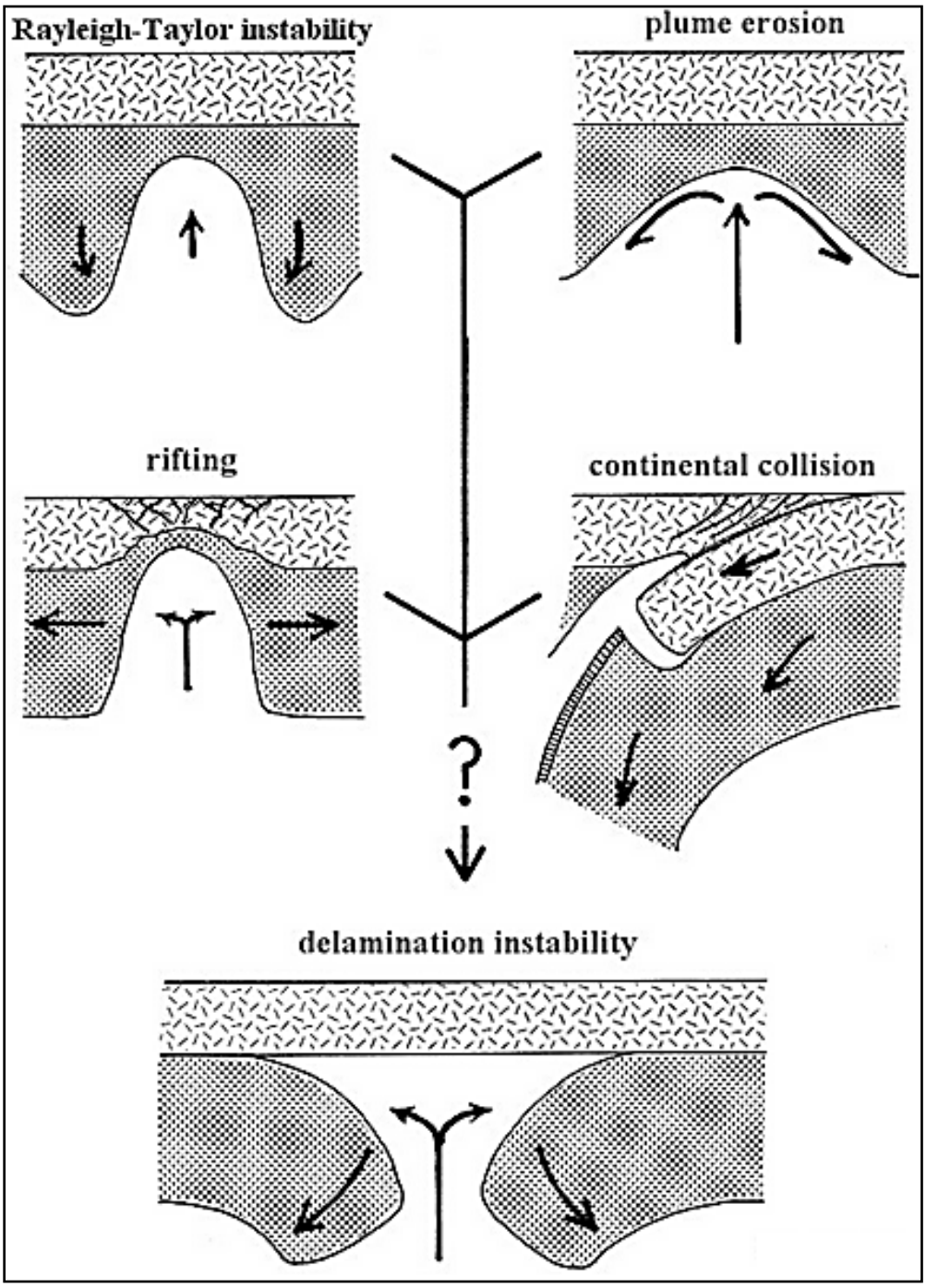

Figure 2.11: Four possible causes of delamination, convective instability, riting , plume erosion or continental collision (after Bird, 1979)

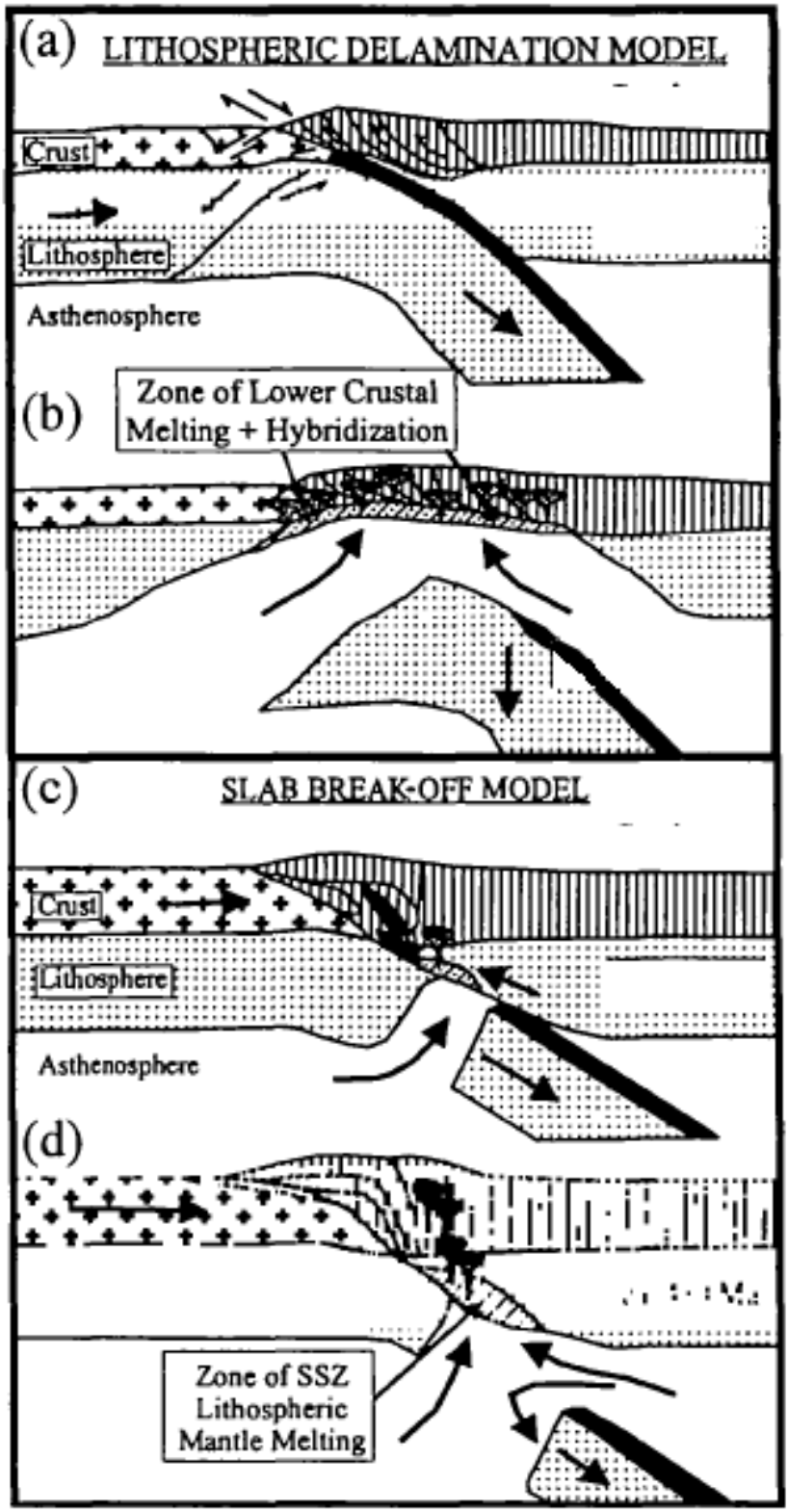

Figure 2.12: Cartoons showing the sequence of events leading to the delamination (a and b) and slab break-off (c and d) after von Blakenburg (1995)

3.0 PETROGRAPHY ANALYSIS

3.1 Introduction

Petrography observation is important to determine the dominant minerals accessory mineral and their inter-relationship (e.x. mineral shape and texture) that form igneous rocks from study area. General description will be discussed for each type of rocks. Interpretation will be discussed in discussion and conclusion sub-chapter. From microscopic textural relationship it is also possible to determine the emplacement of the magma that gradually formed all rocks. . The study area consist of 3 main rock types which are dioritem rhyolite and trachydacite. Summary of petrographic description is shown in Table 3.1

3.2 General Description

3.2.1 Diorite

This rock has varies in minerals sizes from medium grained to coarse grained equigranular with average size from 0.8mm to 1.0mm. Most diorite shows coarse grain pheneritic texture. The coarse grained diorite consists of prominent prismatic hornblende and white colour lath shape plagioclase. Minerallogically, diorite consists of plagioclase + hornblende + biotite + k-feldspar as main minerals and zircon+opaque+rarely apatite as accessories. Plagioclase is the most abundant mineral in diorite which composed approximately 60% - 70% of the rock total composition. The plagioclase are mostly euhedral to subhedral and display albite and Carlsbad albite twinning. There is also plagioclase crystal that shows zoning extinction. Mafic minerals present in this rock are hornblende and biotite and they make up about 10% to 15% of total rock compositions. Biotite composed 5% of total rock mostly formed as subhedral with jagged shape at both

end of the crystals. Their size is from 0.5mm to 0.8mm. Hornblende crystallized as prismatic crystal with size ranging from 0.6mm up to 1.0mm and makes up about 10% of rock compositions.The ratio of length to width for hornlende and biotite can be up to 8:1. Alteration minerals occurred in this rock including sericite and chlorite. The secondary epidote usually formed by replacing plagioclase feldspar through hydrothermal process. K-feldspar mostly shows subhedral shape and consists of 3% of the total rock. Quartz which likely to be the last primary mineral to crystallized composed about 10% in diorite and usually occurs as anhedral crystals. It occurs as interstitial crystal to plagioclase and some of the quartz are the main component of the microgranophyric and less common myrmekitic intergrowth. Microgranophyric is less common in this rock compared to rhyolite and trachydacite as this intergrowth are more common in more felsic rocks. Microgranophyric or granophyric texture is k-feldspar and quartz formed together as skeletal and triangle shape morphologies (refer to sub-chapter 3.5).

3.2.2 Rhyolite

Rhyolite occurs either as porphyritic ~~and~~ or fine grained textured rocks and shows pink to greyish colour. Plagioclase, K-feldpsar and quartz occurs as main phenocrystic phase and also reflect the composition of the groundmass. Some of the rhyolite samples shows patches of secondary epidote which formed due to hydrothermal alteration. Microscopically, the rhyolite consists of plagioclase + K-feldspar + Quartz + biotite as main minerals. Plagioclase, K-feldspar, quartz and biotite occur as main phenocryst phase as well as groundmass with the size ranging from 2.0 - 3.0mm, 2.0 - 3.5mm,<0.1 - 3.0mm and 0.5 - 1.0mm respectively. The groundmass formed as microcrystalline to cryptocrystalline of quartzo-feldspatic compositions. Plagioclase

constitutes about 33% to 35% of total rock composition and formed as lath shape or prismatic crystals. K- feldspar constitutes approximately 35% to 38% of total composition and formed as euhedral to subhedral crystal shape. Quartz constitutes about 25% to 30% and often shows anhedral shape. Like k-feldspar and plagioclase, quartz also formed both as invidual phencryst and also as interstitial within groundmass. Biotite is the only ferromagnesian mineral which constitutes about 2% to 3% of total rock composition. Biotite is strongly pleochroic from light brown to dark brown sometimes replaced by chlorite along the cleavages. The accessory minerals are zircon, apatite and opaque. Zircon formed as inclusion in biotite and usually associated with the pleochroic haloes. Microgranophyric intergrowth of quartz and k-feldspar is the most common intergrowth in rhyolite. There is also occurrence of spherulite which is quite common in rhyolite from study area.. Apatite formed as individual prismatic crystals. Opaque mineral formed as individual mineral and clots. Chlorite, epidote and sericite are the main alteration minerals in rhyolite.

3.2.3 Trachydacite

Most trachydacite is porphyritic and are light to dark grey colour Mineralogically, trachydacite consist of k-feldspar + quartz + plagioclase + biotite as major minerals and zircon + apatite+ opaque as accessory minerals. The phenocrystic phases are plagioclase and K-feldspar. Generally K-feldspar is the most abundant mineral in trachydacite which constitute about 42% to 45% of total rock composition. The crystal usually is euhedral to subhedral with the size 0.3 to 2.5mm. K-feldspar usually formed as individual crystal as well as glomerocryst where the K-feldspar phenocryst is formed in group or clustered together surrounded by groundmass. Plagioclase is the least major mineral in trachydacite which consist about 23% to 26% of

total rock composition. Plagioclase size ranging from 0.5 – 2.0mm and commonly formed as euhedral to subhedral crystals. Plagioclase exhibit albite twinning and carslbad-albite twinning. There is also pericline in plagioclase which develop along with albite twinning. Quartz constitutes approximately 29%-33% of total rock composition. The size of quartz is ranging from 0.7 – 1.1mm and often shows anhedral crystal shape. The main mafic mineral phase is biotite and rarely hornblende. Biotite formed as individual crystal and as interstitial between earlier formed minerals**.** The accessory minerals found in trachydacite are zircon and apatite. Most of the zircon formed as inclusion in biotite and associated with pleochroic haloes. Apatite formed as small individual prismatic mineral. The sizes of zircon and apatite are <0.1mm.The felsic minerals (quartz and feldspar) shows microgranophyric intergrowth of quartz and k-feldspar. However the amount of the intergrowth is lesser compared to rhyolite. Chlorite, epidote and sericite formed as alteration mineral replacing the formed feldspars and biotites.

Rock Types	Rhyolite	Trachydacite	Diorite
Colour	Pink to Light Grey	Dark Grey	Grey to Dark Grey
Main texture	Porphyrictic to Aphanitic	Porphyritic to aphanitic	Pheneritic , equigranular (easily indetified by prismatic hornblende)
Phenocryst Assemblages	Plagioclase, Kfeldspar and Quartz	Plagioclase, Kfeldpsar and Quartz	None
Groundmass	Quartzo Feldspatic	Quartzo-Feldspatic	None
Primary Mineral Assemblages	Plagioclase (33 – 35 %) K-feldpsar (35 - 38 %) Quartz (25 – 30 %) Biotite (2 – 3 %)	K-feldspar (42 – 45%) Plagioclase (23 – 26%) Quartz (29 – 33%) Biotite/Hornblede (2 – 3%)	Plagioclase (60 – 70%) Hornblende (10 – 15%) Biotite (7 – 10 %) K-feldspar (2 – 5%)
Mineral Size	Plagioclase (2.0 – 3.0mm) K-feldpsar (<2.0 – 3.5mm)	K-feldspar (0.3 – 2.5mm) Plagioclase (0.5 – 2.0mm)	Plagioclase (1.5 – 2.5mm) Hornblende (0.6 – 1.0mm)

	Quartz (<0.1 – 3.0 mm) Biotite (0.5 – 1.0mm)	Quartz (0.7 – 1.1 mm) Biotite/Hornblede (<0.8mm))	Biotite (0.5 – 0.8mm) K-feldspar (0.5 – 1.0mm))
Accessory Mineral Assemblages (size < 0.1mm)	Zircon, apatite and opaque	Zircon, apatite and opaque	Zircon, apatite and opaque
Alteration Minerals	Epidote and Chlorite, Sericite	Epidote and Chlorite, Sericite	Epidote and Chlorite, Sericite
Early crystalizing phase	Plagioclase, K-feldspar and quartz	Plagioclase, K-feldspar and quartz	Plagioclase, bioite and hornblende
Late Crystalizing phase	Biotite and opaque	Biotite $\pm$ hornblende and opaque	Biotite and Hornblende
Special Features	- Micrograno phyric intergrowth are common and myrmekitic intergrowth is less common - Biotite formed as interstitial - K-feldspar shows euhedral shape.	- Micrograno phyric is less common compared to to rhyolite. - Biotite formed as interstitial - K-feldspar shows euhedral shape	Occurrence of micrograno phyric intergrowth is not common Biotite and hornblende formed as interstitial

3.3 Photomicrograph of Diorite from study area

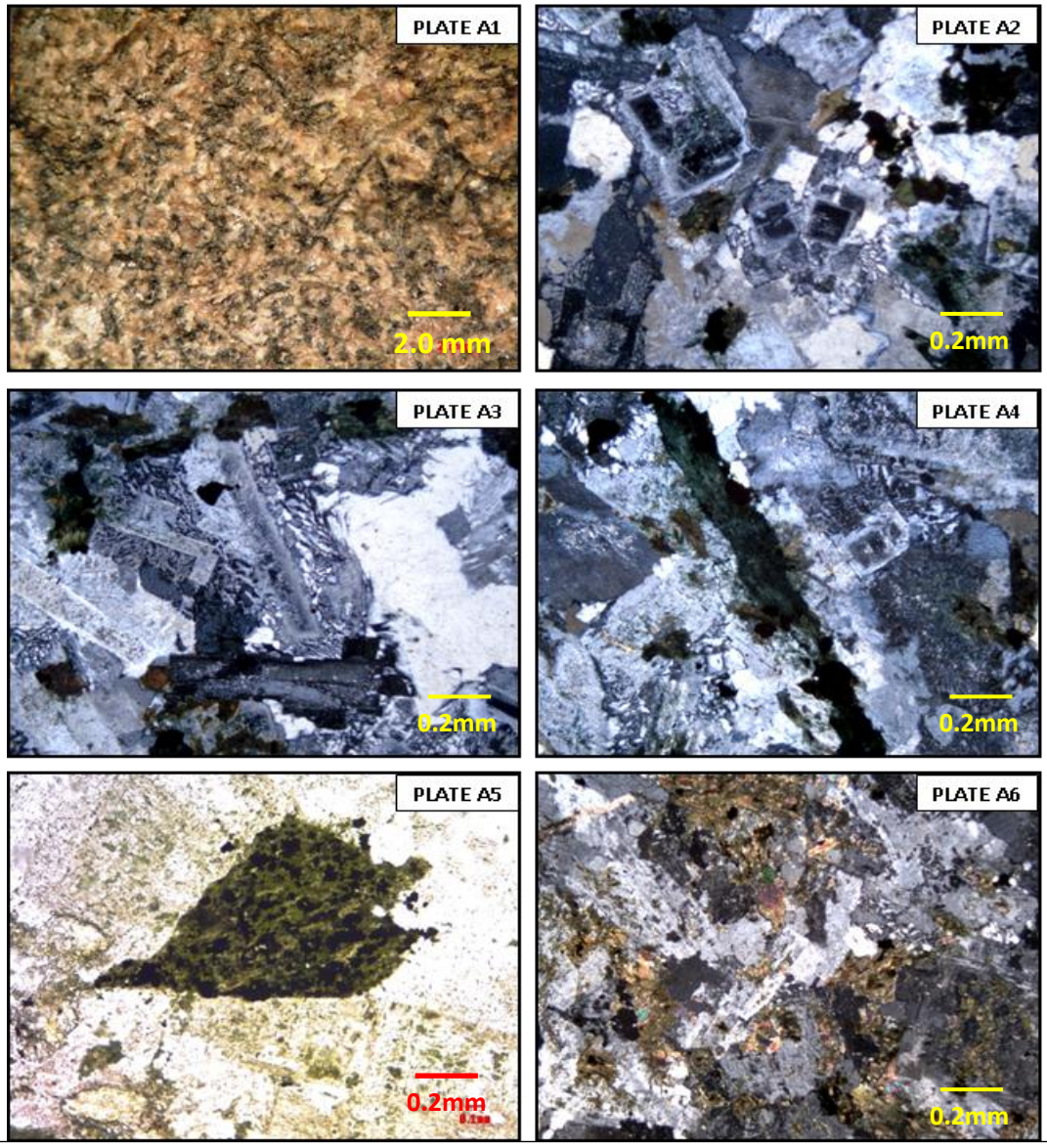

Plate A1: Hand specimen of diorite taken from western part of Pit 3. The diorite shows medium to coarse grained. **Plate A2**: Most of the euhedral plagioclase at the centre of photomicrograph shows zoning extinction. **Plate A3**: Photomicrograph shows that 80% of the sample dominated by euhedral to subhedral plagioclase with interstitial of quartz. Note there are also myrmekitic intergrowth between plagioclase and quartz. **Plate A4**: Photomicrograph view occurrence of prismatic hornblende in diorite sample (green black mineral at the centre part of the microphotograph. **Plate A5**: Micrograph shows occurrence of hornblende with biotite inclusion in sample MIX 4A which may indicates that the biotite was formed by alteration of hornblende. **Plate A6**: Secondary epidote and hornblende form a network surrounding anhedral to subhedral plagioclase.

3.4 Photomicrograph Of Rhyolite From Study Area

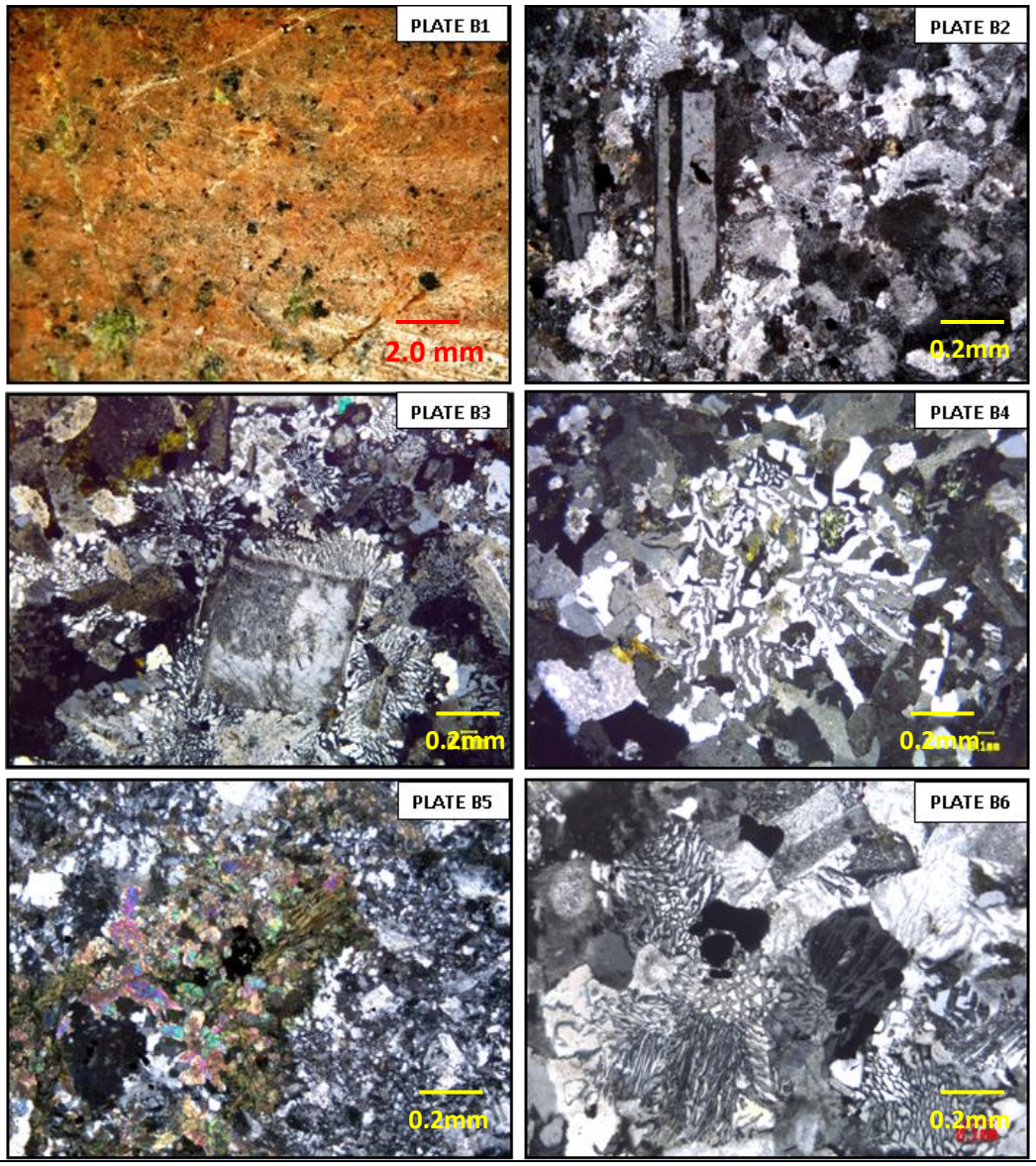

Plate B1: Hand specimen of rhyolite taken from Pit 3 of Pejal quarry. **Plate B2**: Twinning plagioclase phenocryst surrounded by relatively finer grained K- feldspar, quartz and plagioclase. **Plate B3**: Micrograph of euhedral k-feldspar microphenocryst in rhyolite. Note that the k-feldpsar microphenocryst is surrounded by k-feldspar-quartz intergrowth. **Plate B4**: Presence of microgranophyric intergrowth texture in rhyolite.**Plate B5**: Clot in P3C which composed of numerous anhedral secondary epidote is common features in rhyolite. This epidote is an alteration product of plagioclase feldspar (Cox 1979).**Plate B6**: Photomicrograph of rhyolite shows another shape of microgranophyric texture in rhyolite. Note the triangle shapes formed within grain.

3.5 Photomicrograph of trachydacite from study area

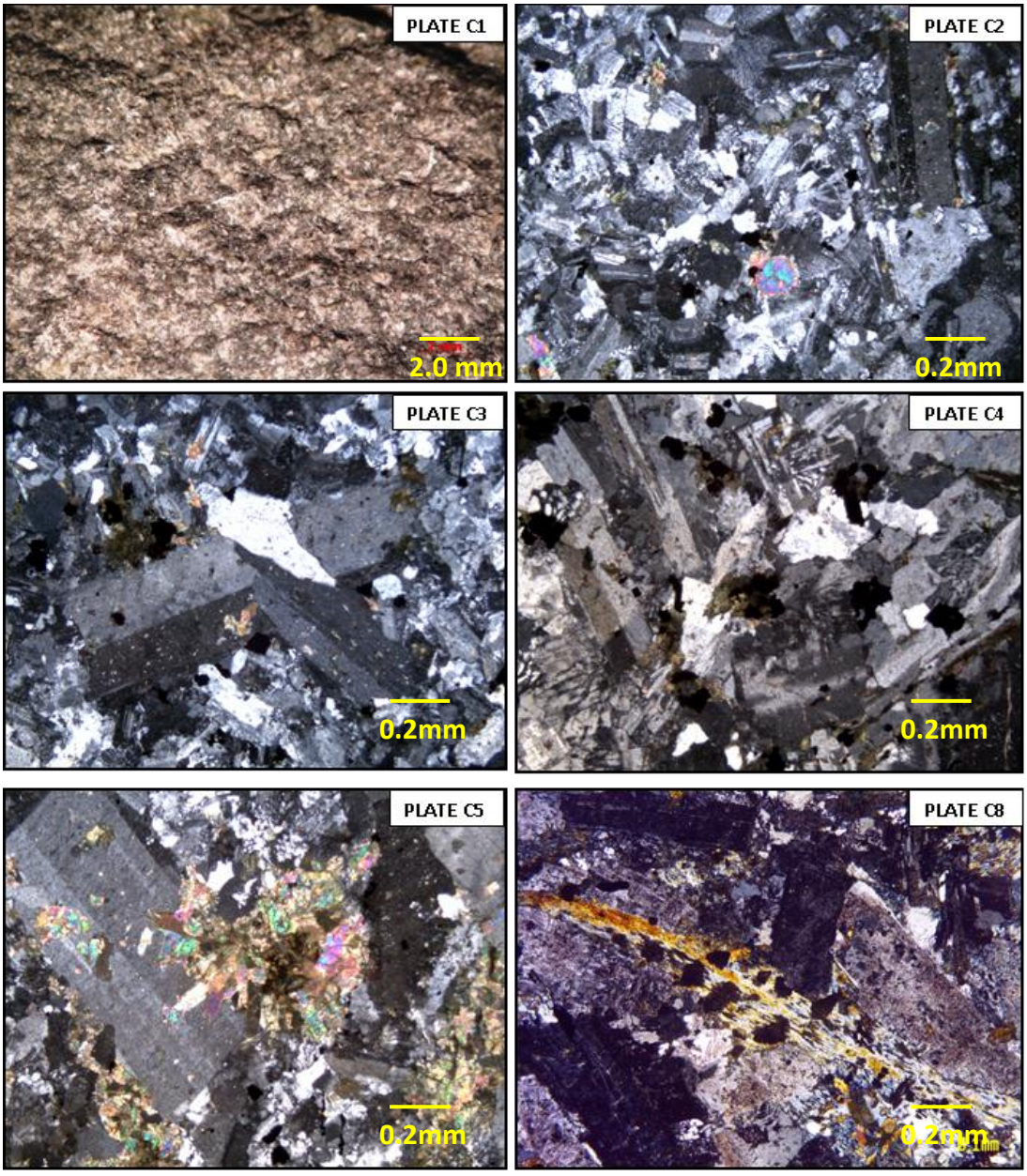

Plate C1: Hand specimen of rhyolite taken from Pit 3 of Pejal quarry. **Plate C2**: General view of sample P3J showing that rhyolite are composed of mainly K-feldspar and Quartz. Note that most of the K-feldspar shows good shape while quartz shows clear irregular shape. **Plate C3**: K-feldspar shows euhedral shape and formed glomercryst or glomeroporphyritic texture in sample P3J. **Plate C4**: K-feldspar and quartz intergrowth forming microgranophyric texture in trachydacite. **Plate C5**: Photomicrograph shows the occurrences of secondary epidote inclusion in Plagioclase in P3K samples. **Plate C6**: Photomicrograph shows biotite formed as interstitial in trachydacite.

3.6 Discussion and Conclusion

Petrographic studies can give several informations about the occurrence of magma mixing, implication of mineral intergrowth and spherulite towards magma emplacement, hydrothermal alteration and A-type classification.

- There are 3 rock types exposed in the study area. They are diorite, rhyolite and trachydacite. All these 3 rocks have sharp contact and there is no evidence of magma mixing between these magmas (e.x. hybrid rock). There are 2 types of volcanic rocks and 1 type of plutonic rock found within the study area. The main volcanic rock types are rhyolite and trachydacite and the plutonic rock is diorite.
- Microgranophyric texture is common in all rocks from study area although rhyolite content more micrographic intergrowth compared to trachydacite and diorite. Microgranophyric or granophyric texture is k-feldspar and quartz formed together as skeletal and triangle shape morphologies. Some of the microgranophyric texture shows formation of k-feldspar as nucleus or core at the center of intergrowth. The size of the k-feldspar nucleus are varies. Following experiment studies on granophyric texture on the Long mountain A-type granite (Morgan and London 2012), the occurrences of the microgranophyric texture in all rocks from study area suggest that the magma that produce micrographic intergrowth has undergone undercooling in high viscosity silicate magma in range of 50 -150^{O}C which is initially H_2O undersaturated (<2.9 wt% according to Tuttle and Bowen, 1958) and became equilibrium as water saturated magma at final emplacement (0.5kbar) (Morgan and London 2012). The occurrence of feldspar phenocryst enclosed by microgranophyric intergrowth shows that some k-feldspar has crystallized before the intergrowth and quartz. The occurrence of microgranophyric intergrowth

marked the process undercooling stage where this process is restricted only to the formation of the microgranophyric texture before individual quartz are formed.

- The occurrences of interstitial biotite in all rocks from study area indicate that the biotite is of annite type. The stabilization of annite in late crystallization sequence attributed to progressive enrichment in H_2O in residual melt upon crystallization of feldspar and quartz. Annite is enrich in fluorine which can be used as an indicator of magmatic and fluid-rock interaction processes associated with melt (Markle and Piazolo, 1998; Selby and Nesbitt, 2000)
- The occurrences of radial spherulitic texture also indicate the magma has undergone undercooling process. However, the rate of undercooling shown by spherulite is higher compared to the microgranophyric of granophyric intergrowth (e.g. Fenn, 1977; Morgan and London, 2012). Regardless their difference in temperature range, undercooling of high viscosity silicate liquid is the key process toward formation of crystallization of granophyric or microgranophyric (Morgan and London, 2012).
- Mineral alteration is common in all rocks from study area (e.g chlorite and epidote). The replacement of biotite mineral to chlorite is common in granitic composition (Parry and Downey, 1982; Eggleton and Banfield, 1985). The water that contained in the host rock is the catalyst to the formation of the chlorite. The water provides hydrogen cation (H^+) which will react with the chemically unstable biotite and produce chlorite + Mg^{2+} (e.g. Parry and Downey, 1982). With example of igneous biotite from Gold Hill Utah, Parry and Downey (1982) suggest that the alteration of the biotite by chlorite took place at near $200^{O}C$.
- Other alteration mineral such as epidote which altered from plagioclase feldspar. The alteration process of plagioclase to formed epidote is called saussuritization. Saussuritization process by which calcium-bearing plagioclase feldspar is altered to a

characteristic assemblage of minerals called saussurite (Cox, 1979). Residual fluids present during the late stages of magmatic crystallization can react with previously formed plagioclase feldspar to form epidote. The epidote will be spread through the plagioclase or located near its outer margin. The replacement possibly took at higher temperature than chlorite which is 320OC (e.g Keith et al., 1968)

- The occurrence of the euhedral k-feldspar, interstitial biotite and association with microgranophyric intergrowth shown in all rocks from Ramunia are similar to the A-type rocks elsewhere (King et al., 1997;Shen et al., 2011; Li et al., 2012). These features are important in petrographic and field features of A-type rocks although the useful of this features are still uncertain (e.g. Collins et al., 1982; Whalen et al.,1987; Landenberger and Collins, 1996).

4.0 GEOCHEMISTRY

4.1 Introduction

This chapter will describe in detail the geochemical variation of volcanic rocks from the study area. 30 samples have been analysed for major, trace and REE elements. Each of the rock type will be describe separately. All rocks will be classified using TAS diagram (Middlemost. 1994) and will be used throughout the thesis. Petrogenesis of the magma based on the geochemistry will be discussed at the end of this chapter.. Result of the analysis is presented in Table 4.1

Table 4.1: Whole rock major and trace element composition for all rocks from Teluk Ramunia

Sample	P2A	P2B	P2G1	P3B	P3C	P3E	P3F	P3G	P3H	P3J
Type	Rhyolite	Rhyolite	Rhyolite	Rhyolite	Rhyolite	Rhyolite	Rhyolite	Rhyolite	Rhyolite	Rhyolite
Major Elements										
SiO2	72.4	72	72.4	72.1	71.8	73	71.9	72.5	73.4	70.3
Al2O3	12.69	12.6	12.73	12.63	12.94	11.98	12.51	12.37	11.9	13.33
Fe2O3	3.16	3.32	3.27	3.42	3.61	3.68	3.37	3.15	3.35	3.88
CaO	0.97	0.94	1.51	2.37	1.25	1.04	1.28	1.34	1.88	1.21
MgO	0.12	0.1	0.23	0.19	0.12	0.22	0.15	0.13	0.18	0.13
Na2O	3.92	3.72	5.09	3.66	3.55	3.29	3.62	3.06	3.29	4.13
K2O	4.72	4.76	2.78	3.45	4.99	3.93	4.12	5.18	3.98	4.73
MnO	0.04	0.07	0.07	0.06	0.06	0.06	0.07	0.07	0.12	0.08
TiO2	0.35	0.25	0.29	0.23	0.27	0.25	0.26	0.23	0.22	0.3
P2O5	0.03	0.02	0.02	0.02	0.02	0.03	0.03	0.02	0.02	0.02
BaO	0.15	0.16	0.12	0.14	0.19	0.18	0.17	0.19	0.16	0.25
LOI	0.58	0.62	0.68	1.07	0.54	1.05	0.97	0.7	0.77	0.7
SUM (%)	99.13	98.56	99.19	99.34	99.34	98.71	98.45	98.94	99.27	99.06
Trace Elements										
Ba	1625	1572	1163	1304	1883	1746	1643	1828	1566	2635
Be	4	4	2	3	3	3	2	3	2	3
Co	1	0.9	1.6	1.8	0.7	0.8	1.1	1.2	0.9	1.5
Cs	4.1	3.4	5.2	2.7	3.4	3.2	3	6	3.4	5
Ga	20.4	20.3	19.7	20	20.3	18.9	19.6	18.9	18.1	20.7
Hf	10	9	9.2	8.4	9.3	9.1	9	8.4	8.5	8.4
Nb	18.5	19.6	17.2	18.8	19.2	17	18.1	17.3	17.8	17.4
Rb	181.1	206.5	115.7	128.5	176.2	155.8	151.4	196.5	155.9	187.9
Sn	6	7	4	5	6	5	5	3	5	5
Sr	155.9	131.2	158.5	247.7	162.1	133.9	139.1	125.6	164.6	180.2
Ta	1.6	1.4	1.2	1.4	1.3	1.3	1.2	1.3	1.2	1.3
Th	32.9	28.8	28.9	28.4	29.1	26.6	28.2	26.9	26.7	25.8
U	7.9	7.8	6.8	6.6	7.1	6.9	6.9	6.8	6.8	6.3
W	2.1	2.4	3.2	6.4	4.4	1.8	3	7.2	3.2	6.4
Zr	365.5	350.9	330.1	317.5	332.2	332.7	318.9	316.4	308.5	306.1
Y	57.1	59.7	50.3	49.8	49.7	47.8	50.5	53.6	50.5	52.2
La	67.1	71.8	68	59.6	64.5	60.2	63.4	66.3	60.8	65.4
Ce	132.1	139.2	134.8	119.3	128.8	120.8	122.3	132.6	120	134.8
Pr	14.91	15.81	15.55	13.5	15.09	13.7	14.13	14.96	14.21	15.48
Nd	55.9	60.6	58.6	50.9	56.1	53.2	53.3	55.8	50.4	58.9
Sm	10.32	10.61	10.52	9.59	10.02	9.4	9.5	10.11	9.88	10.5
Eu	1.49	1.57	1.65	1.58	1.53	1.68	1.47	1.53	1.81	2.29
Gd	9.72	10.34	9.72	8.92	9.08	8.85	8.81	9.47	9.15	10.26
Tb	1.6	1.68	1.54	1.46	1.5	1.4	1.45	1.54	1.48	1.63
Dy	9.36	9.89	8.96	8.57	8.93	8.12	8.48	9.05	8.84	9.29
Ho	1.92	1.99	1.83	1.62	1.7	1.64	1.72	1.93	1.79	1.92
Er	5.98	5.81	5.21	4.82	5.27	4.69	5.04	5.49	5.27	5.37
Tm	0.87	0.9	0.77	0.69	0.78	0.72	0.74	0.81	0.77	0.8
Yb	5.6	5.93	5.19	4.49	5.34	4.64	5.09	5.46	5.09	5.28
Lu	0.87	0.89	0.8	0.68	0.79	0.73	0.8	0.82	0.78	0.83
Mo	2	2	1.8	1.7	2.4	0.8	1	1.6	2.6	2
Cu	4.9	4.2	9.9	10.7	13.4	6.1	9	10.2	7.3	14.5
Pb	13.2	26.1	118.3	606.2	77.2	22.7	52.3	37.5	41.2	74.2
Zn	26	48	116	333	53	41	64	54	38	82
Ni	3.4	2.7	4	4.8	3.1	3.1	4.3	3.7	4.7	3.7
As	0.8	6.8	2	3.6	1.7	<0.5	0.6	60	7.9	9.1
Normative Minerals										
Quartz	29.66	30.19	29.39	33.08	29.53	36.25	32.24	29.24	35.47	25.79
Ortoclase	27.89	28.11	16.43	20.38	29.45	23.21	24.33	27.89	23.49	27.95
Albite	33.15	31.47	42.06	30.94	30	27.8	30.63	33.41	27.8	34.93
Anorthite	3.09	3.62	3.67	7.85	4.67	5.27	5.7	3.26	2.98	3.87
H2O/LOI	1.05	0.95	1.04	1.07	0.8	1.1	0.97	0.7	0.77	0.68

Table 4.1, continued: Whole rock major and trace element composition for all rocks from Teluk Ramunia

Sample	P3M	TRP1	TRP2	TRA	TR5	TRG3	TRG4	TRG5	P2C	P2E
Type	Rhyolite	Rhyolite	Rhyolite	Rhyolite	Rhyolite	Rhyolite	Rhyolite	Rhyolite	Tra-dacite	Tra-dacite
Major Elements										
SiO2	72.2	73.6	74.4	70	71.1	70.8	70.1	70.9	64.6	63.5
Al2O3	12.8	12.55	12.53	13.56	13.81	13.71	13.95	13.93	14.85	17.02
Fe2O3	3.73	2.18	2.07	4.14	2.9	3.01	3.08	2.94	4.87	5.36
CaO	0.91	0.27	0.58	2.01	1.11	0.82	1.04	1.11	2.57	1.34
MgO	0.14	0.12	0.1	0.34	0.26	0.28	0.29	0.25	0.91	0.72
Na2O	3.95	3.74	3.8	4.26	4.21	4.3	4.14	4.25	4.85	8.65
K2O	4.72	4.78	4.74	3.5	4.49	4.65	4.53	4.5	3.98	0.21
MnO	0.06	0.04	0.04	0.11	0.07	0.07	0.07	0.08	0.13	0.15
TiO2	0.25	0.17	0.16	0.25	0.25	0.25	0.29	0.27	0.6	0.68
P2O5	0.02	0.02	0.01	0.05	0.04	0.05	0.05	0.05	0.16	0.19
BaO	0.19	0.1	0.1	0.13	0.18	0.19	0.17	0.16	0.15	0.03
LOI	0.7	0.96	0.96	1.1	0.92	0.93	1.03	0.96	1.25	1.37
SUM	99.67	98.53	99.49	99.45	99.34	99.06	98.74	99.4	98.92	99.22
Trace Elements										
Ba	1856	1020	1000	1340	1663	1857	1799	1689	1518	181
Be	2	3	3	4	3	4	4	3	4	2
Co	1.4	1.8	1.6	2.6	2.1	2.3	2.6	2.4	5.9	4
Cs	2.9	3	2.8	3.1	2.8	6.5	3.1	2.9	2.9	1.6
Ga	19.4	21.5	20.9	22.5	19.4	19.6	21.3	19.7	21.5	27.2
Hf	8.5	7.8	7.5	8.4	8.3	9	8.4	9	8.4	8
Nb	17.1	17.7	19	14.2	15.5	15.4	16.1	15.7	12.8	16.5
Rb	188.3	230.7	220	144.9	191.2	194.9	196.8	195.4	155.8	6.3
Sn	3	4	5	14	5	14	5	5	5	10
Sr	147.5	53.2	59.6	162.1	118	135.7	132.6	117.6	233	143.2
Ta	1.3	1.4	1.6	1.2	1.1	1.1	1.2	1.1	0.8	1.2
Th	28	34.3	39.6	32.2	30.2	29.7	31.1	27.9	27.2	24.7
U	7	8.4	9.8	7.5	6.3	7.3	7.5	6.8	6.8	6.5
W	4	2.8	3.3	3.3	3.3	3	2.6	3.3	2.3	4
Zr	328.6	241.3	223.6	330	336.7	345.8	324.9	350.3	312.4	303.3
Y	45.2	54.7	46.8	40	40.4	33.3	45.8	35.5	43.5	52.2
La	62.2	75.1	61.9	47.6	77.3	43.1	55.3	39.3	60.1	57.2
Ce	123.4	153.2	128.7	96.7	150.1	90.4	109.5	81.4	112.6	117.2
Pr	13.97	16.7	13.73	10.76	15.43	10.08	12	8.84	13.02	13.64
Nd	51.8	63.6	48.8	40.5	52.8	37.7	47.2	35.2	47.2	49.8
Sm	9.23	11.58	9.15	7.2	8.63	6.8	8.38	6.51	8.57	9.22
Eu	1.53	0.9	0.61	1.12	1.17	0.99	1.18	0.98	1.56	1.76
Gd	8.17	10.58	8.37	6.57	7.53	6.01	7.98	6.22	7.74	8.81
Tb	1.37	1.68	1.35	1.09	1.17	0.98	1.27	1.01	1.23	1.39
Dy	8.09	9.6	7.99	6.45	6.84	5.73	7.39	5.94	7.02	8.18
Ho	1.6	1.91	1.59	1.37	1.41	1.19	1.61	1.22	1.43	1.68
Er	4.69	5.73	4.66	4.12	3.98	3.59	4.77	3.84	4.16	4.98
Tm	0.71	0.88	0.76	0.64	0.62	0.55	0.73	0.6	0.62	0.75
Yb	4.99	5.69	5.11	4.36	4.3	3.57	4.89	3.93	4.25	5.11
Lu	0.77	0.84	0.73	0.65	0.63	0.57	0.74	0.61	0.64	0.76
Mo	1.5	1.5	1.8	1.2	1.2	1.1	1.3	1.2	1.3	0.4
Cu	4.8	5.3	13.7	4.7	4.8	5.5	4.5	4.5	3.8	9.8
Pb	31.9	22.7	19.8	15.1	12	51.3	19.5	11.4	23.6	1118.9
Zn	49	51	47	89	57	108	76	53	87	1777
Ni	5.1	3.7	5.4	3.7	4	4.3	3.6	3.9	2.6	1.9
As	0.8	1.6	1.1	1.3	1.8	1.8	1.5	2	2.3	3
Normative Mineral										
Quartz	29.24	32.8	32.71	27.58	26.26	25.84	26.08	26.26	15.74	8.99
Ortoclase	27.89	28.22	28	20.65	26.55	27.43	26.72	26.55	23.49	1.22
Albite	33.41	31.63	32.15	36.03	35.93	36.35	34.98	35.93	41.01	73.16
Anorthite	3.26	1.41	3.03	7.54	5.48	4.12	5.18	5.48	7.01	5.45
H2O/LOI	0.7	0.96	0.96	1.1	0.96	0.93	0.9	0.96	1.25	1.37

Table 4.1, continued: Whole rock major and trace element composition for all rocks from Teluk Ramunia

Sample	P2G2	P3N	P3O	P3K	P1G	MIX2A	MIX4A	P1I	HBL LONG
Type	Tra-dacite	Tra-dacite	Tra-dacite	Tra-dacite	Tra-ande	Diorite	Diorite	Diorite	Diorite
Major Elements									
SiO2	64.7	64.9	66.7	64.9	59.4	65.8	58.7	64.1	64.4
Al2O3	14.72	14.09	14.02	14.63	15.39	14.76	15.34	15.14	14.41
Fe2O3	5.26	7.32	6.46	6.08	7.69	4.89	8.49	6.18	6.78
CaO	2.38	1.98	2.17	2.76	3.62	2.2	5.02	2.75	2.45
MgO	0.87	0.41	0.32	0.29	1.65	0.66	1	1.01	0.43
Na2O	4.5	5	4.8	5.13	4.25	4.46	3.8	4.48	4.26
K2O	4.51	4.16	3.68	3.42	4.16	4.26	3.99	3.46	4.15
MnO	0.12	0.21	0.15	0.15	0.24	0.15	0.24	0.18	0.17
TiO2	0.58	0.54	0.48	0.45	1.01	0.52	0.89	0.74	0.53
P2O5	0.16	0.11	0.09	0.07	0.37	0.13	0.3	0.21	0.11
BaO	0.18	0.17	0.17	0.15	0.21	0.15	0.14	0.16	0.19
LOI	0.87	0.6	0.64	0.79	1.55	1.01	1.39	1.21	0.74
SUM	98.85	99.49	99.68	98.82	99.54	98.99	99.3	99.62	98.62
Trace Elements									
Ba	1632	1793	1822	1651	2107	1582	1492	1541	1960
Be	4	4	3	4	4	4	4	4	4
Co	5.1	1.9	2	1.5	7.4	3	5.8	6.2	2.5
Cs	20.9	3.1	3.6	6.4	15.9	12.2	24.2	10	15.5
Ga	19.8	20	22.7	25.2	22.8	20.6	27.6	22.6	22.8
Hf	6.9	7.5	7.4	6.6	6.1	9.1	6.5	5.7	6.8
Nb	16.4	20.1	15.7	15.9	13.7	13.7	12.5	15.6	16.1
Rb	237.8	168.1	149.8	144.3	255.7	215.7	242.5	170.4	233.6
Sn	4	4	4	5	6	5	9	4	5
Sr	292.1	240.9	237.7	241	354.5	275.8	315.7	289.4	320.5
Ta	1.1	1.5	1.1	1.1	1	1	0.8	1.2	1.1
Th	21.7	22.7	22.9	20.8	19.3	23.8	19.6	20.2	21.7
U	5	5.7	6.2	4.9	5	6.4	5.1	4.9	5.6
W	4	5.5	7.7	6.5	4.2	4.2	9.6	3	2.8
Zr	228.2	269.7	284.7	249.2	225.3	348.1	245.8	199.1	277
Y	46.2	53.1	53.2	45.8	44.5	44.9	50.8	39.5	44.5
La	59.1	58.3	60.1	54.8	46.2	51.6	56.2	50.8	49.5
Ce	119.4	115.9	119.7	107.3	97.2	103.9	117.8	106	105.8
Pr	13.7	13.72	14.05	12.82	11.37	11.81	14.12	11.99	11.97
Nd	50.6	55.8	53.3	49.6	44.4	45.4	54	47.3	46
Sm	9.37	10.16	10.3	9.09	8.82	8.37	10.3	8.37	8.67
Eu	1.82	2.38	2.44	2.67	1.83	1.62	2.57	1.75	2.2
Gd	8.58	9.91	9.77	8.59	8.35	7.83	9.89	7.82	8.33
Tb	1.39	1.54	1.58	1.39	1.29	1.27	1.53	1.21	1.31
Dy	8.28	9.01	9.11	8.28	7.84	7.64	8.83	6.86	8.04
Ho	1.61	1.81	1.86	1.66	1.51	1.52	1.79	1.39	1.63
Er	4.6	5.31	5.53	4.83	4.38	4.58	5.11	4.02	4.61
Tm	0.66	0.79	0.78	0.69	0.66	0.67	0.76	0.62	0.7
Yb	4.46	5.38	5.19	4.54	4.41	4.43	4.85	3.91	4.7
Lu	0.66	0.81	0.79	0.72	0.63	0.65	0.69	0.57	0.67
Mo	1.5	1.7	1.8	2.2	1.1	4.1	1.2	1.4	2.4
Cu	3.9	4.3	6.1	5.9	4.2	5.2	4.4	4.3	8.1
Pb	16	38.2	80.4	22.6	28.2	24.3	34.2	15.8	72.6
Zn	64	60	57	55	98	56	124	85	107
Ni	2.7	2.4	3.3	3.2	2.7	3	2.6	3.3	2.5
As	3.9	1.6	3.2	2.5	3.4	6.1	7.9	2.6	112.3
Normative Mineral									
Quartz	16.17	16.48	20.72	17.17	10.61	18.72	12.08	18	18.93
Ortoclase	26.61	24.55	21.71	20.21	24.55	25.16	23.55	20.43	24.49
Albite	30.08	42.77	40.59	42.37	35.93	37.71	32.15	37.87	36.03
Anorthite	6.85	3.73	5.87	6.79	10.66	7.68	13.02	10.99	7.96
H2O/LOI	1.4	0.6	1.2	1.3	1.25	1.12	1.39	1.21	0.74

4.2 Analytical procedure

4.2.1 X- ray fluorescence (XRF)

Loss of Ignition

About 1.0 gram of dry rock sample powder is put into the crucible and heated at 1000°C for 60 minutes. After 60 minutes heated, the samples will be left cooled and weight lost are measured (LOI). The value of LOI can be obtained from the calculation below.

$$LOI = [(b - a)/(c - a)] \text{ X } 100$$

Fusion Disc (Major Element)

Sample powder of 0.6g is mixed with the Flux (Lithium Tetraborate) with factor 8 (1 sample: 8 flux). So about 4.8g of flux is mix with the sample powder in the fusion crucible. The fusion crucible is then installed on the fusion machine (Vulcan Fusion) and the fusion process is start. The heating and fusion process will take about 9.45 minutes (567 seconds) and the cooling will take about 6 minutes (360 seconds) until the fused glass bead is ready. Analysis of ACME laboratories standard rocks (STD SO-18 and STD SY-4D) indicate that both analytical precision and accuracy for all major are better than 0.5% - 1.0%

4.2.2 ICP-MS

Reagent HF and HNO3 were used and purified by su-boiling distillation. A laboratory PTFE bombs were cleaned using 20% HNO3 heated to 100°C for 1 hour. 100mg of sample powder were placed into the PTFE bomb. 1ml of HF (38%) and 0.5ml of HNO3 (68%) were added to each if the samples powder. Then the PTFE bombs were placed on a hot plate and left to dry in order to remove silica in the solution through evaporation. After that, 1ml of HF and 0.5ml HNO3 was added again. The seal bomb were then placed in an electric oven and heated to 190°C for 12 hours. After 12 hours heated, the bombs are left to

be cooled then unsealed. 1ml of 1μml^{-1} Rh solution was added as standard and placed on a hot plate (approximately 150°C) and left to dry. 1ml of HNO_3 was put into the PTFE bomb and left to dry followed by the same step for 1 more time. The final residue was re-dissolved by adding 8ml of 40% HNO_3, resealing the bombs and placed them back at 110°C electric oven and leave for 3 hours. After cooling, distilled de-ionized (UPW) water was mix with the final solution until they reach 100ml. The standard materials used for this analyses were STD SO-18, STD SY-4(D), STD DS8 STD CSC and STD OREA S45CA. Analysis of ACME laboratories standard rocks (STD SO-18 and STD SY-4D) indicate that both analytical precision and accuracy for trace and REE elements are better than 0.5%.

4.3 Major Element Variations

Based on TAS classification (Middlemost, 1994), all samples from study area are plot into rhyolite, trachydacite and diorite (Figure 4.1). Selected Harker diagrams for major elements are illustrated in Figure 4.2. The ranges of SiO2 for rhyolite, trachydacite and diorite are 70% - 74.4%, 63.5% – 66.7% and 58.7% – 65.8% respectively. The felsic rock is considered as highly evolved as the SiO_2 content is more than 70%. In general all Al2O3, Fe2O3, CaO, MgO, MnO, TiO2 and P2O5 show increasing trends with increasing SiO2. A gap of 5.2% occurs between the rhyolite and trachydacite and diorite. Most rocks have high K_2O and Na_2O content (> 4%). K_2O and Na_2O shows no systematic trend with increasing SiO2. Rhyolite, trachydacite and diorite have high total alkali content (Na2O+K2O) which ranging from 7.11% to 9.16%. The value of K2O/Na2O of rhyolite (mostly more than 1.0) is slightly higher than trachyte and diorite (<1.0). Total alkali Silica (Na2O + K2O) vs SiO2 diagram display decreasing trend for rhyolite and trachyte with increasing SiO2 except for diorite rock which display increasing trend with increasing silica content. In K2O vs.SiO2 diagram (after Peccerillo and Taylor, 1976) the samples are plot in high- K calc alkaline

and shoshonitic affinity (Figure 4.3). Mole of $Al_2O_3/(CaO+Na_2O+K_2O)$ and $Al_2O_3/(Na_2O+K_2O)$ are plot against SiO2 shows all trachydacite and diorite samples are metaluminous whereas rhyolite is plot in meta-peraluminous (Figure 4.4a and 4.4b). The Fetot/Fetot+MgO for rhyolite, trachydacite and diorite are 0.95, 0.91, 0.89 respectively. Diagram Fetot/(Fetot+MgO) against SiO2 of Frost (2011) shows that they are plots in within ferroan and A-type field (Figure 4.5).

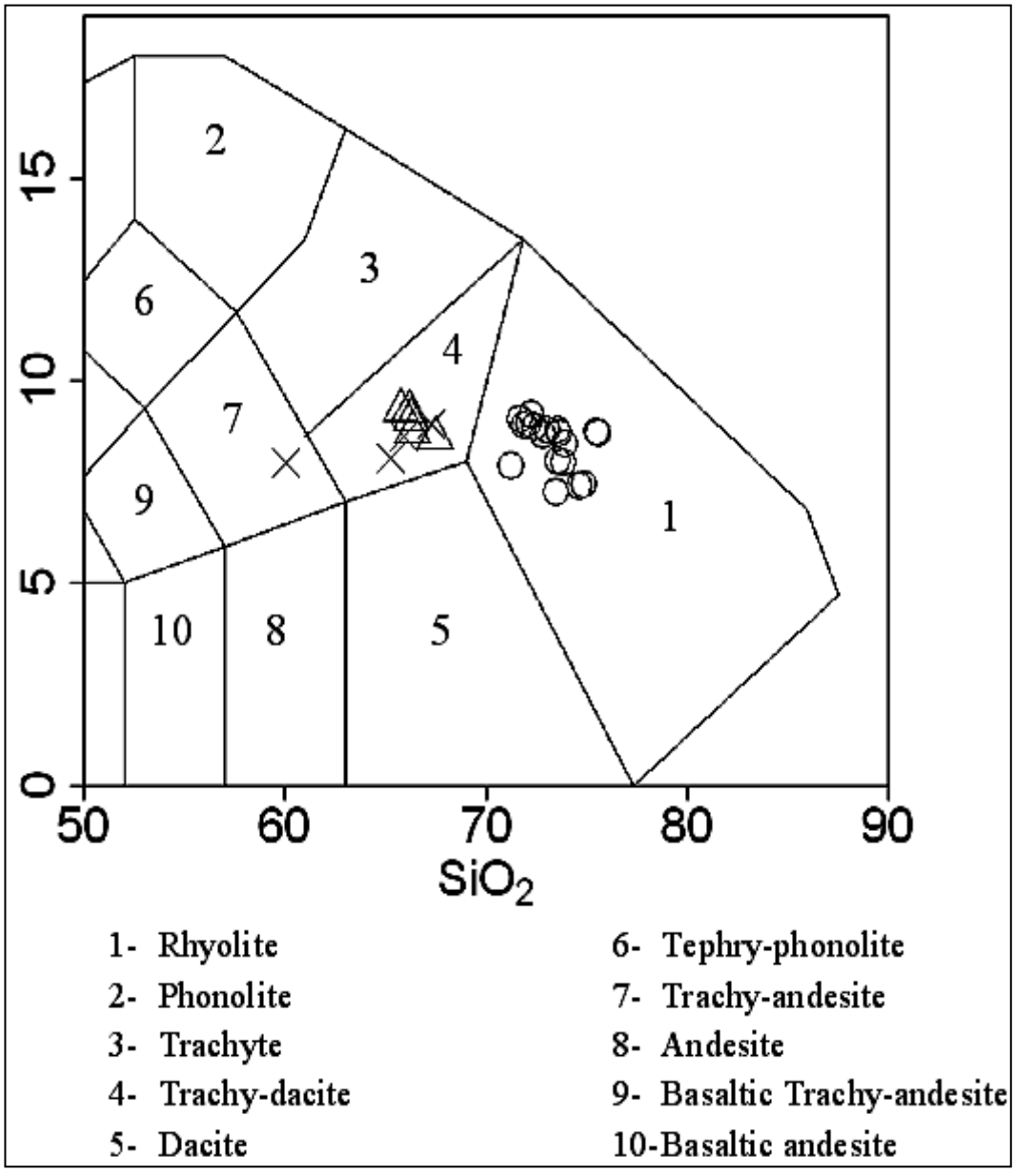

Figure 4.1: TAS volcanic classification (modified after Middlemost (1994). Note the volcanic rocks are plot into rhyolite, trachy-dacite and trachy-andesite.

○ Rhyolite △ Trachy-dacite ✕ Diorite

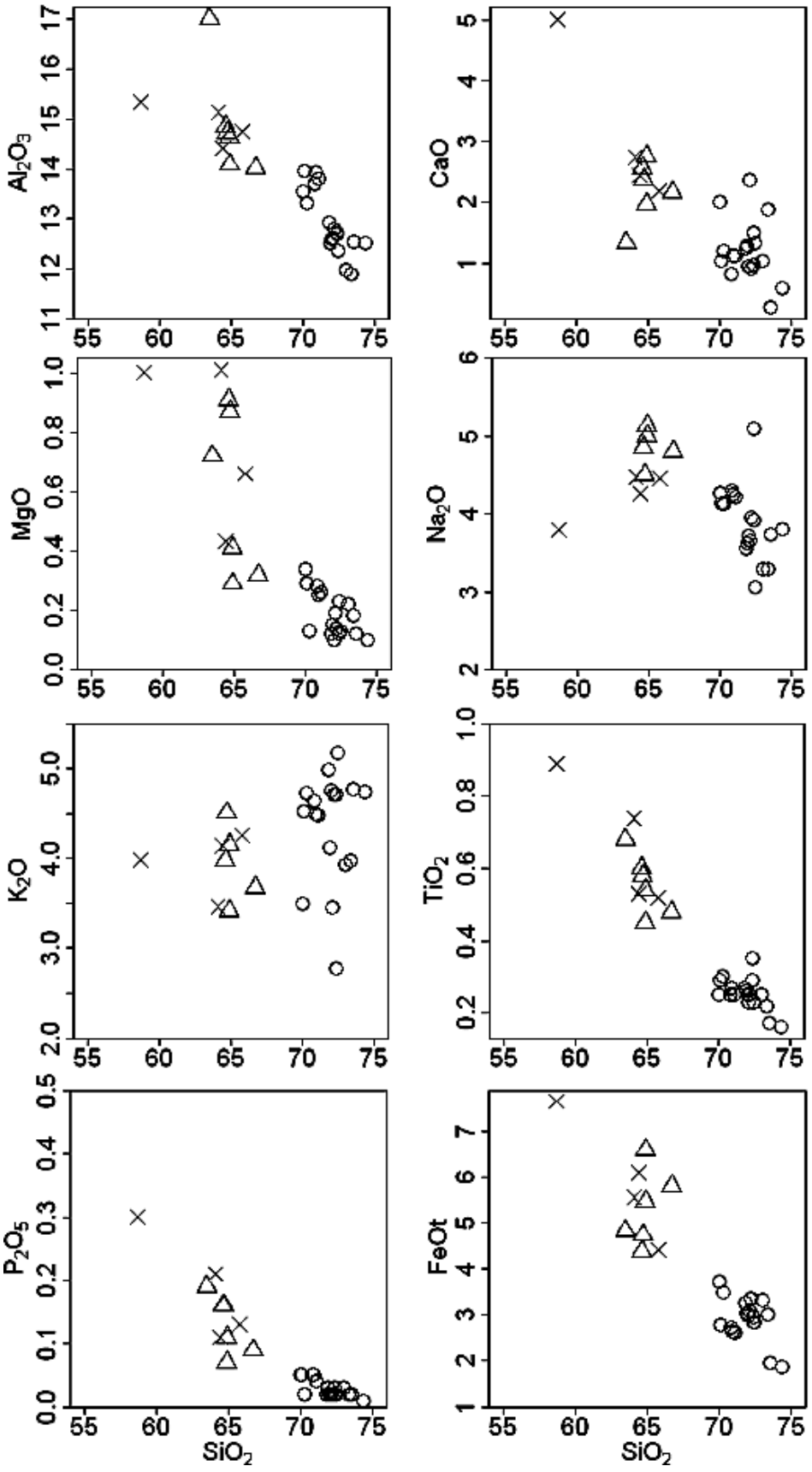

Figure 4.2: Harker diagram for major element plot of igneous rock from Ramunia

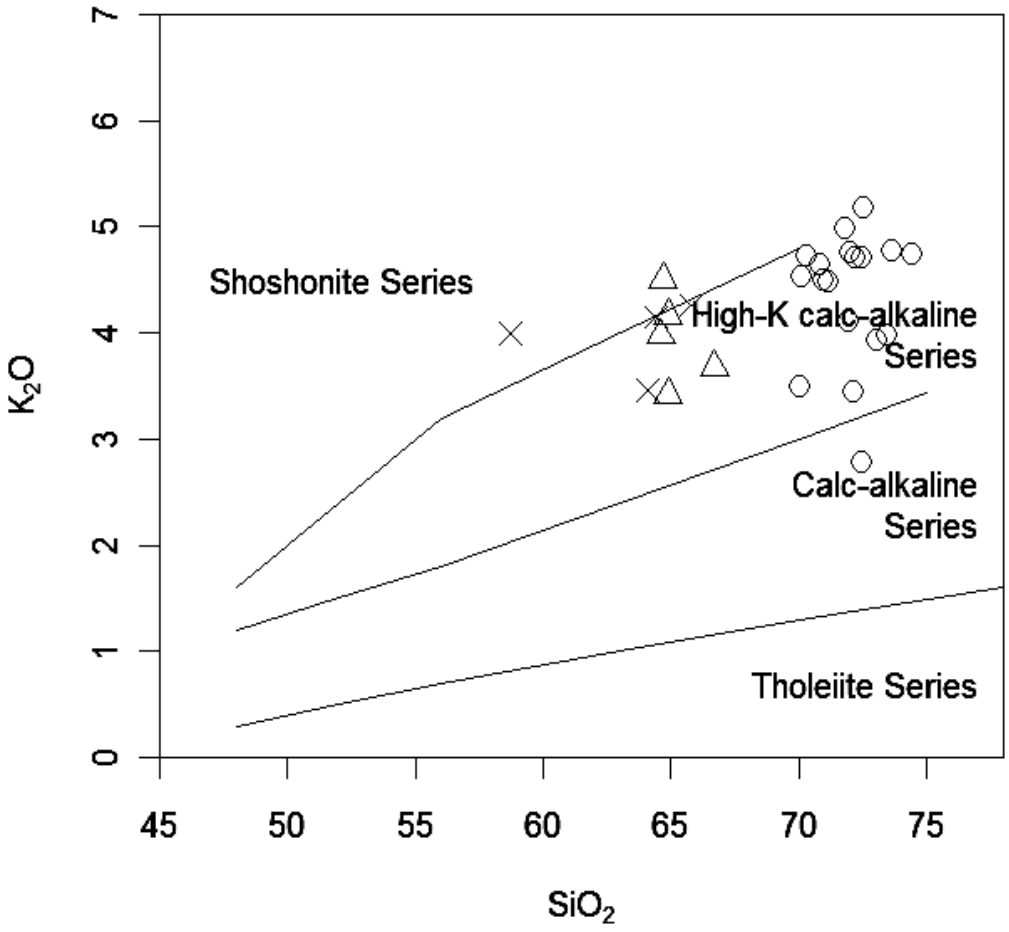

Figure 4.3: K_2O vs SiO_2 diagram shows that most of the rocks from Ramunia are plot into High-K calc alkaline series

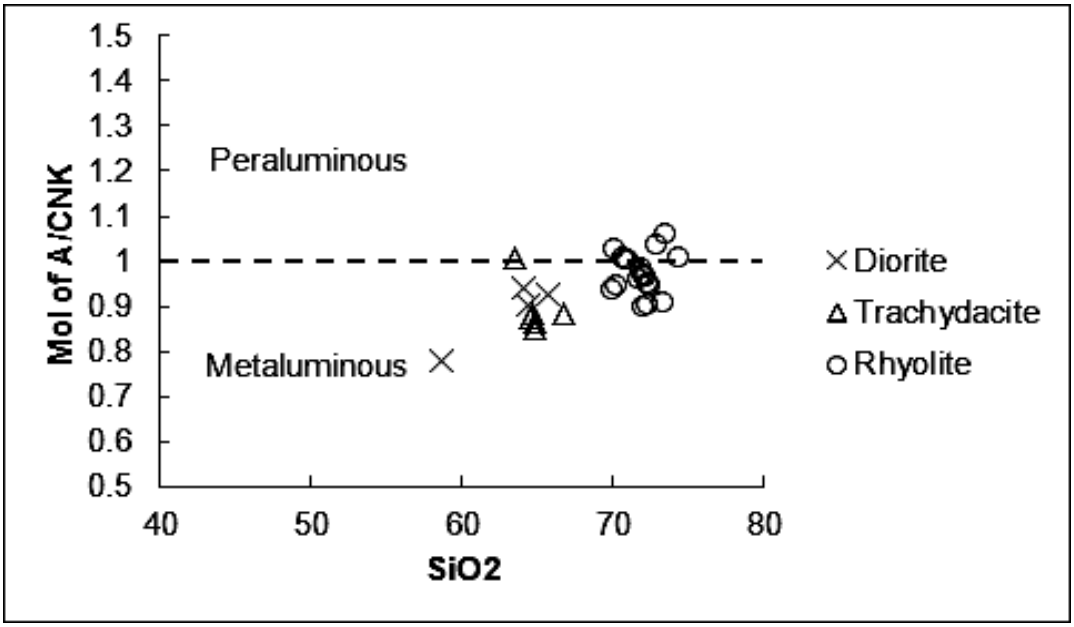

Figure 4.4a : Mol of Al2O3/(CaO+Na2O+K2O) against SiO2 After Shand (1943). Most volcanic and plutonic rock from Teluk Ramunia shows

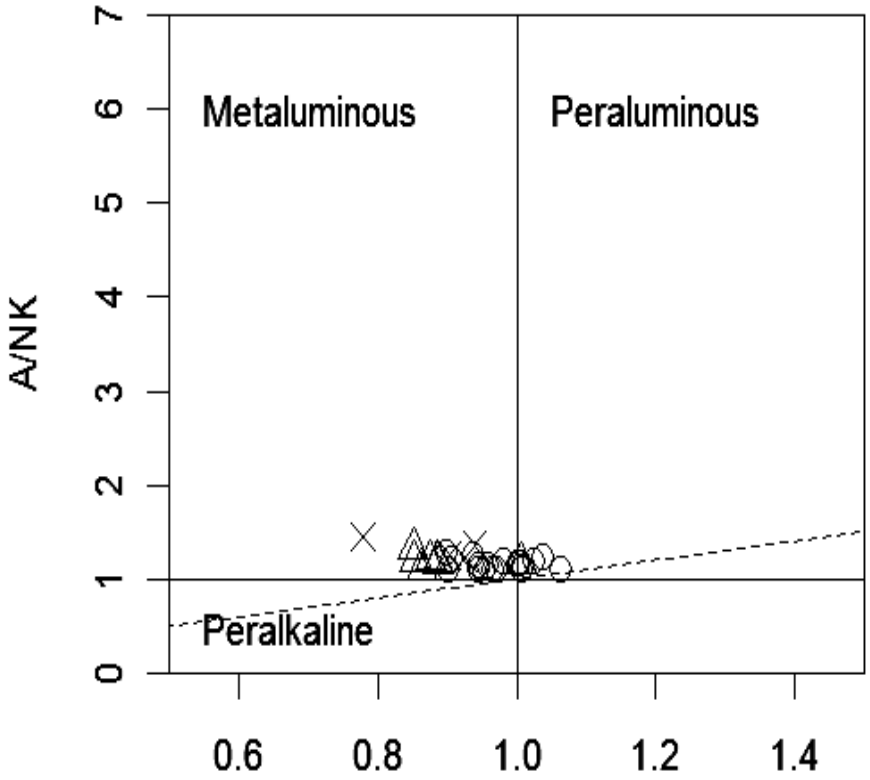

Figure 4.4b: Mol of Al2O3/(Na2O+K2O) against mol of Al2O3/(CaO+Na2O+K2O) after Shand (1943). Most volcanic and plutonic rock from Teluk Ramunia shows charateristic from Metaluminous to weakly Peraluminous.

Rhyolite Trachy-dacite Diorite

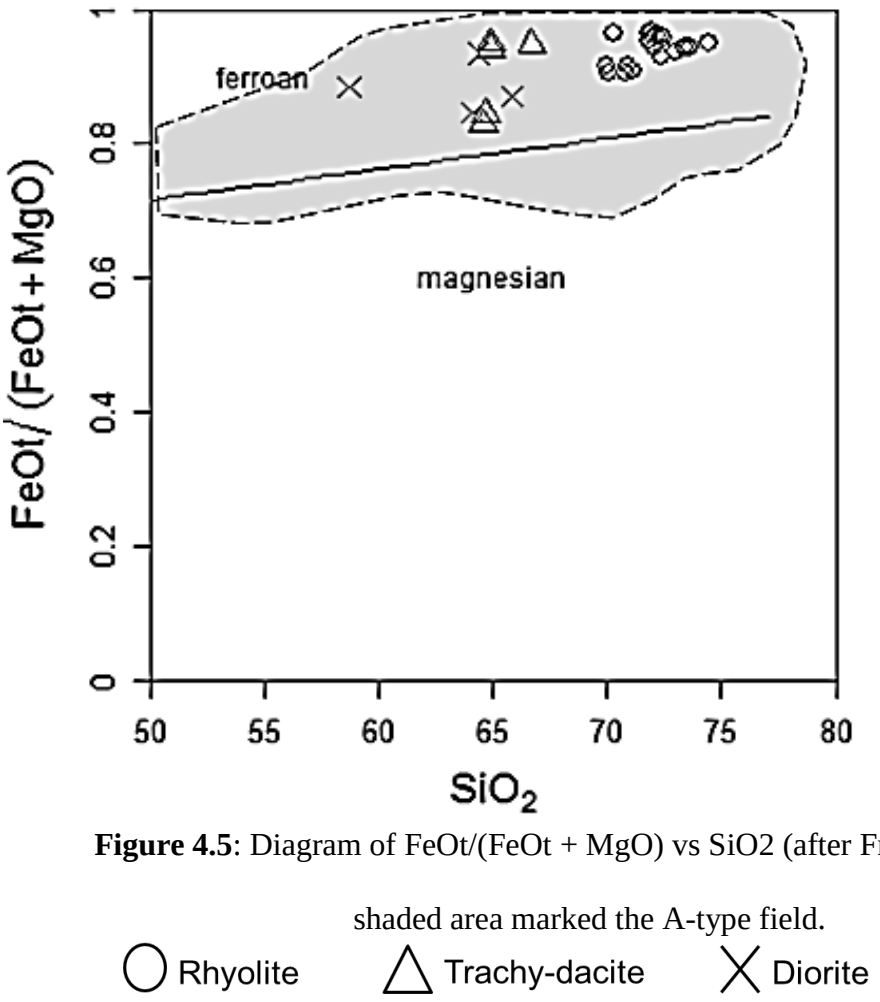

Figure 4.5: Diagram of FeOt/(FeOt + MgO) vs SiO2 (after Frost (2001). The shaded area marked the A-type field.

4.4 Trace Element Variation.

Trace element Harker diagrams were plotted for all samples are plotted in Figure 4.6. In general, Sr, Zr, Ba, Co, Ga, Hf shows decreasing trends with increasing SiO2 content. Trend for Rb, W and Zr shows decreasing trend although they are quite scatter. The content of Ba in rhyolite is ranging from 1000 - 2635ppm with a mean of 1622 ppm. The other LIL element such as Rb and Sr are low which is less than 250ppm. Primordial mantle normalized extended element plot for rhyolite, trachydacite and diorite are given in Figure 4.7. In general, all rocks show roughly parallel and smooth pattern with no significant crossover. They are characterized by Nb, Ta, Sr, P and Ti negative anomalies

without any significant enrichment. Relative to primordial mantle, the changes on trace elements concentration ratios for all rocks are large; enrichment range from 150 to 300 times for Rb and 7 to 20 times for Y. The ratios of depletion range from 20 to 40 times for Nb and Ta, 2 to 15 times for Sr, 0.4 to 15 times for P and 0.7 to 4 times for Ti. This depletion may be related to the fractionation of apatite, plagioclase and sphene. In triangular plot of Ba-Rb-Sr for all rocks from study area shows the vector trend is toward Ba with increasing SiO_2. Diagram of Th/Nb vs Zr shown in Figure 4.8 shows the arrow vector is toward AFC (Assimilation-Fractional crystallization). The average values of 10000Ga/Al ratios in rhyolite, trachydacite and diorite is 2.94, 2.87 and 2.96 respectively thus signify A-type characteristic. All rocks shows low average Sr/Y value which are 2.98, 4.78, 6.72 respectively and contained restricted range of Nb/Ta ratio (Nb/Ta=11 – 14). The average value of Y/Nb for all rocks from study area is from 2.7 – 4.6 which is higher than the value of the mantle sources (Y/Nb < 1.2). Average value of Ca/Sr ratio for rhyolite, trachydacite and diorite are 60.38, 68.15 and 73.3 respectively. Clarke (1992) has proposed that the high ratios of K/Rb in igneous rocks are typical normal in magmatic process. The low ratio of K/Rb can be exceptionally obtain if the magma is affected from fluid interaction and crustal contribution. All rocks shows higher high field strength elements content (220.2 ppm – 394.2 ppm), high K/Rb (136.6ppm – 235.1ppm) ratio and very low Rb/Ba ratio (0.07 ppm – 0.23 ppm). K/Rb ratios of Ramunia rocks are higher compare to the Mahneshan granitoid, northeast Iran which has moderate ratio of K/Rb (Saki, 2010) thus implicate less magma-fluid interaction and crustal contribution in magma.

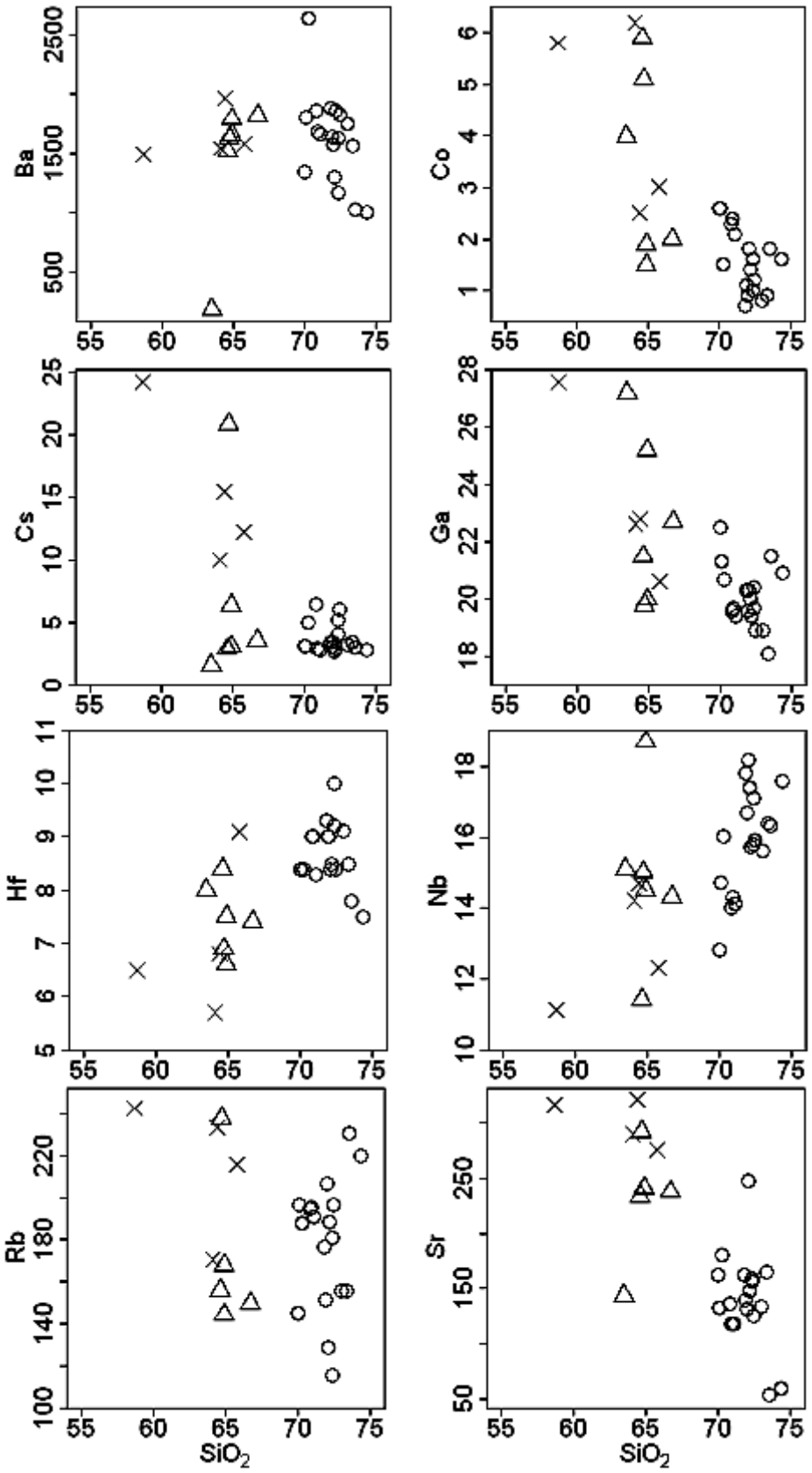

Figure 4.6: Harker diagram for selected trace element plot of rcok samples from Ramunia

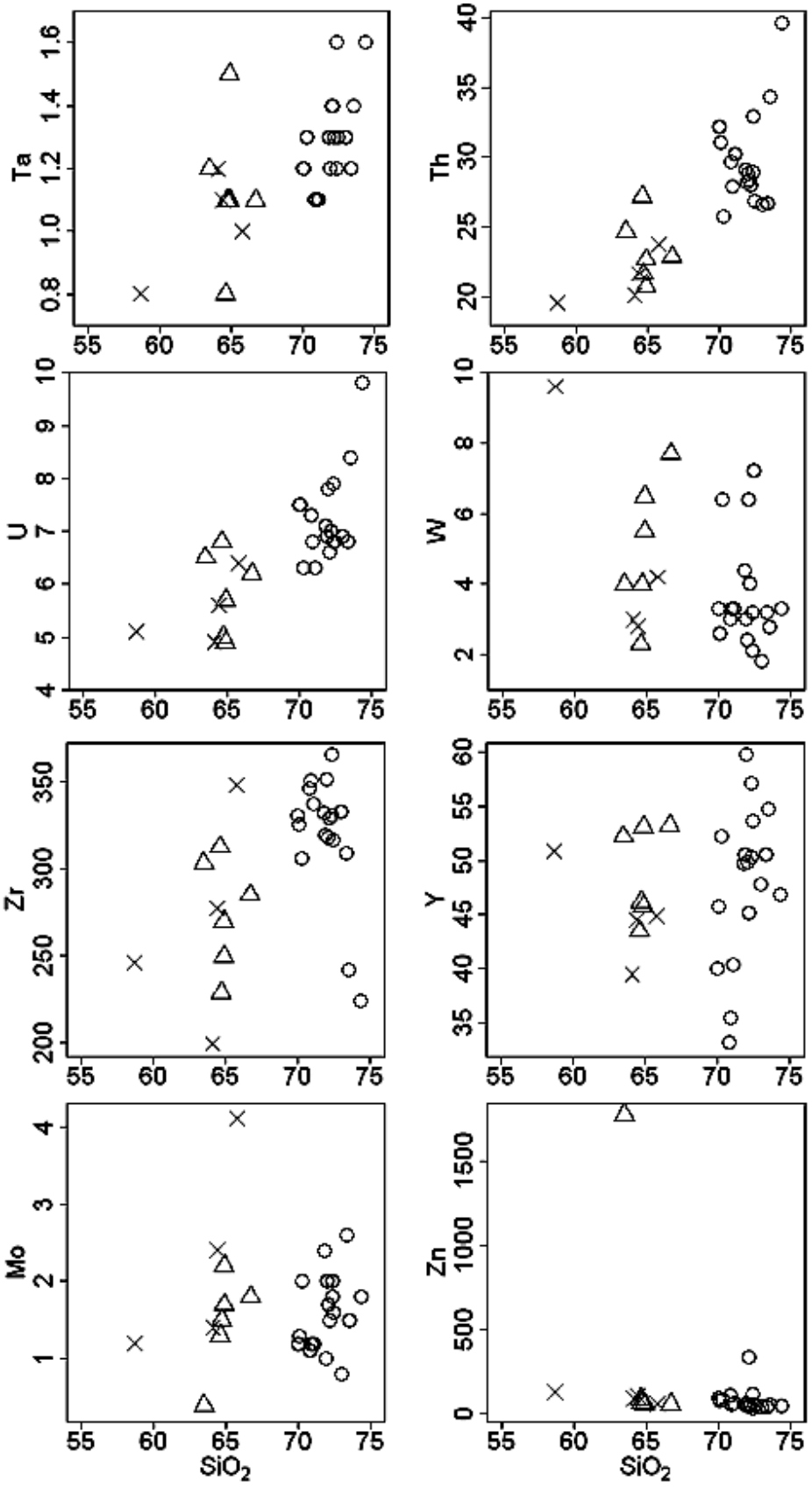

Figure 4.6, continued: Harker diagram for selected trace element plot of igneous rock from Ramunia

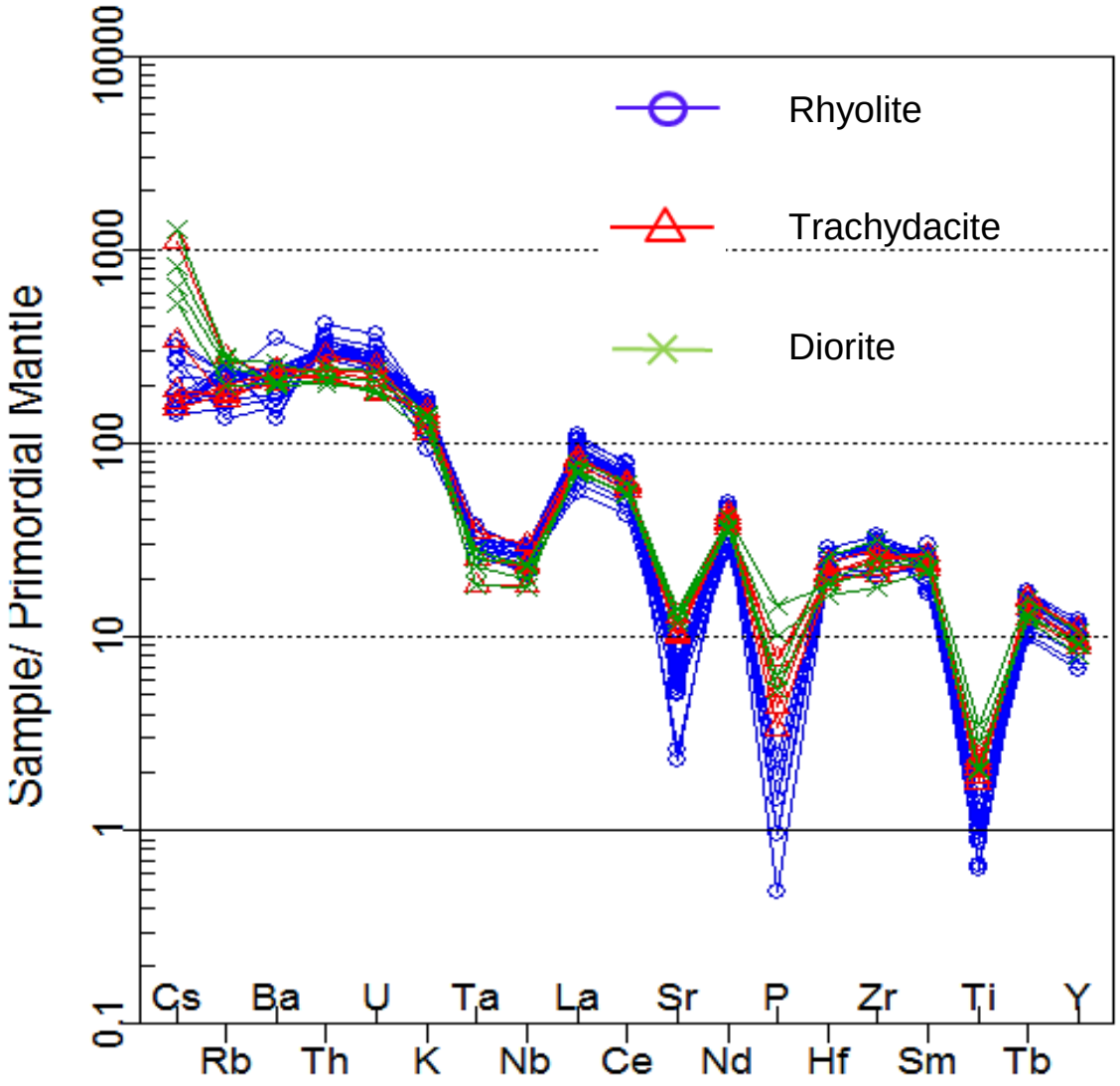

Figure 4.7: Multi-elements spidergrams normalized to Primitive Mantle after Sun and Mcdonough. (1989).

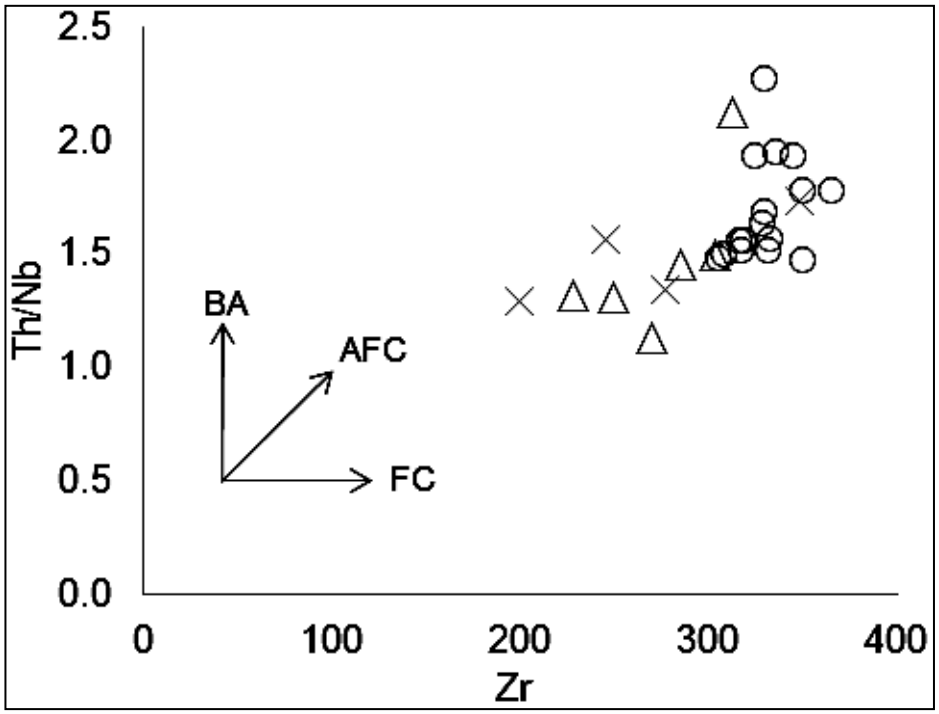

F**igure 4.8**: Diagram Th/Bn versus Zr shows that Ramunia rocks are pointing toward AFC (after Nicolae and Saccani 2003). BA =Bulk assimilation, AFC = Assimilation Fractional Crystalization), FC= Fractional Crystalization

4.5 Rare Earth Trace Elements

Rare earth elements for all samples from Ramunia are shown in Table 4.1 (La – Lu). The REE chondrite normalized pattern in all rocks from study area have similar trends to the A-type from other studies (e.g. Whalen et al., 1996; Landenberger and Collins, 1996; Han et al., 1997; Zhao et al., 2008; Shen et al., 2011. They display sub-parallel LREE (La – Sm) pattern, roughly flat HREE (Gd – Lu) pattern and negative Eu anomalies (Figure 4.9). The ratio of $(La/Yb)_N$ for rhyolite, trachydacite and diorite are 10.0 - 18.0, 10.8 – 14.1 and 10.5 – 13.0 respectively. All rocks have high ratios of [(La/Lu)N = 6.7 – 12.7] clearly shows higher light rare earth elements enrichments. Values of $(Gd/Lu)_N$ for rhyolite, trachydacite and rhyolite are 1.42, 1.53 and 1.62 respectively. (Eu/Eu*=

$Eu_N/\sqrt{[(Sm_N).(Gd_N)]}$ ratios for rhyolite, trachydacite and diorite is 0.42 – 1.32, 1.22 – 1.82 and 1.20 – 1.55 respectively.

Rhyolite shows large negative Eu anomalies compared to trachydacite and diorite. Trachydacite and diorite display almost identical negative Eu anomaly. The negative Eu anomalies in all rocks indicate the plagioclase fractionation as the partition coefficient for Eu is high in plagioclase and K-feldspar (Pearce and Norry, 1979; Nash and Crecraft, 1985; Mahmood and Hildreth, 1983). HREE shows nearly flat pattern which indicate that the source rock does not retain a HREE rich minerals such as garnet and allanite as HREE especially shows high partition coefficient in garnet and allanite.

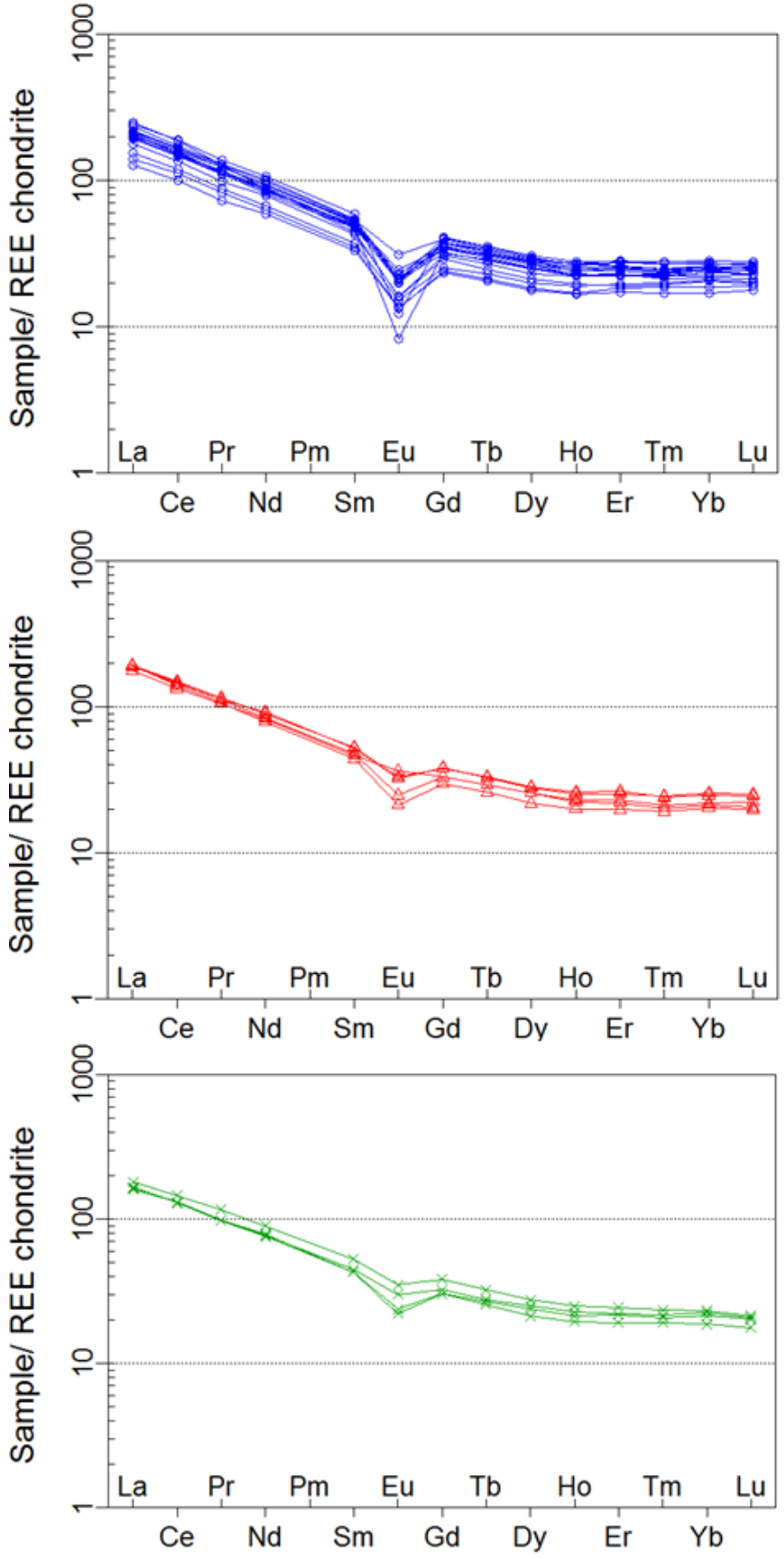

Figure 4.9: REE normalized to chondrite after Boynton 1984. Note the difference of Eu anomalies between rhyolite and trachydacite.

4.6 Rocks classification of rhyolite, trachydacite and diorite from Ramunia (A-type) and comparison to the I and S type from Peninsular Malaysia.

The igneous rocks can be divided into I, S, M and A types according to the alphabetical classification (see reviews in Bonin, 2007). Several attempts have been made to differentiate A-type rocks from other type of rocks (Loiselle and Wones, 1979; Whalen et al., 1987; Eby, 1990). The A-type magma are suggested to have been produced by combination of partial melting and fractionation from magma source that slightly different chemical composition to that I-type source (e.g. Anderson and Cullers, 1978; Cullers et al., 1981; Collins et al., 1982; Anderson, 1983; Clemens et al., 1986; Whalen et al., 1987; Wormald and Price, 1988; Creaser et al., 1991; Landenberger and Collins, 1996). The term A-type are widely used to describe the occurrence of the granite in anorogenic setting (Loiselle and Wones, 1979). King et al, (1997) has suggest that A-type igneous that have aluminous characteristic should be characterized as Aluminous type to replace the A-type

Generally the A-type rocks have high Fe(total)/[(Fe(total) + MgO)], $Na_2O + K_2O$, Ga/Al, HFSE, lower CaO, display large negative anomaly for Eu and yield higher REE content compared to the I and S type granitoid (Loiselle and Wones, 1979; Collins et al., 1982; Whalen et al., 1987; Whalen and Currie, 1990; Eby, 1992; King et al., 1997; Bonin, 2007, Zhao et al., 2008; Dargahi et al., 2010; Shen et al., 2011 and reference therein).

In major and trace elements discrimination diagrams of Whalen et al. (1987) shown in Figure 4.10, most of rocks from study area are plot into the A-type field while the S-type are clearly plot into FG-OGT field and I-S type field (Figure 4.11). Apart from that, the rocks classification of Frost (2001) in binary diagrams ($Fe_{total}/(Fe_{total} + MgO)$versus SiO_2 shows that Ramunia rocks are also plot into A-type field thus strongly suggest that the rhyolite, trachydacite and diorite should be classified as A-type rocks (Figure 4.5).

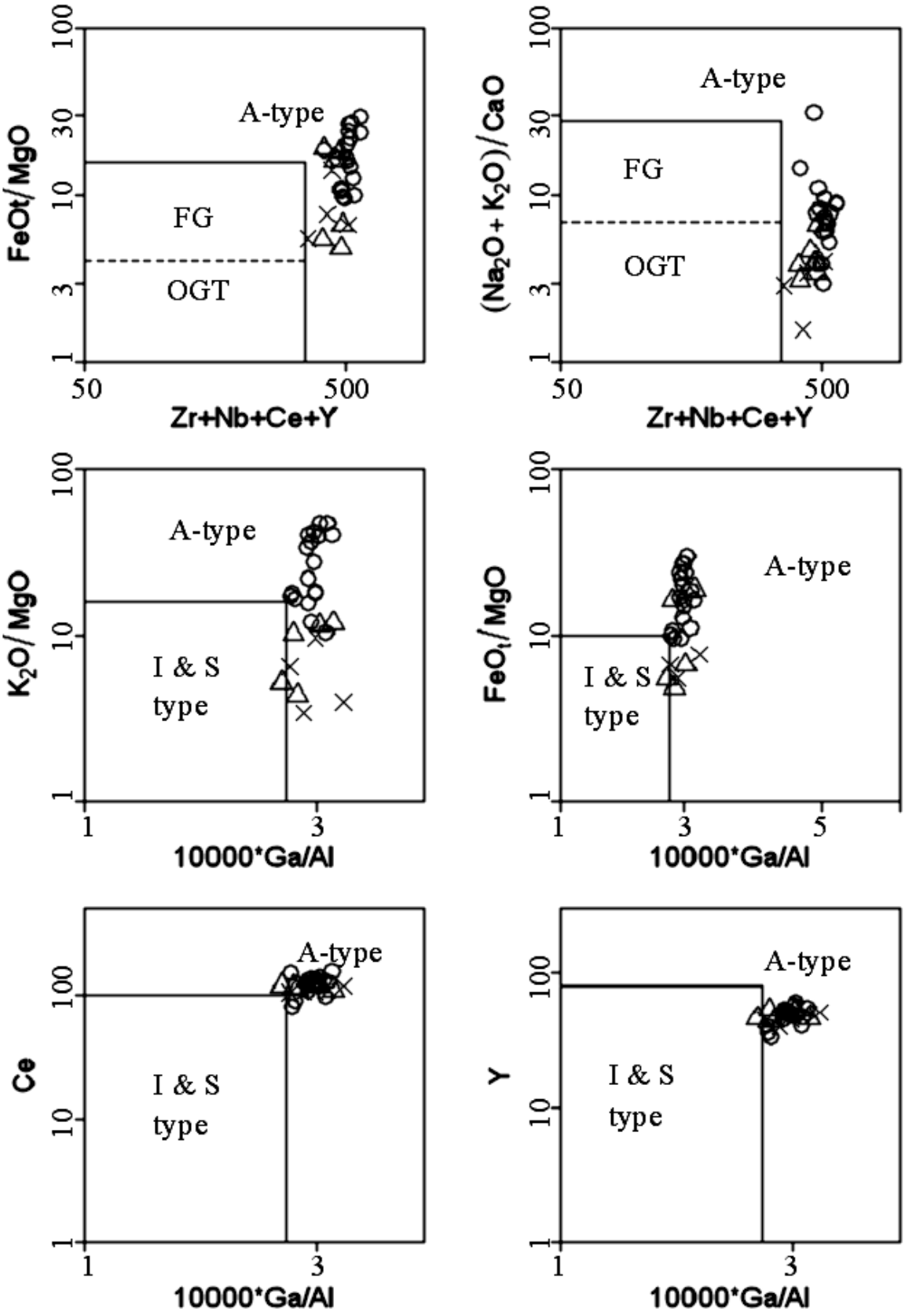

Figure 4.10: Discrimination diagrams after Whalen et al. (1987). Note that rhyolite, trachydacite and diorite are plot into A-type field.

○ Rhyolite △ Trachy-dacite ✕ Diorite

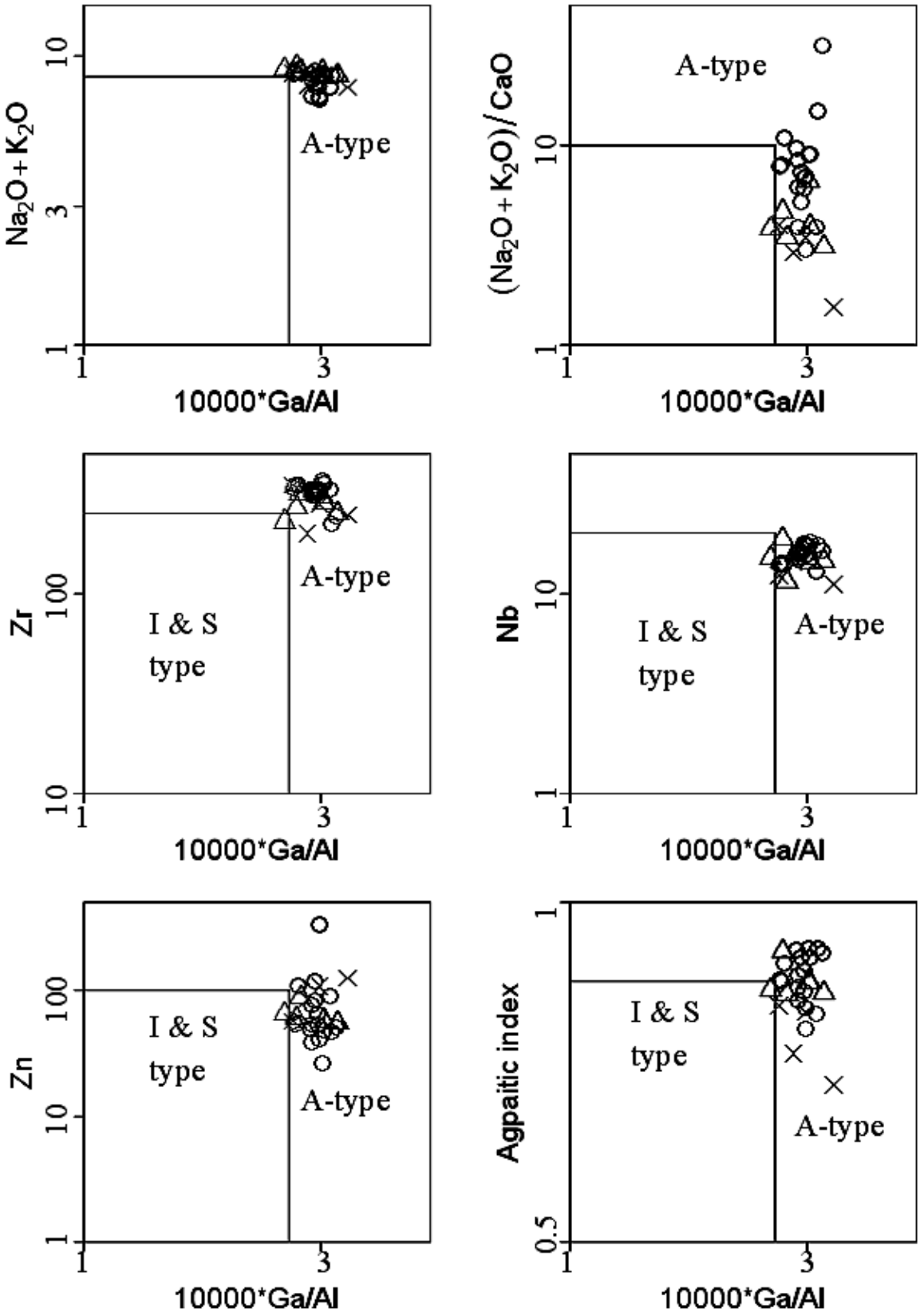

Figure 4.10, continued: Discrimination diagrams after Whalen et al. (1987). Note that rhyolite, trachydacite and diorite are plot into A-type field

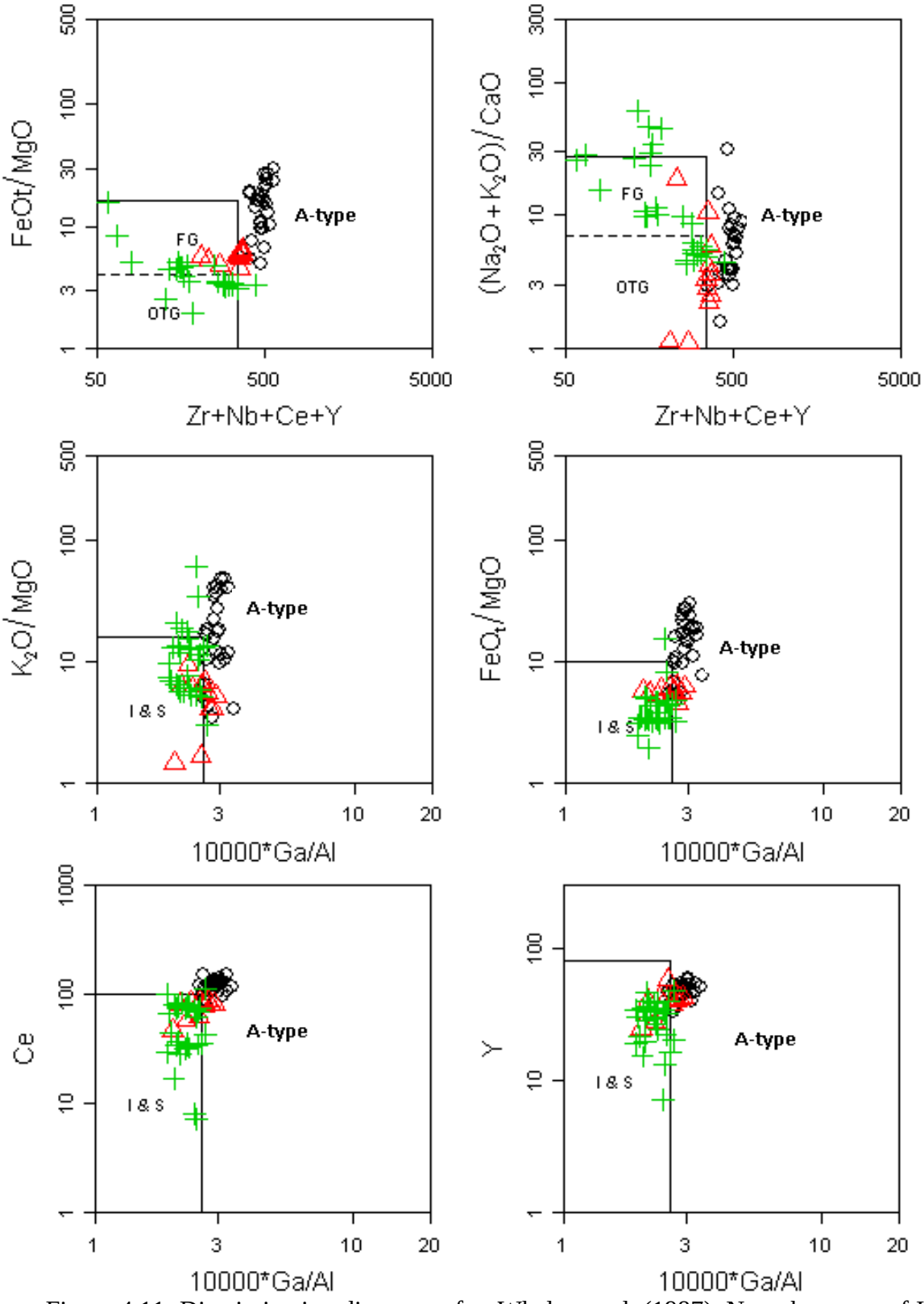

Figure 4.11: Discrimination diagrams after Whalen et al. (1987). Note that most of I and S type from Peninsular plotted in FG-OTG and I-S field while A-type Ramunia are plotted in A-type field

A-type Ramunia

I-type Peninsular Malaysia

S-type Peninsular Malaysia

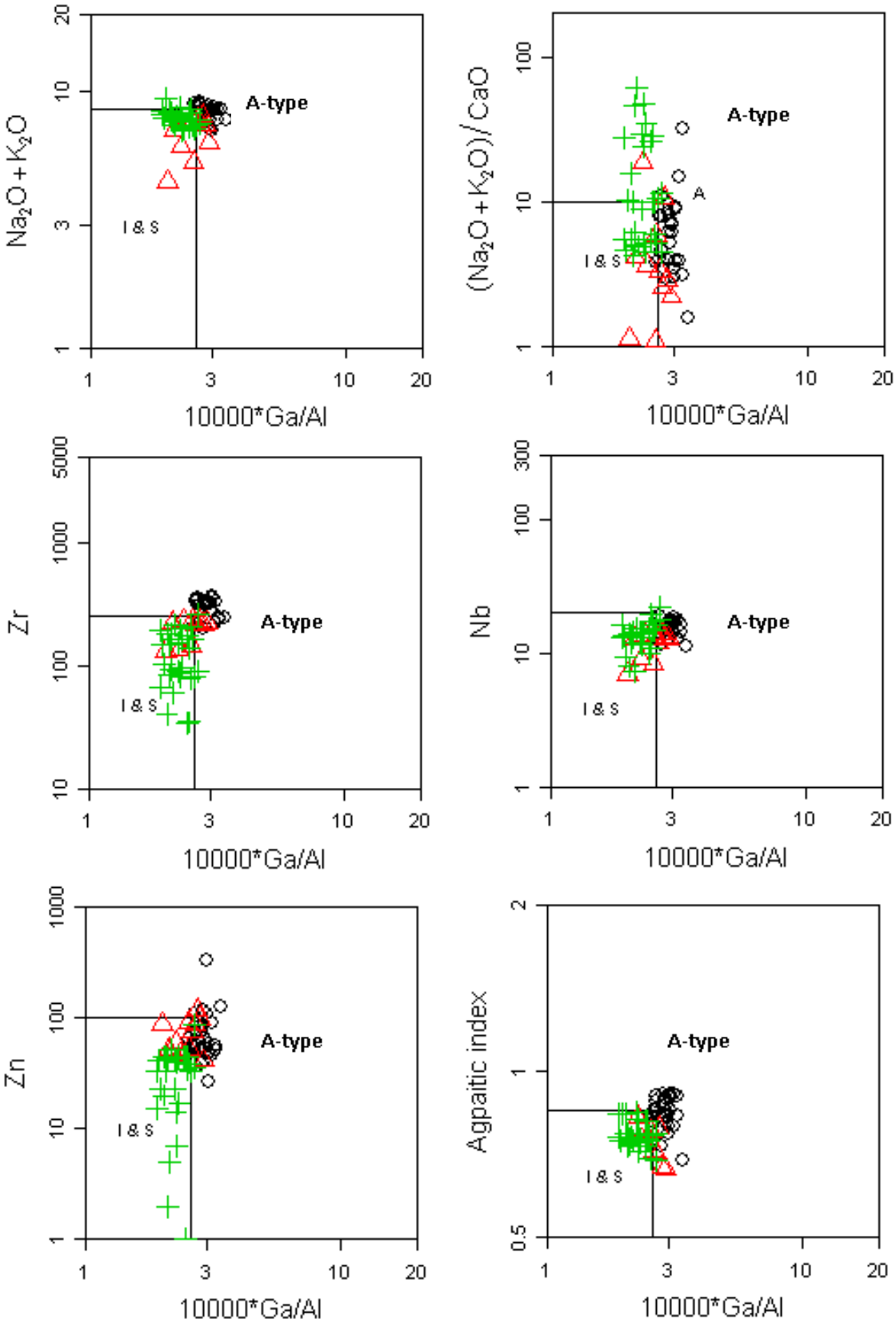

Figure 4.11,continued: Discrimination diagrams after Whalen et al. (1987). Note that most of I and S type from Peninsular plotted in FG-OTG and I-S field while A-type Ramunia are plotted in A-type field

A-type Ramunia I-type Peninsular Malaysia S-type Peninsular Malaysia

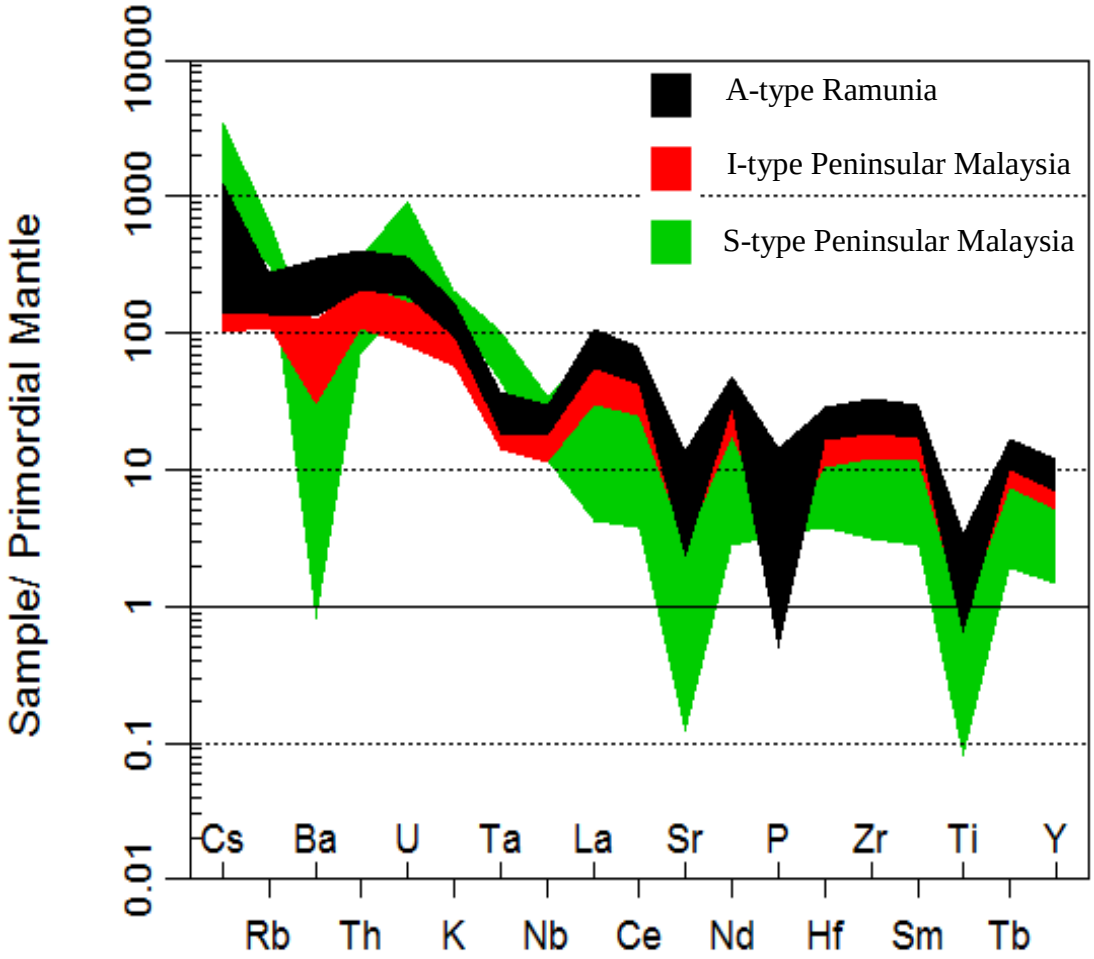

Figure 4.12a: Multi-elements spidergram normalized to Primitive Mantle after Sun and Mcdonough. (1989). Note the S-type shows very different pattern compared to the A-type Ramunia. Although generally I-type shows similar pattern with A-type however the I-type shows clear Barium negative anomaly (Ba) which is not seen in A-type Ramunia. [data for S-type taken from Nyien (2014) and I-type from Syai (2012)]

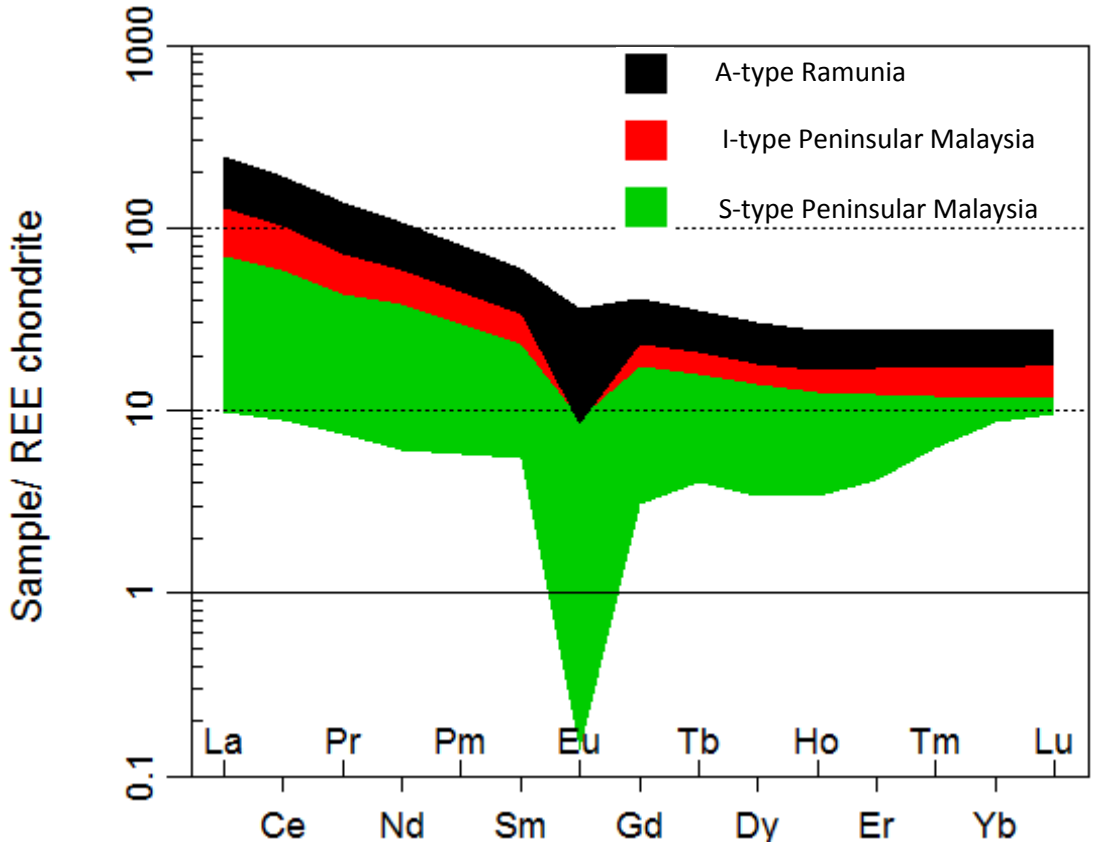

Figure 4.12b: Rare earth elements (REE) spidergram normalized to chondrite after Boynton 1984. Note the A-type Ramunia yield higher REE content compared to typical I and S type from Peninsular Malaysia. [data for S-type taken from Nyien (2014) and I-type from Syai (2012)]

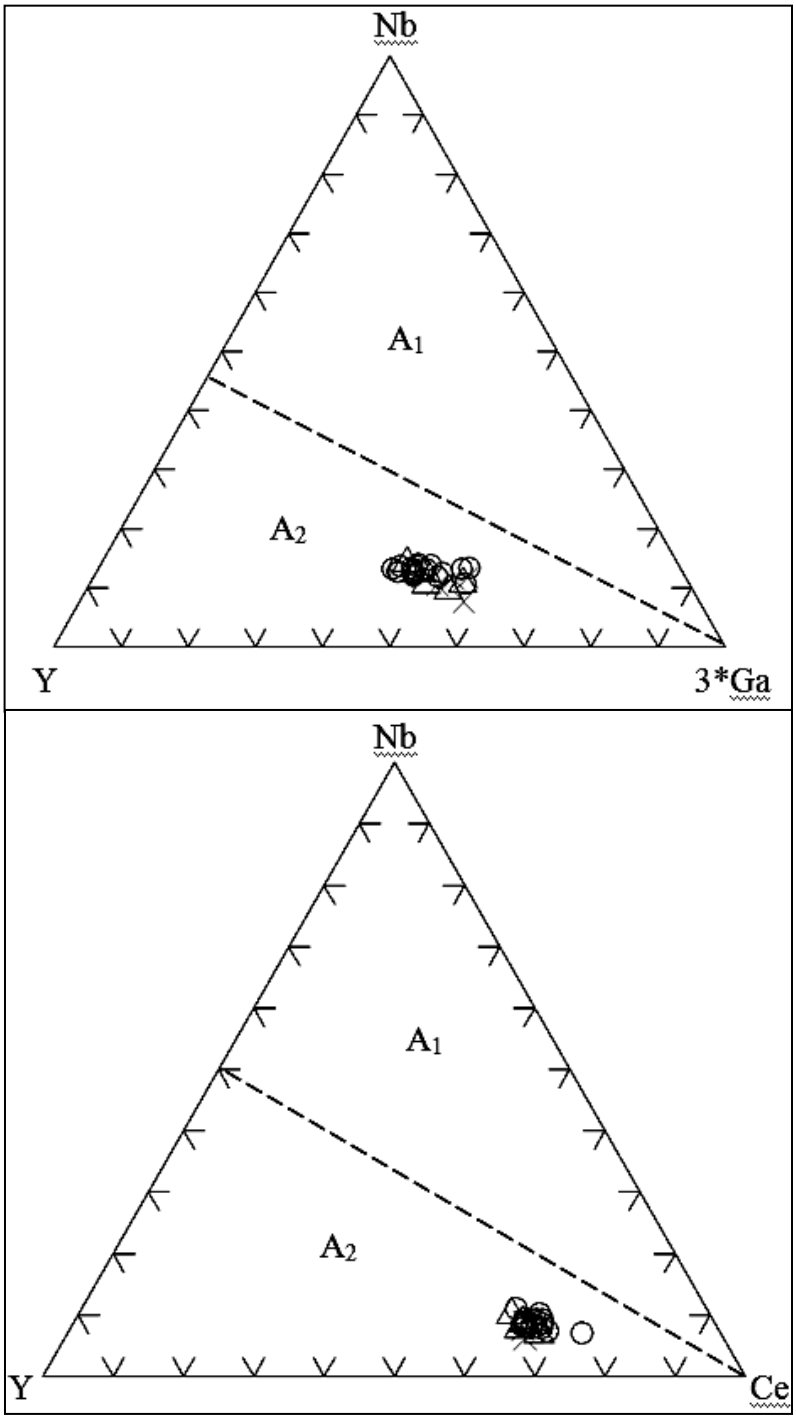

Figure 4.13: Discrimination diagrams of a) Nb – Y – 3Ga and b) Nb – Y – Ce shows all Igneous rocks from Teluk Ramunia are plotted within A2 field. The A1 and A2 are the subdivision of the A-type magma by Eby (1992). A1 = intraplate magmatism, A2 = Post Collision

Comparison on the multi-elements and REE spidergrams clearly shows that the A-type Ramunia have very distinct chemical characteristic compared to the I and S-type from Peninsular Malaysia (Figure 4.12a and 4.12b) [data for S-type taken from Nyien (2014) and I-type from Syai (2012)]

4.7 Zircon (Zr) Saturation Thermometry

In felsic and intermediate rock the occurrence of zircon, monazite and apatite are common. Zircon, monazite and apatite saturation temperatures can be calculated from whole rock geochemical analysis to estimate the temperature of the magma forming rhyolite, trachyte and diorite by using the experimental model of Watson and Harrison (1983), Watson and Harrison (1984), Harrison and Watson (1984), Montel (1993) and Piccolli et al. (1999).

4.8 Magma thermometry

In felsic and intermediate igneous rocks, the occurrence of zircon as accessory mineral is common. Zircon or zirconium saturation temperature can be calculated from whole rock geochemical analysis to estimate the minimum temperature of the magma source that formed the magmatic rocks using the experimental models of Watson and Harrison (1983) and Watson and Harrison (1984).

Zircon saturation temperatures were calculated using this following equation from Watson and Harrison (1983) :

$$T\ Zr\ saturation\ ^{o}C = \frac{12900}{ln\ (D_{Zr}) + 3.8 + 0.85\ (M - 1)} - 273.15$$

Where D_{Zr} is the ratio of 497644 to the concentration of Zr in ppm and M is the cationic ratio [(100 Na + K + 2Ca)/(Al.Si)] of the whole rock concentration of SiO_2, Al_2O_3, Na_2O, K_2O and CaO.

$$= \frac{100\ Na + K + 2Ca}{Al.Si}$$

Results of the Zr saturation temperatures calculations including with error for Ramunia A-type, Eastern Belt I-type and Western belt S-type are shown in Table 4.2.

4.9 Discussion On Saturation Thermometry And Estimated Depth Of Melting Of A-Type Ramunia Source

The estimation of magma temperatures for A-type, I-type and S-type are given in Table 2. Figure 4.14 shows most of the samples from Ramunia are more than $750^{O}C$. It is clearly shows that A-type yield higher Zr saturation temperature (826 ± 5 °C) compared to the I-type (775±3°C) and S-type (763 ± 4 °C). and are comparable with temperature estimates for A-type magmas elsewhere [e.g. Guimares, et al., 2005 (869 ^{O}C) , 1996; Jiang et al ($820^{O}C$), 2005 and Zhao, 2008 (880 ^{O}C); Yang, S.Y., 2012 (~ $810^{O}C$]. High saturation temperatures shown by Ramunia A-type can be explained by high heat which contributed by the upper mantle contemporaneous with crust extension. Given an average magma temperature of 826 ^{o}C (from the magma saturation estimates) and a surface temperature of 30 ^{o}C (since Indochina was located near the equator in the Middle Triassic, see Metcalfe, 2013) and assuming a geothermal gradient of 35/km such as might be expected in a stretched back arc. Considering the average lithostatic pressure gradient is 0.027 GPa/km (e.g. Christensen and Mooney, 1995) with Beta factor of 2, the magma source that formed

A-type Ramunia might have been generated at a depth of about 11.8km at lithostatic pressure of about 0.32 GPa or 3.2 kbar .

Table 4.2: Table shows zircon saturation temperature for A-type, I-type and S-type rock (data for I and S rocks are taken from Cobbing et al.,

A(Ramunia)	I (eastern)	S(Western)
TZr.sat.C	TZr.sat.C	TZr.sat.C
852.6	777.9	786.9
851.3	784.6	778.8
834.8	767.5	773.9
831.9	784.2	795.8
843	775.7	744.1
856.7	771.5	770.4
844	775.2	762.2
839.1	773.7	780.1
832.7	797.7	771.8
830.8	779.2	749.8
843.1	745.1	716.9
828.2	828.1	738.4
815.5	752.1	778.7
836.5	746.2	782.8
847.9	773.9	778.8
851.2	767.3	793.8
846.6	754.3	746.6
851.7	825.4	789.2
810.7	774.1	763.1
784.7	793	779.6
795.6	779.8	726.4
807.9	755.6	712.6
787.6	760.5	775.9
831.3	754.1	754
759.7	761.9	785.5
779.4	756.3	761.5
805.2	812.8	713.3
	790.6	727.6
	809.7	776.7
	779.3	791.3
	775.7	750.4
	780.8	735.3
	783.4	770.1
	762	792.3
	770.9	766
	774.8	761.5
	770.9	764.7
	761.2	783.7
	764.8	788.8
	761.9	772.2

Mean	826	775	763
Std. Deviation	26.06	21.66	24.70
Std. Error	5	3	4
T.Zr °C	826 ± 5 °C	775±3°C	763 ± 4 °C

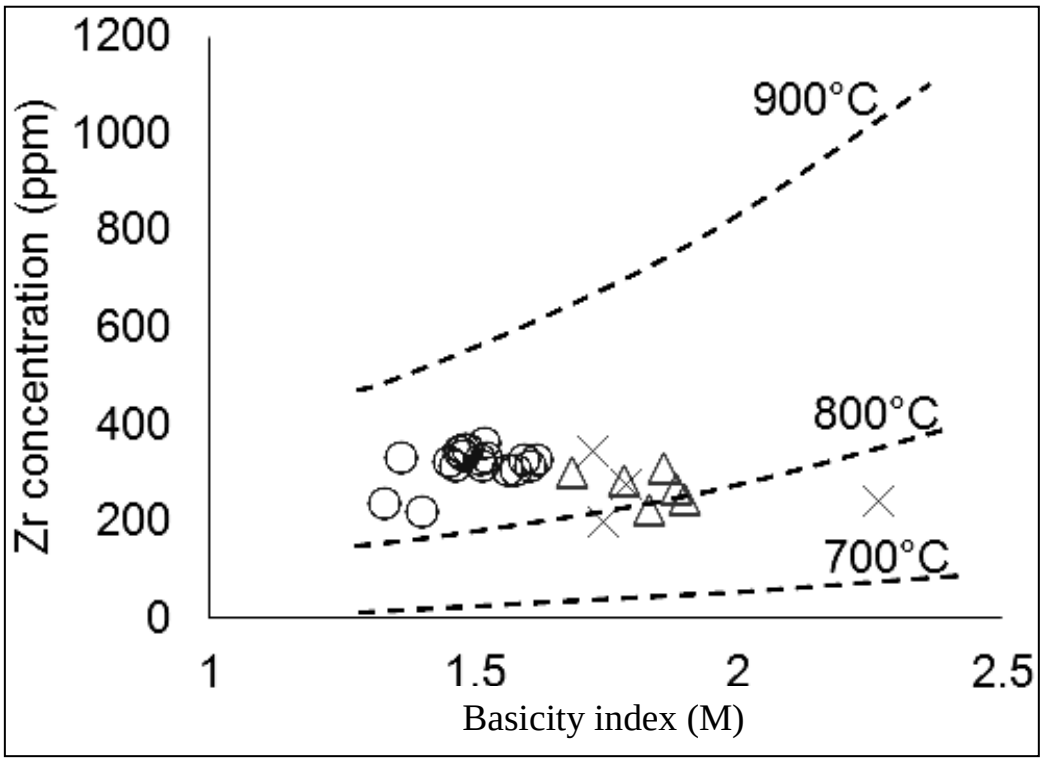

Figure 4.14: Zr concentration in ppm versus melt basicity index (M) after Watson and Harrison 1983. Note that most of the rocks from Ramunia are plot roughly around $800^{O}C$ – $850^{O}C$. The dashed temperature lines are constructed using Zr saturation (in ppm) with fixed temperature using equation Zr sat. = $497644/D_{Zr}$

4.10 Magmatic Evolution

Petrographically there is no evident in term of texturally as well as compositional for magma mixing and contamination in rhyolite, trachydacite and diorite from Ramunia. There is no occurrence of mafic rock composition within study area. Most major and trace elements (ex. Al_2O_3,CaO,MgO,TiO_2,Sr,Th and etc.) show increasing and decreasing with increasing SiO_2 content reflect the significant of fractional crystallization processes (eg. K-feldpsar + plagioclase + biotite + hornblende and minor apatite) during the evolution of the magma suite. However the considerable scattered variation in the Harker major and trace elements plots is attributed to the porphyritic /phenocryst nature of the volcanic rocks (Cox et al., 1979; Wilson, 1994). Na_2O shows scattered pattern with increasing SiO_2 to some

extent which could be explained by chlorite partly replacing feldspars and biotite by late hydrothermal alteration (Dargahi et al., 2010). However the effect of the hydrothermal alteration appears to be less important or negligible or less important on most trace elements because of their immobile nature. Scattered variation in the major and trace Harker diagrams is attributed to the porphyritic/phenocryst nature of the volcanic rocks (Cox et al. 1979; Wilson, 1994). Rhyolite, trachydacite and diorite exhibits J-shape on Rb/Sr vs SiO_2 diagram **(**Figure 4.15**)** which suggest the feldspar crystallization play major role in magmatic evolution. All rocks shows negative anomalies in Sr and Eu are shown in Figure 4.7 and Figure 4.9 which implicate major role of plagioclase and k-feldpsar in fractional crystallization during magma evolution. Large ion lithophile (LIL) modelling shows that k-feldspar play important role rather than plagioclase during magmatic evolution (Figure 4.16a, 4.16b and 4.17).

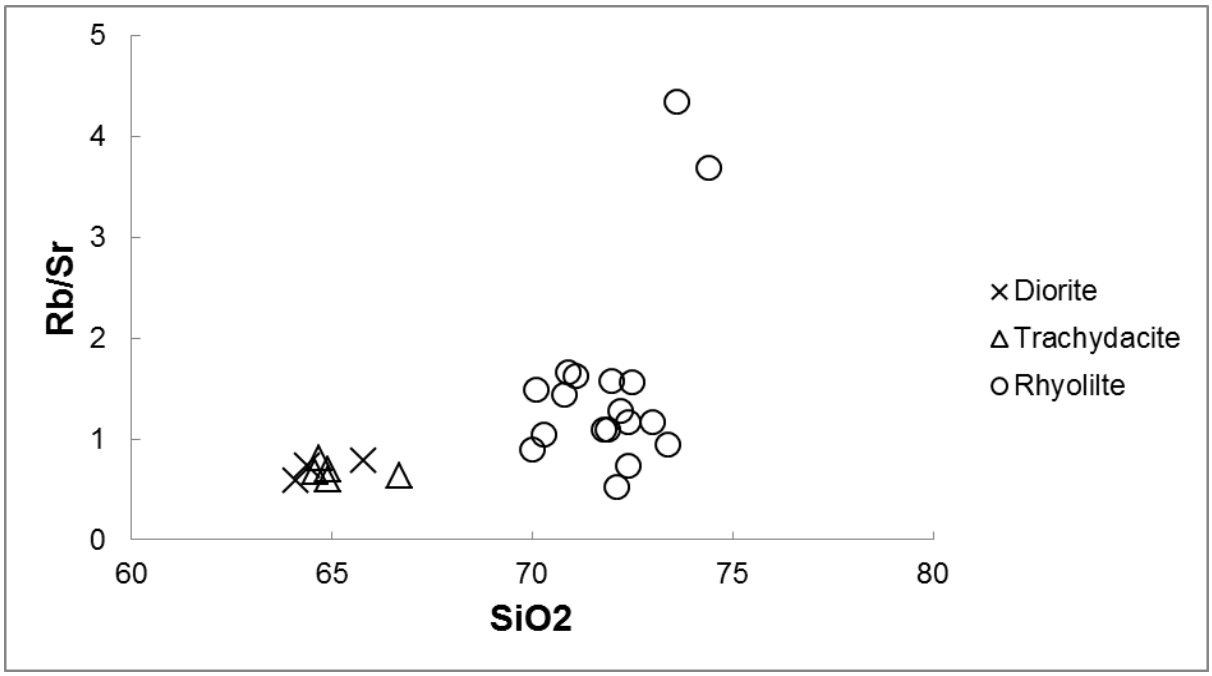

Figure 4.15: Rb/Sr vs SiO2 diagram show J shape which implicate the feldspar crystallization play major role in magmatic evolution.

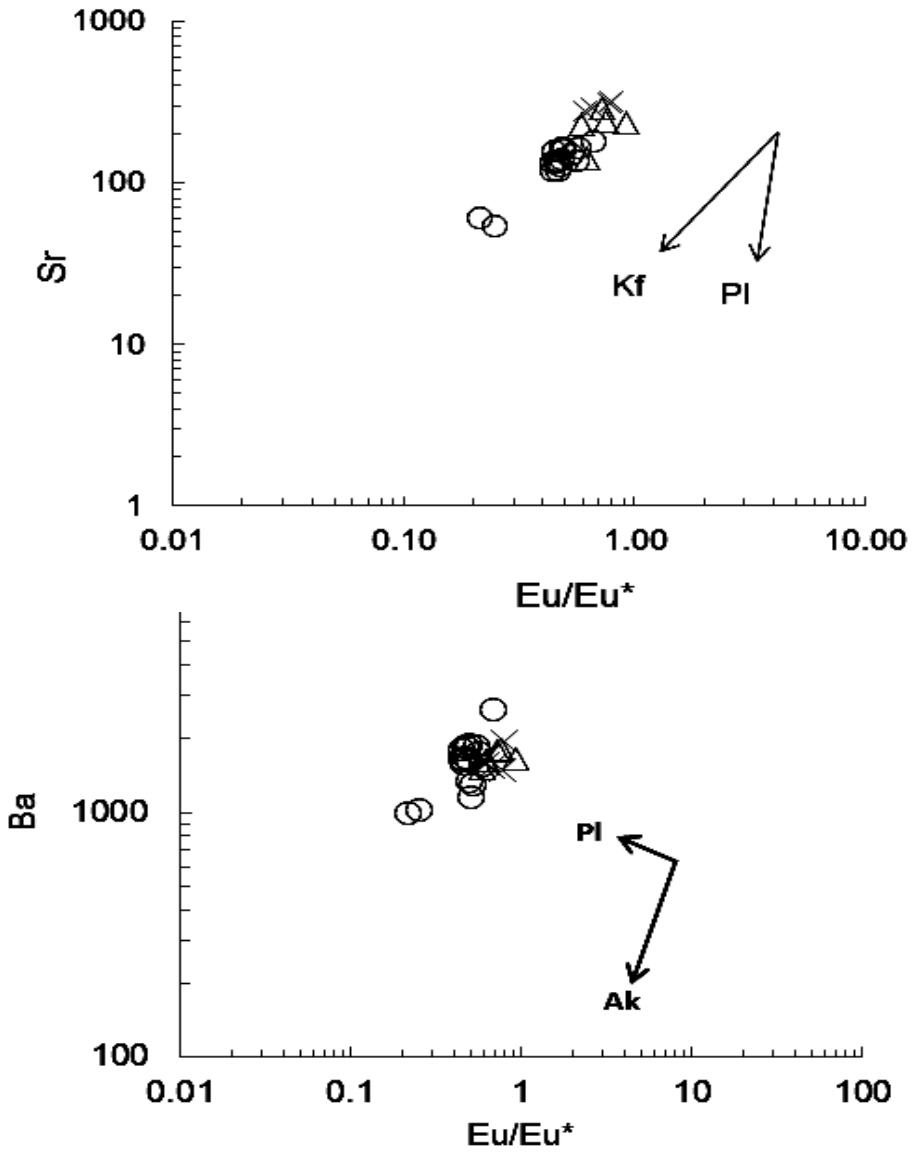

Figure 4.16 : Diagram of (a) Ba versus Eu/Eu*, Sr vs Eu/Eu* after Eby (1990). From diagram above it is clearly shows that fractionation of plagioclase play control in magma evolution. Eu/Eu* = $Eu_N/\sqrt{Gd_N} \times Sm_N$ where N is the subscript for chondrite normalized after Boynton 1984.

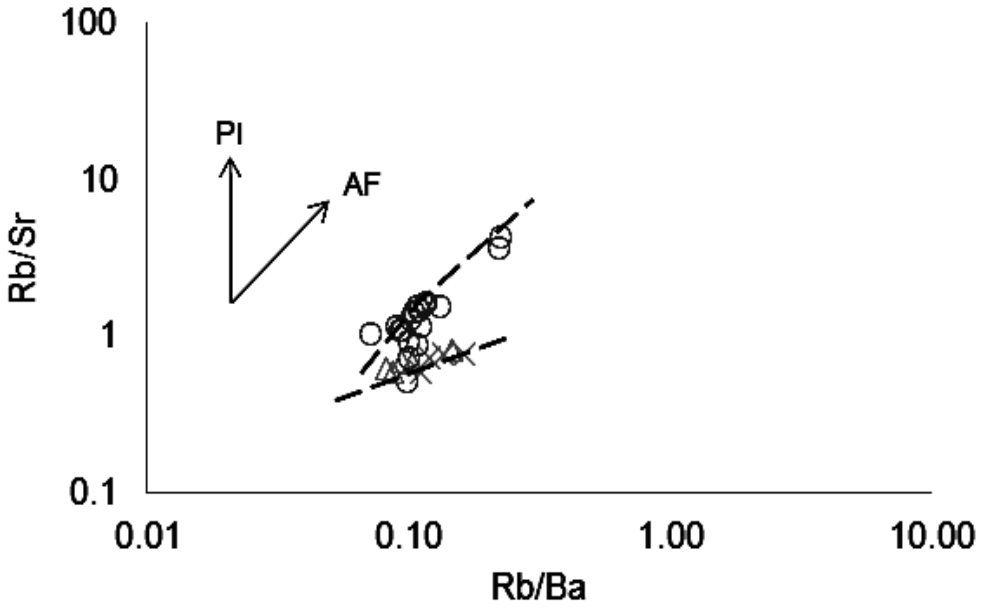

Figure 4.17: Large ion lithophile element modelling for rhyolite, trachydacite and diorite from Ramunia (e.g. Guimaraes et al., 2005). Vector arrow trends shows K-feldspar play dominant role in the melt during fractionation. Note that the rhyolite has different trend with trachydacite and diorite with implicate that they are non-comagmatic.

Low Ca/Sr ratio (<70) yield by all rocks from study area indicate that the plagioclase extraction from the melt on the earlier fractionation process was limited (e.g. Landenberger and Collins, 1992) which support the less important of plagioclase compared to K-feldspar. But note must be taken that plagioclase also play role during evolution although it is less important compared to k-feldspar. This is because of low Ca/Sr (<70) value which indicating that the removal of plagioclase in earlier fractionation phase was limited (e.g. Landenberger and Collins, 1996). Other than that, they have high ratio of K/Rb and low ratio of Rb/Ba suggests that the enrichment of K reflects melting rather than biotite (Landenberger and Collins.1996; Jiang et al., 2005). Negative spike in Ta and Nb might as well implicate involvement of crustal materials in the source or crustal contamination (Xu et al., 1984; Chazot and Bertrand, 1995). From multi-element variation spider-diagram and REE spidergram, each rocks shows difference in enrichment/depletion. The difference in

RE enrichment/depletion, occurrence of magma mingling, 5.4% SiO_2 gap and different vector trend shown in Figure 4.15 suggest that the rhyolite is not co-magmatic with the trachydacite and diorite. The high concentration of Th and U reflects the more evolved igneous rocks most probably because the high content of zircon in felsic compared to mafic. In fact the fractional crystallization and assimilation occurred contemporaneously which can be clearly seen in Th/Nb vs Zr of Nicolae and Saccani (2003**)** where the vector plot point toward Assimilation-Fractional crystallization (Figure 4.8**)** although the trends is not very clear. The high content of HREE in all rocks from study area reflects the magma source contained pyroxenes (Mark, 1999). High concentration of HFSE (ex. Zr, Nb, Hf and Ta) coupled with high HREE content implies that they were derived from dehydrated source rocks (Collins et al., 1982; Whalen et al., 1987). The source rock was possibly dehydrated during thermal event but not to a point where it is geochemically depleted (Landenberger and Collins, 1996: Zhao et al., 1997).

4.11 Source rocks potential of the A-type rocks from study area

A-type rocks especially granite have been extensively studied since it was introduced by Loiselle and Wones (1979) because of the unusual geochemical characteristic and tectonic setting (e.g. Collins et al., 1982; Clemens et al., 1986; Whalen et al., 1987; Creaser et al., 1991; King et al., 1997; Bonin, 2007). There are several mechanisms or genetic model proposed to explain the generation of A-type rocks; a) fractional crystallization of alkaline basaltic magma (Loiselle and Wones, 1979; Turner et al., 1992); b) partial melting of relatively refractory lower crustal granulites (Collins et al., 1982; Whalen et al., 1987); c) partial melting coupled with high temperature of tonalite and granodiorite (Creaser et al., 1991; King et al., 1997; Patino Douce, 1997) and d) partial

melting of charnockite or dry rocks which are non-depleted melt, anhydrous, alkali feldspar rich granulitic protolith (Landenberger and Collins, 1996; Jiang et al., 2005).

The fractionation of basalt is a certain mechanism that can create the A-type magmas (Loiselle and Wones, 1979; Turner et al., 1992). One of the closest example from Padthaway Ridge in South Australia where the A-type granite is formed from basaltic parental magma (Turner et al., 1992). Fractionation of the alkaline basaltic magmas is not suitable mechanism to form the Ramunia A-type because one of the dyke has been analyse for major and trace elements and they shows much lower REE content (and high field strength elements content compared to the rhyolite , trachydacite and diorite. In order for the dyke (mafic dyke) to be suitable source for Ramuni rocks, they must contain higher REE content and also HFSE. Other than that, the volume of mafic composition which represent only by mafic dyke is insufficient to form the large volume of Ramunia volcanic. High content of high field strength element (HFSE) yield by Ramunia A-type rocks (>300ppm for Zr+Nb+Ce+Y) need a basaltic precursor that contained highly enriched in HFSE elements (e.x King et al., 2001; Chen, Y., 2013). However spidergrams shows that mafic dyke within Teluk Ramunia contained low amount of REE and HFSE content (Figure 4.18). There is no isotopic age yet to be done on the dolerite dyke within the study area. However Ghani et al., (in manuscript) has determine the age of most dyke from Eastern Peninsular and they age are varies from 178.5 Ma – 124 Ma (Jurassic – Cretaceous). Volcanic from Ramunia has been dated about 238$\pm$2 Ma (Middle Triassic) and shows that the Ramunia rocks are plausibly not related to the dolerite dyke from the studyarea.

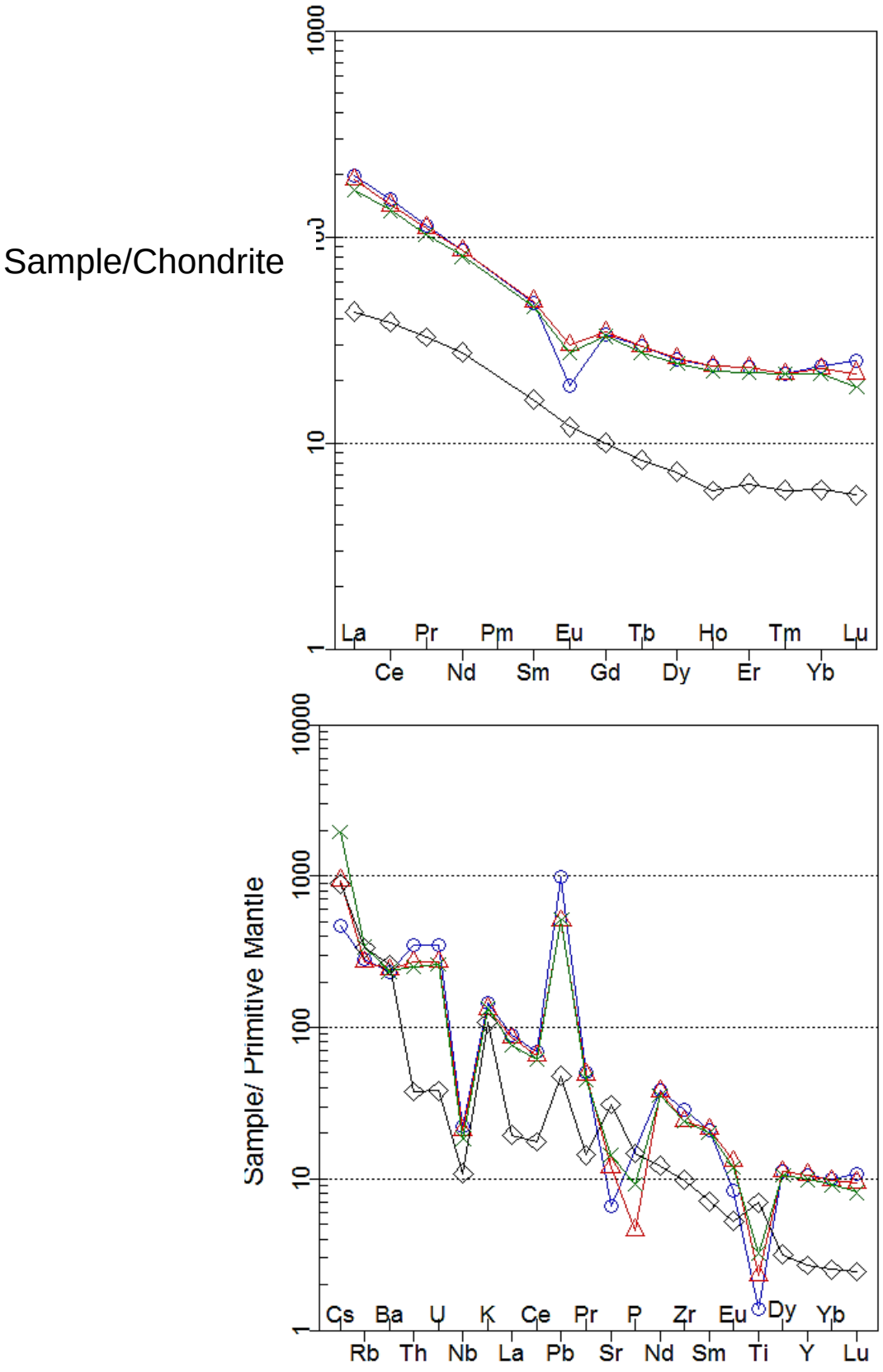

Figure 4.18: Spidergrams of a) Rare Earth Element. b) Multi-

Element of Ramunia volcanic with basalt

Some other possible mechanism that can formed the A-type magma are the granulite and charnockite (e.x. Landenberger and Collins, 1996; Jiang et al., 2005; Zhao et al., 2008;Yang et. al., 2012). Granulite is a high grade metamorphic rocks which form at high pressure and temperature where the protoliths may originated from igneous and sedimentary source. The mineralogy of the granulite are strongly influenced by the type of the protolith bulk chemistry. As for charnockite, latest definition by Frost (2011) define that charnockite is an orthopyroxene – (or fayalite) bearing granite rocks that is clearly of origin or that is present as orthogneiss within a granulite terrain. In term of mineralogy the granulite of igneous origin have the same mineral characteristic with charnockite. Most of the rocks from Teluk Ramunia shows metaluminous to weakly peraluminous characteristic based on Aluminium saturation index (Figure 4.4a and Figure 4.4b). It shows that these rocks are formed by igneous source and parametamorphic granulite is not a suitable to become A-type Ramunia source. Charnockite and mafic granulite is not suitable to be source because they mainly contained garnet which indicates high pressure formation. The lowest SiO_2 shown by Ramunia A-type is 58.7% which mean that the source must be mafic – intermediate composition. However mafic – intermediate granulite (data taken from Turner et al., 1992) shows low average content of High field strength elements (Zr+Nb+Hf+Y = 167) compared to Ramunia A-type (Zr+Nb+Hf+Y = 378) which strongly suggest that mafic-intermediate granulite is not suitable to be the source of Ramunia A-type plus there is no occurrence of granulite nearby the study area to confirmed the granulite to be the Ramunia A-type source rock.

Patino Douce (1997) has done experimental melt on tonalite and granodiorite at low pressure (4kbar) melting. From the experimental melt it is possible that partial melting low pressure (4kbar) of dehydrated metaluminous tonalite and granodiorite might produce the metaluminous – weakly peraluminous Ramunia A-type volcanic because they shows

similar geochemical characteristic (e.x high Fe_{total} and high HFSE). Most of the Ramunia rocks shows slightly higher value of Ga/Al which can be explained by the low pressure residual assemblages dominated by the plagioclase. This is because partition coefficient value of Ga/Al for plagioclase is only about ~0.5 and occurrence of clinopyroxene will give higher Ga/Al values. The high Fetot/MgO shown by granodiorite is generally same due to crystallization of orthopyroxene during melting at low pressure. The flat HREE trend shows by all ramunia rocks may indicate presence of orthopyroxene (Mark, 1999). The flat HREE pattern shows that there is absence of garnet in the source which indicate low pressure melting. Patino also demonstrate that A-type rocks can be formed by low pressure melting of tonalite and granodiorite. This was supported by the low melting depth (Partial melting of the tonalite-granodiorite may explained the contemporaneously of formed of A-type and I-type from Eastern belt of Peninsular Malaysia.

4.12 Integrated petrogenetic model in forming the A-type magma/rocks

Melting experiment of tonalite and granodiorite has been demonstrated by Patino Douce (1997) and shows that shallow dehydration melting of granitoids that contain hornblende and biotite can generates metaluminous A-type which is same with metaluminous Ramunia A-type. Writer try to do a cartoon model showing the formation of the Ramunia A-type rocks. In early discussion, it has been mentioned that there are extension process occur on the lower crust during Middle Triassic due to oceanic slab roll back. Due to the lower crust extension, the mafic under-plating derived mantle will intrude and ascending toward the middle crust and the heat from the mantle input will definitely partial melt the country rock at the middle crust (in this case tonalite and granodiorite). The pressure of the crust has been decrease due to the extension process which make the low pressure incongruent melting possible. The partial melting of the granodiorite will create

the A-type magma and formed the Ramunia volcanic suite when they crystallized. The dominant occurrence of I-type rocks on the Eastern Belt Peninsular Malaysia can be explained from different types of rock derivation.

4.13 Implication of the A-type magma on Peninsular Malaysia geotectonic during Anisian (Early Middle Triassic)

The magmatism on the eastern belt of Peninsular Malaysia are believed to be related to the volcanic arc during Permo-Triassic. The plutonism and volcanism are trending parallel to the Bentong Raub Suture Zone which is north-south trend. These magmatism are generally formed during the subduction of the Paleo-Tethys oceanic crust beneath the Indochina block (Mitchell, 1977; Hutchison, 1989a; Metcalfe, 2000b; Sevastjanova 2011; Searle, 2012). The occurrence of the A-type rocks including rhyolite, trachydacite and diorite from Ramunia give the implication that there is extensional setting occurred during middle Triassic as pink rhyolite from Ramunia is dated 238$\pm$2 Ma (Oliver et al, 2013) with U-Pb dating. As mentioned before, the A-type are believed to be closely related with the within plate or post collisional setting. Discrimination diagrams of Pearce (1984) shows that most of the rhyolite, trachydacite and diorite from Ramunia were plotted in the intersection of volcanic arc and within plate tectonic setting. Pearce (1996) has modified the discrimination diagram of Rb vs (Y+Nb) suggesting that the igneous rocks that are plotted within the intersection of volcanic arc and within plate should be classified as post-collisional setting (Figure 4.19**)**. Other ternary discrimination diagrams from Eby (1992) also support this post-collisional setting. However these tectonic events fail to explain the occurrence of the A-type rocks because of the volcanic arc still occurring during Middle Triassic (~238 $\pm$ 2 Ma) thus exclude the suitability of within plate and post-collisional tectonic setting. Tectonic discrimination triangular plot of Harris et al. (1986) and high ratio

of Nb/Ta (Green, 1993) shows that A-type rocks from Ramunia are related to the volcanic arc setting. However the occurrences of the A-type rocks give strong implication of crustal extension.

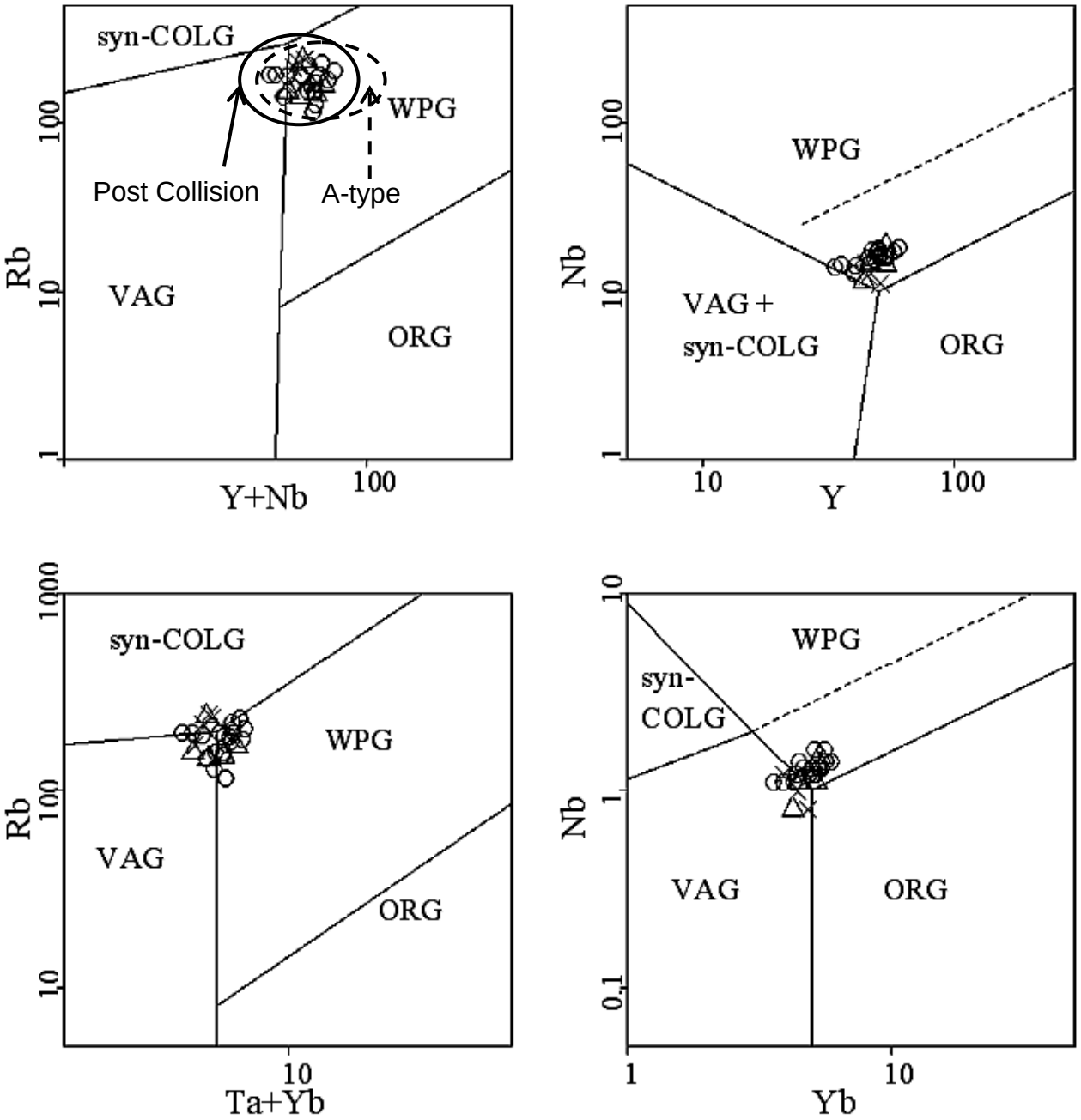

Figure 4.19: Tectonic discrimination diagram of (a) Rb versus (Y+Nb), (b) Rb versus (Ta+Yb), (c) Nb versus Y and (d) Ta versus Yb after Pearce et al. (1984). The continuous circle line indicate post collision field (Pearce, 1996) and the dashed circle shows A-type magma (Whalen et al., 1987).

A suitable explanation is needed to explain the occurrence of the extension during the volcanic arc regime. Ryall 1982 has done cross section magnetic studies on the central belt of Malay Peninsula and there is evidence of thinning crust mainly on the central belt (Figure 4.20**)**. Most of the Ramunia rocks show the characteristic of high-K calc alkaline which reflects the geodynamic environment of transitional regimes from subduction to continental collision (Barbarin 1999) which may implicate late subduction (no collision yet). Therefore the most suitable to explain the crustal extensional during volcanic arc setting is oceanic slab-roll back which is consistent with the geochemical characteristic of the Ramunia rocks and the age (Anisian). The slab-roll back will pull the crust to be pulled because of the high density of the oceanic crust. This geodynamic model is the most suitable tectonic environment to explain the occurrence of the A-type magma which is related to the crust extensional. During the continuous of the subduction process, the angle of the subducted oceanic plate will get more which will trigger lower crust extension and back arc basin extension (Bourgois et al.,1996; Sample and Reid, 2003). The value of slab dip (α_d) will be increase as the age of the subduction becoming older (Lallemand et al., 2005). The Upwelling athenosphere mantle flow is the main factor that will increase the slab dip angle (α_d) **(**Figure 4.21b**)** (Heuret and Lallemand, 2005 ; Lallemand et al.,, 2005). The schematic cross section illustrating the oceanic subduction leading to slab-rollback is shown in Figure 4.21a**.** The Semantan basin on the central belt could be formed during the back-arc extension. There is evident of volcanic rocks interbedded with the metasediment there (Jaafar 1976) which is juxtaposition with the crustal extension during slab-roll back. However there are not enough evidence to support this assumption because the basin can also formed during post-collision which is not related to the volcanic arc. The A-type magma that formed all rock from study area must be generate during the process of the

slab-roll back which eventually will lead to the opening of the back-arc basin (Semantan Basin?). After the lower crust has start extend, the underplated mantle derived mafic magma will intrude into the exposed extension area and melt the lower crustal rocks. Melting of the lower crust and middle crust will lead to the generation of the I–type and A-type rocks found on the eastern belt of Peninsular Malaysia. The slab-roll back related extension is consistent with the tectonic proposed by Oliver et al (2013). In the paper he proposed the oceanic slab-roll back of Paleo-tethys plate based on the U-Pb zircon age younging from eastern to western across the Peninsular Malaysia.

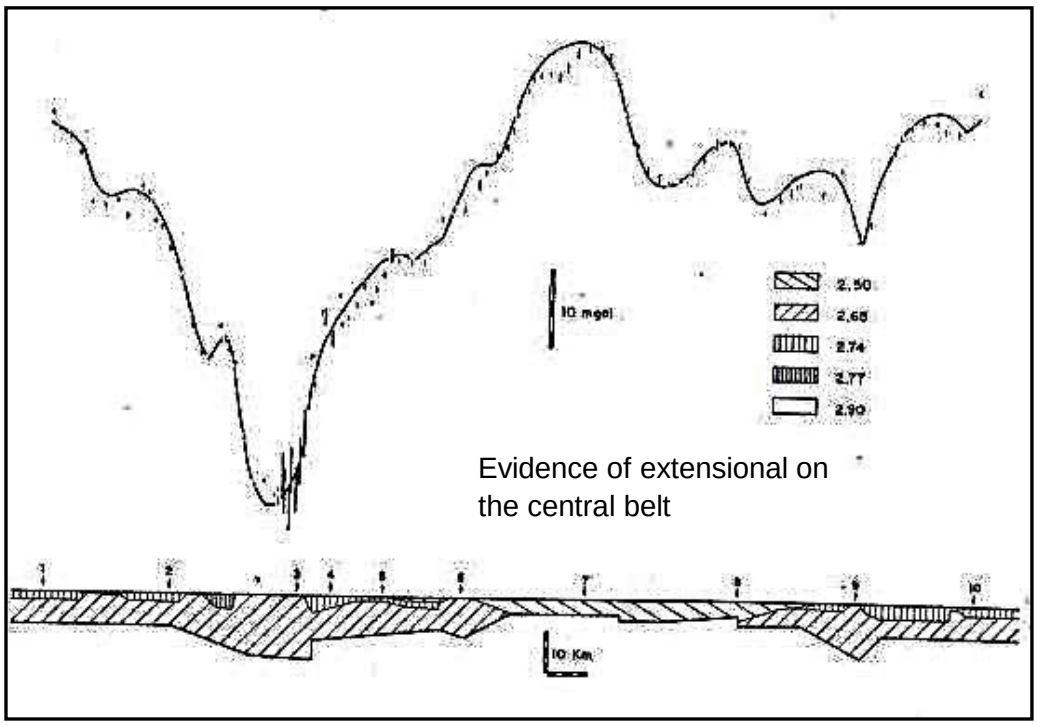

Figure 4.20: Diagram of observed Bouguer gravity and calculated gravity for a model with no granite in the Central back. However there is no Moho Line shown. Gravity profile supports the occurrence of extensional in Peninsular Malaysia (profile taken from Ryall, 1982).

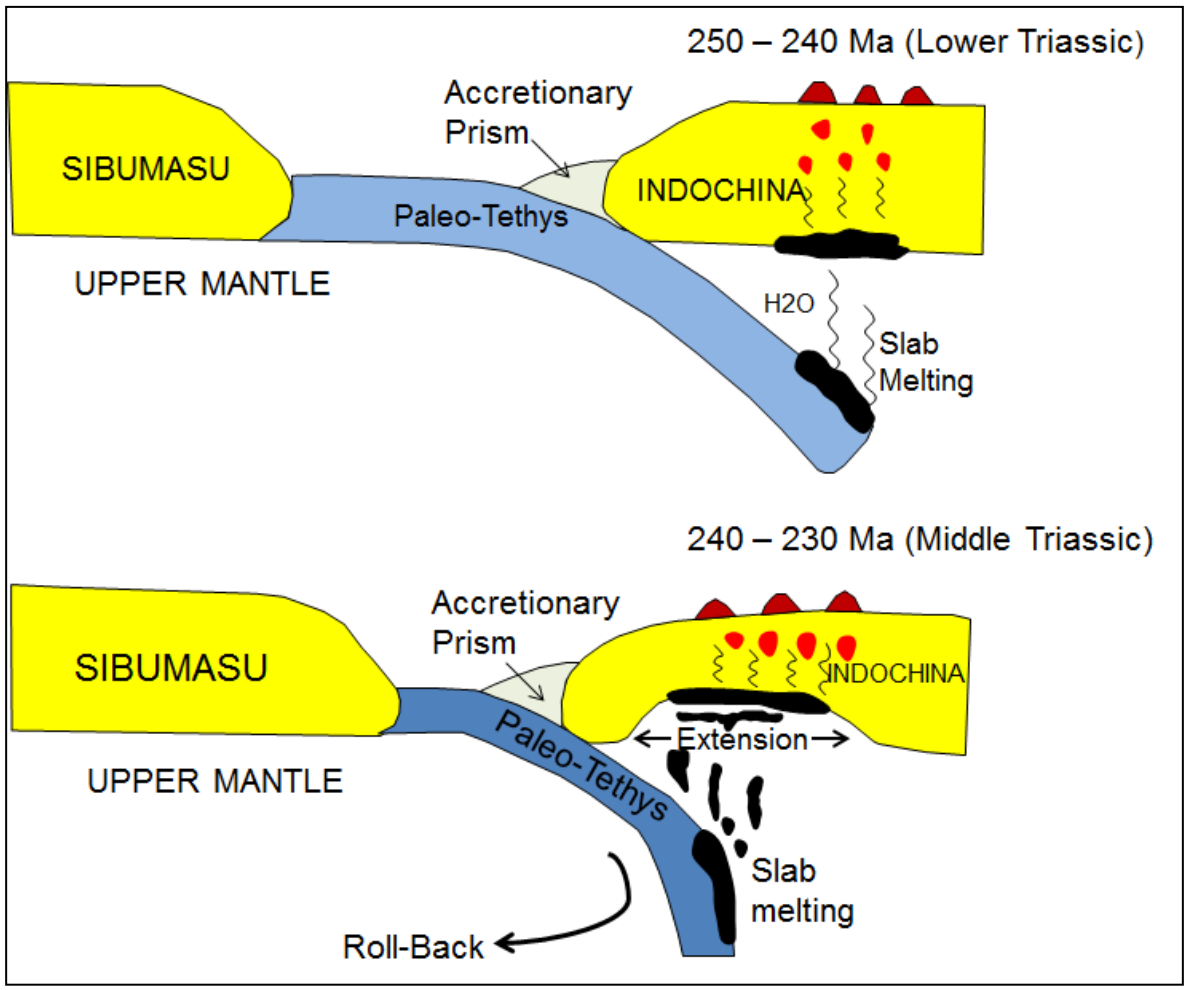

Figure 4.21 a: Schematic diagram showing the tectonic setting for (a) partial melt of the subducted Paleo-tethys ocean which lead to the generation of the volcanic arc magmatism. (b) the angle of subducted oceanic crust is getting steeper because of the slab-roll back which then will lead to crustal extension. During this time the A-type magma will generate from the partial melting of the dry rock at lower crust.

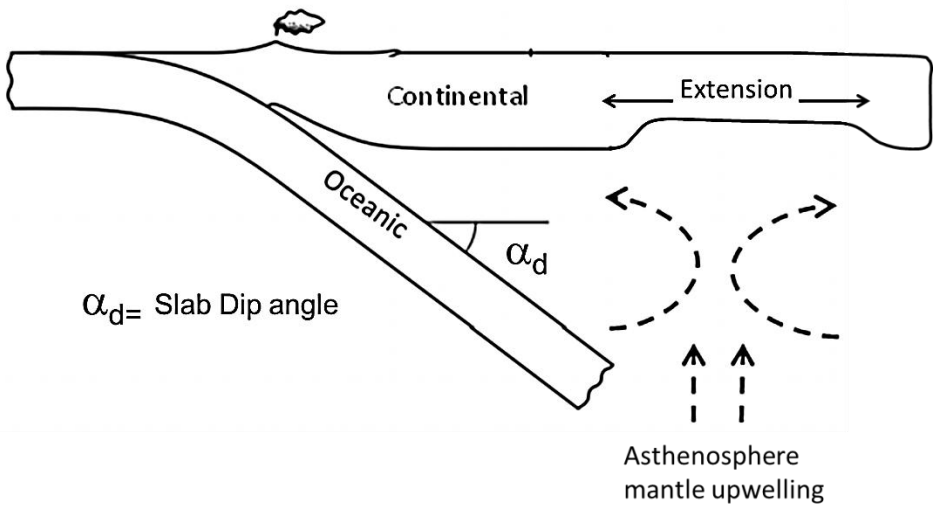

Figure 4.21 b: Diagram illustrating the relation between Slab dip angle and asthenospheric flow force.

5.0 CONCLUSION

5.1 Introduction

In this chapter the writer will summarize all the conclusions that has been proposed in each chapter before. New interpretation can be made based on the geological finding from the study area.

5.2 Summary of conclusion on volcanism within Teluk Ramunia

Based on fieldwork, petrographic and geochemistry study there are 3 types of igneous rocks found within study area which located in Teluk Ramunia. They are diorite, rhyolite and trachydacite. Occurrence of the micro-granophyric texture in all rocks shows that they are emplaced at sub-volcanic environment. Rhyolite is formed from the same source rock with trachydacite and diorite. However based on geochemistry charateristic the rhyolite is not formed within same magmatic pulse with trachydacite and diorite. The rhyolite, trachydacite and diorite strongly shows A-type characteristic thus the writer suggest it can be called A- type Ramunia. Lower pressure partial melting of tonalite-granodiorite are highly possible to be the source rock of A-type Ramunia. Most of the studies on A-type rocks indicate that they are very close related with the extensional magmatism. Based on published U-Pb zircon isotope dating on rhyolite from study area (238$\pm$2 Ma from Oliver et al., 2013), the extensional is occurred during volcanic arc setting thus exclude the mechanism of delamination and slab-break off. The most suitable to explain the occurrence of A-type Ramunia during volcanic arc setting is the effect of pull-slab or slab-roll back during subduction process. Based on previous studies, slab roll back of subducted oceanic crust is the main factor that lead to mantle lithosphere extension under

the central belt of Peninsular Malaysia. The slab roll back geodynamic setting on Peninsular Malaysia has been proposed by Oliver et al. (2013).

5.3 New Finding

From petrographic and geochemistry analysis the writer found the occurrence of A-type rocks which consists of rhyolite, trachydacite and diorite. The A-type always give implication of magmatism due to crustal extension and high temperature magma sources with average Zr saturation temperature of 826 ^{O}C. Most of the A-type from other places are closely related of either post-collision or intraplate magmatism. In the case of the A-type rocks found within study area, the age of the volcanic rock is rather old to be correlate with the post-collision magmatism (Middle Triassic). It is because the main tectonic event that occurred during the time is volcanic arc setting. Therefore the best tectonic to explain the formation of the A-type is slab roll back or slab pull back that can lead to crustal extension.

5.4 Future work suggestion.

The rock samples that have been analysed in this research are only constrained on the south eastern part of peninsular Malaysia. It is very important to study on the occurrence of the A-type rocks which are likely can be found on the eastern belt of Peninsular Malaysia. Studies on the volcanic rocks on the eastern belt of Peninsular Malaysia should be more thoroughly especially on geochemistry characteristic. Previous study has shown that there are association of the I-type and A-type rocks in volcanic arc settings. They are more likely to have formed within the back arc regime. The occurrence of A-type might give important clue about the contribution of slab roll back, slab delamination or slab break-off which can lead to extension of the lithospheric mantle and will continue to the back-arc deformation. Other than that, the Peninsular Malaysia igneous

rocks have lack of isotopical data which make it hard to interpret the relationship between the mantel output with the crustal contribution. In case of Ramunia volcanics, it is crucial to do isotopical studies as the A-type magma have strong relation to the mantle contribution, crustal contamination and fractional crystallization.

REFERENCES

Anderson, J.L., & Cullers, R.L., (1978). Geochemistry and evolution of the Wolf River Batholith, a late Precambrian rapakivi massif in northern Wisconsin. *Precambrian Research, 7,* 287-324.

Anderson, J.L., (1983). Proterozoic anorogenic granite plutonism of North America. *Geological Society of America Memoir, 161,* 133-154.

Aw, P.C., (1967). Ignimbrite in central Kelantan, Malaya. *Geological Magazine, 104,* 13 – 17.

Barbarin, B., (1999). A review of the relationship between granitoid types, their origins and their geodynamic environments. *Lithos, 46,* 605 – 626.

Batchelor, R.A., & Bowder, P. (1985). Petrogenetic interpretation of granitoid rock using multicationic parameters. *Chemical Geology, 48,* 43 – 55.

Bean J.H. (1972). Geology, petrography and mineral resources of Pulau Tioman, Pahang. *Geological Survey of Malaysia Map Bulletin, 5,* 92.

Bird, P. (1979). Continental Delamination and Colorado Plateau. *Journal of Geophysical Research, 13,* 7561 – 7571.

Bohlen, S.R., & Lindsley, D.H. (1987). Thermometry and barometry of igneous and metamorphic rocks. *Annual Review of Earth and Planetary Sciences, 15,* 397 – 420.

Bonin, B., 2007. A-type granites and related rocks: evolution of a concept, problems and prospects. *Lithos, 97,* 1–29.

Bonin, B., & Giret, A. (1985). Contrasting roles of rock-forming minerals in alkaline ring-complexes. *Journal of African Earth Sciences, 3,* 41 – 49.

Bourgois, J., Lagabrielle, Y., Moigne L., J., Urbina, O., Janin M.C.H., & Beuzart, P. (1993). Preliminary results of a field study of the Taitao Peninsula. *Geology, 24(8),* 723 – 726.

Boynton, W.V. (1984). Cosmochemistry Of The Rare Earth Elements : Meteorite Studies. In: Henderson, P (Eds.), Rare Earth Element Geochemistry. *Elsevier, Amsterdam,* 63 – 114.

Bradford, E.F. (1965). *The geology and mineral resources of the Gunong Jerai area, Kedah, Malaya*. (Unpublished doctoral dissertation). University of London, London.

Bradford, E.F. (1972). *The geology and mineral resources of the Gunong Jerai area, Kedah.*(*pp.* 242). Geol. Soc. Malaysia Dis. Memoir.

Chakraborty, K.R. (1995). Genting Sempah volcanic Complex: Genetic implication for the Main Range granite. *Geological Society of Malaysia Warta Geologi, 21,* 216 – 217.

Chappell, B.W., & White, A.J.R. (1987). The importance of residual source material (restite) in granite petrogenesis. *Journal of Petrology, 28,* 1111 – 1138.

Chazot, G., & Bertrand, H. (1995). Genesis of silicic magmas during Tertiary Continental rifting in Yemen. *Lithos, 36,* 69 – 84.

Chen, Y., Zhu, D.C., Zhao, Z.D., Meng, F.Y., Wang, Q., Santosh, M., Wang, L.Q., Dong, G.C., Mo, X.X. (2013). Slab breakoff triggered ca. 113 Ma magmatism around Xainza area of the Lhasa Terrane, Tibet. Gondwana Research (in manuscript).

Chong, F.S., & Yong, S.K. (1967). Report on the Jengka Triangle, Pahang 1966. Proceedings of the Senior Officers Departmental Conference 1966. *Geol. Survey Dept. West Malaysia*.

Christensen, N., & Mooney, W. (1995). Seismic velocity structure and composition of the continental crust: A global view. *Journal of Geophysical Research, 100(6),* 9761 – 9788.

Chung, S.K. (1959). Geological inverstigation of pulau Bunting. Geological Survey Department, West Malaysia, (Unpubl. Report GS 58/F/031/33).

Chung, S.L., Chu, M.F., Zhang, Y., Xie, Y., Lo. C.H., Lee, T.Y., Lan, C.Y., Li, X., Zhang, Q., &Wang, Y. (2005). Tibetan tectonic evolution inferred from spatial and temporal variations in post collisional magmatism. *Earth Science Reviews, 68,* 173 – 196.

Clarke, D. B. (1992). Granitoid Rocks. Topics in the Earth Sciences 7. Ta–Sn–Li mineralization in the granite at Beauvoir, French Massif Chapman & Hall, (pp. 283). London.

Clemens, J.D., Holloway, J.R., & White, A.J.R. (1986). Origin of an A-type granite : experimental constraints. *American Mineralogist, 71,* 317 – 324.

Clemens, J.D., & Wall, V.J. (1981). Crystalization and Origin of some peraluminous (S-type) granitic magmas. *Canadian Mineral. 19,* 111- 132.

Cobbing, E.J., Pitfield, P.E.J., derbyShire, D.P.F. & MAlliCk, D.I.J. (1992). The Granites of the Southeast Asian Tin Belt. *Overseas Memoirs of the British Geological Survey,* 10.

Collins, W.J., Beams, S.D., White, A.J.R., & Chappell, B.W. (1982). Nature and origin of A-type granites with particular reference to Southeastern Australia. *Cont. to Min. and Petrology, 80,* 189 – 200.

Cox, K.G., Bell, J.D., & Pankhurst R.J., (1979). *The Interpretation of Igneous Rocks* (pp. 450). Allen and Unwin, London.

Creaser, R. A., Price, R. C. & Wormald, R. J. (1991). A-type granites revisited: assessment of a residual-source model. *Geology, 19,* 163 - 166.

Creaser, R.A., Price, R.C., & Wormald, R.J. (1991). A-type granites revisited : assessment of a residual-source model. *Geology, 19,* 163 – 166.

Cullers, R.L., Koch, R.J. & Bickford, M.E. (1981). Chemical evolution of magmas in the proterozoic terrane of the St. Francois Mountains, southeastern Missouri 2. Trace element data. *Journal of Geophysical Research, 86(10),* 388 – 10,401.

Dargahi, S., Arvin,. M., Pan, Y., & Babaei, A. (2010). Petrogenesis of post-collisional A-type granitoids from the Urumieh – Dokhtar magmatic assemblage, Southwestern Kerman, Iran : Constraints on the Arabian – Eurasian continental collision. *Lithos, 115,* 190 – 204.

Davies, J., & Von Blanckenburg, R., (1995). Slab breakoff: a model for syncollisional magmatism and tectonics in the Alps. *Tectonics, 14,* 120 - 131.

Eby, G.N., 1990. The A-type Granitoids, A Review of Their Occurrence And Chemical Characteristics and Speculations On Their Petrogenesis. *Lithos, 26,* 115 – 134.

Eby, G.N., 1992. Chemical Subdivision Of the A-type granitoids : Petrogenetic and Tectonic Implications. *Geology, 20,* 641 – 644.

Eggleton, R.A., & Banfield, J.F. (1985). The alteration of granitic biotite to chlorite. *American Mineralogist, 70,* 902 – 910.

Ellison, A.J, & Hess, P.C. (1986). Solution behavior of +4 cations in high silica melts: Petrologic and geochemical implications. *Contribution to Mineralogy and Petrology, 94,* 353 – 351.

Fenn, P.M., (1977), The nucleation and growth of alkali feldspars from hydrous melts. *Canadian Mineralogist, 15,* 135–161.

Ferrari, C. (2004). Slab detachment control on mafic volcanic pulse and mantle heterogeneity in central Mexico. *Geology, 32,* 77 – 80.

Fitch, F.H., 1952. The geology and mineral resources of the neighbourhood of Kuantan, Pahang. *Geologcial Survey Department Federation of Malaya Memoir, 6,* 144.

Foley, S., Tiepolo, M., & Vannucci, R. (2002). Growth of early continental crust controlled by melting of amphibolite in subduction zones. *Nature, 417(6891),* 837 – 840.

Frost ,C.D., & Frost, B.R. (2011). On ferroan (A-type) granitoids: their compositional variability and modes of origin. *Journal of Petrology, 52(1),* 39 – 53.

Frost, B.R., Barnes, C.G., Collins, W.J, Arculus, R.J., Ellis, D.J., & Frost, C.D. (2001). A Geochemical Classification for Granitic Rocks. *Journal of Petrology, 42,* 2033 – 2048.

Frost. B.R., & Frost, C.D. 2008. On Charnockites. *Gondwana Research, 13,* 30 – 44.

George B. Morgan & David London. (2012). Process of granophyre crystallization in the Long Mountain Granite, southern Oklahoma. *Geological Society of America Bulletin, 124(7 – 8),* 1251 – 1261.

Gerya, T.V., Yuen, D.A., & Maresch, W.V., 2004. Thermomechanical modelling of slab detachment. *Earth and Planetary Science Letters, 226,* 101 – 116.

Ghani A.A. (2006). Batuan volkanik dari Pulau Tinggi dan Pulau Sibu Johor. *Geol. Soc. Malaysia Bull, 52,* 63 – 66.

Ghani A.A., (2009). Volcanism. In Hutchison, C.S., Tan, D.N.K. (Eds). *Geology of Peninsular Malaysia* (pp. 197 – 210). Malaysia: University of Malaya and Geological Society of Malaysia.

Ghani, A.A., & Singh N. (2005). Petrology and Geochemistry of the Sempah Volcanic Complex, Peninsular Malaysia. *Geological Society of Malaysia Bulletin, 51,* 103 – 121.

Gobbett, D.J. (1965a). The Lower Palaeozoic rocks of Kuala Lumpur. *Federation Museums Journal, 9,* 67 – 79.

Green, T.H. (1995). Significance of Nb/Ta as an indicator of geochemical processes in the crust-mantle system. *Chemical Geology, 120,* 347 – 359.

Grubb, P. L. C. (1962). Serpentinization and chrysotile formation in the Matheson ultrabasic belt northern Ontario. *Economic Geology, 57,* 1228-1246.

Grubb, P. L. C. (1972). Origin of Darling Range Bauxites; A Reply. *Economic Geology, 67(7),* 981 – 982.

Grubb, P.L.C. (1965). Undersaturated potassic lavas and hypabassal intrusives in North Johor. *Geological Magazine, 102,* 338 – 346.

Grubb, P.L.C. (1968). Geology and Bauxite Deposits of the Pengerang Area, Southeast Johor. *Geol. Soc. Malaysia Dis. Memoir, 14,* 125.

Guimaraes, I.P., Filho, A.F.D.S., Melol, S.C., & Macambira, M.B. (2005). Petrogenesis of A-type Granitoids from the Alto Moxoto and Alto Pajeu Terranes of the Borborema Province, NE Brazil: Constraints from Geochemistry and Isotopic Composition. *Gondwana Research, 8(3),* 347 – 362.

Han B.F., Wang S.G., Jahn, B.M, Hong D.W., Kagami H., Sun, Y.L. 1997. Depleted-mantle source for the Ulungur River A-type granites from North Xinjiang, China: geochemistry and Nd–Sr isotopic evidence, and implications for Phanerozoic crustal growth. *Chemical Geology, 138,* 135–159.

Harris, N.B.W., Pearce, J.A., Tindle, A.G., 1986, Geochemical characteristics of collision-zone magmatism. In: Coward, M.P. and Reis, A.C. (Eds.), Collision tectonics. *Spec. Publ. Geol. Soc. 19,* 67 – 81.

Harrison, T.M., & Watson, E.B. (1984). The behavior of apatite during crustal anatexis: Equilibrium and kinetic considerations. *Geochim. Cosmochim. Acta, 48,* 1467-1477.

Heli, Ming Xing Ling, Cong Ying Li, Hong Zhang, Whng Ding, Xiao Yong Yang, Wei Ming Fan, Yi Liang Li & Wei Dong Sun. (2011). A-type granite belts of two chemical subgroups in central eastern China: Indication of Ridge Subduction. *Lithos, 150,* 26 – 36.

Heuret, A., Lallemand, S. (2005). Plate motions, slab dynamics and back-arc deformation Physics of the Earth and Planetary Interiors, *149,* 31–51.

Hirose, K. (1997). Melting experiments on lherzolite KLB-1 under hydrous conditions and generation of high-magnesian andesitic melts. *Geology, 25,* 42–44.

Hirose, K., & Kawamoto, T. (1995). Hydrous partial melting of lherzolite at 1 GPa: the effect of H2O on the genesis of basaltic magmas. *Earth and Planetary Science Letters, 133,* 463–473.

Hutchison C.S. (1973a). Volcanic activity. In Gobbett D.J., Hutchison C.S. (Eds.), *Geology Of The Malay Peninsula* (pp. 177 – 213). Canada : Wiley-Interscience.

Hutchison C.S., & Tan D.N.K. (2009). Geology of Peninsular Malaysia. U. Malaya and Geol. Soc. Malaysia, 479.

Hutchison, C.S. (1989a). Geological Evolution of South East Asian. *Oxford monographs on geology and geophysics* (pp. 368). Clarendon Press. Oxford

I.Temizel & M. Arslan. (2008). Petrology and Geochemistry of Tertiary volcani rocks from the Ikizce (Ordu) area, NE Turkey : Implications for the evolution of the eastern Pontide paleo-magmatic arc. *J. Asian Earth Sciences, 31,* 439 – 463.

Irvine, T.M., Baragar, W.R., 1971. A guide to the chemical classification of common volcanic rocks. Canad. *J. Earth Sci, 8,* 523 – 548.

Ismail, M.A., Azman A. Ghani, Rozi M. Umor, & Noran A.S. (2003). Geochemistry and Petrology of Volcanic Rock from Tioman Island. *Geological Society of Malaysia Bulletin, 46,* 415 – 419.

J. Bourgois, H. Martin, Y. Lagabrielle, J. Le Moigne & J. Frutos Jara. (1996). Subduction erosion related to spreading-ridge subduction: Taitao peninsula (Chile margin triple junction area). *Geology, 24,* 723 - 726.

Jaafar, A. (1976). The geology and mineral resources of the Karak and Temerloh areas, Pahang. *Geol. Soc. Malaysia Dis. Memoir*, 15.

Jiang Y.H, Ling, H.F., Jiang, S.Y., Fan, H.H., Shen W.Z., & Ni P. (2005). Petrogenesis of a Late Jurassic Peraluminous Volcanic Complex and its High Mg, Potassic, Quenched Enclaves at Xiangshan, Southeast China. *Jour. Petrology, 6,* 1121–1154.

Keith, T.E.C., Muffler, L.K.P., & Creamer, M. (1968). Hydrothermal epidote formed in the Salton Sea geothermal system, California. *America Min. 53,* 1635 – 1644.

King, P.L., Chappell, B.W., Allen, C.M., & White, A.J.R. (2001). Are A-type granites the high temperature felsic granites? Evidence from fractionated granites of the Wangrah Suite. *Australian Journal of Earth Sciences, 48,* 501 – 514.

King, P.L., White, A.J.R. Chappell, B.W., & Allen, C.M. (1997). Characterization and origin of aluminous A-types granites from Lachlan Fold Belt, Southeastern A-types granites from Lachlan Fold Belt, Southeastern Australia. *Journal of Petrology, 38,* 145 – 170.

Klimm, K., Holtz, F., & King, P.L. (2008). Fractionation vs. magma mixing in the Wangrah Suite A-type granites, Lachlan Fold Belt, Australia: experimental constraints. *Lithos, 102,* 415 – 434.

Landenberger, B., & Collins, W.J. (1996). Derivation of A-type granite from a dehydrated charnockitic lower crust: evidence from chaelundi complex, Eastern Austalia. *Journal of Petrology, 35,* 145 – 170.

Lallemand, S., A. Heuret, & D. Boutelier (2005), On the relationships between slab dip, back-arc stress, upper plate absolute motion, and crustal nature in subduction zones, Geochem. Geophys. Geosyst, *6,* 1 – 18.

Le Bas M. J., Le Maitre R. W., Streckeisen A. & Zanettin B., 1986. A chemical classification of volcanic rocks based on the total alkali-silica diagram. *J. Petrology, 27,* 745 – 750.

Li, H., Ling, M.X., Li, C.Y, Zhang, H., Ding, X., Yang, X.Y., Fan, W.M., Li, Y.L, Sun., & W.D. (2012). A-type granite belts of two chemical subgroups in central eastern China: Indication of ridge subduction. *Lithos, 150,* 26 – 36.

Liew T.C. (1977). Petrology and structural relationships of rhyolite rocks and microdiorite East of Genting Sempah, Pahang (pp. 68).

Liew, T.C. (1983). Petrogenesis of Peninsular Malaysia granitoid Batholiths. (Unpublished doctoral dissertation). Australian National University.

Loke, M.H., Lee, C.Y., & Van Klinken, G. (1983). Interpretation of regional gravity and magnetic data in Peninsular Malaysia. *Geological Society of Malaysia, 16,* 1 – 21.

Loiselle, M.C., & Wones, D.R. (1979). Characteristic and origin of anorogenic granites. Abstracts of papers to be presented at the Annual Meetings of the Geological Society of America and Associated Societies, San Diego, CA, *11,* 468.

Searle, M. P., Whitehouse, M. J., Robb, L. J., Ghani, A. A., Hutchison, C. S., Sone, M., Ng, S. W.-P., Roselee, M. H., Chung S.-L., & G. J. H. Oliver. (2012). Tectonic evolution of the Sibumasu-Indochina terrane collision zone in Thailand and Malaysia: constraints from new U -Pb zircon chronology of SE Asian tin granitoids. *Journal of the Geological Society 2012, 169,* 489 – 500.

Macdonald, S. (1968). The geology and mineral resources of north Kelantan and north Trengganu. *Mem. Geol. Survey Dept. W. Malaysia, 202,* 10.

Mahood, G., & Hildreth W. (1983). Large partition coefficients for trace elements in high silica rhyolites. Geochem. Cosmochim. *Acta. 47,* 11 – 30.

Maniar, P.D., & Picooli, P.M. (1989). Tectonic discrimination of granitoids. *Geol. Soc. Amer. Bull, 101,* 635 – 643.

Mark,G. (1999). Petrogenesis of Mesoproterozoic K-rich granitoids, southern Mt. Angelay igeneous complex, Cloncurry district, northwest Queensland. Australian *Journal of Earth Sciences, 46,* 933 – 949.

Markle, G. & Piazolo, S. (1998). Halogen-bearingminerals in syenites and high-grade marbles ofDronning Maud Land, Antarctica: monitors of fluid compositional changes during late-magmatic fluid-rock interaction processes. *Contrib. Mineral. PetroL, 132,* 246–268.

Metcalfe, I. (2000). The Bentong Raub Suture Zone. *Journal Of Asian Earth Sciences, 18,* 691 – 712.

Metcalfe, I., Sivam, S.P., & Stauffer, P.H. (1982). Stratigraphy and sedimentology of the Middle Triassic rocks exposed near Lanchang, Pahang, Peninsular Malaysia. *Geological Society of Malaysia Bulletin, 15,* 19 – 30.

Middlemost, E. A. K. (1994). Naming materials in magma/igneous rock system. *Earth Sci. Rev., 37,* 215–224.

Mitchell, A.H.G. (1997). Tectonic settings for emplacement of South East Asian tin granites. *Geological Society of Malaysia Bulletin, 9,* 123 – 140.

Moghzani A.M. (2003). Geochemistry and petrogenesis of a high- K calk alkaline Dokan Volcanic Suite, South Safaga area, Egypt : the role of late Neoproterozoic crustal extension. *Precambrian Research, 125,* 161 – 178.

Montel, J.M. (1993). A model for monazite/melt equilibrium and application to the generation of granitic magmas. *Chem. Geol., 110,* 127-146.

Mountains, East Antarctica: implications for charnockite petrogenesis and Proterozoic crustal evolution. *Precambrian Research, 81,* 37–66.

Mustaffa, K.S., & Ghani, A.A. (2003). 'Mantle plume' type magmatism in the Central Belt of Peninsular Malaysia and its tectonic implications. *Bull. Geol. Soc. Malaysia, 4,* 49 – 70.

Nany, M.T. (1983). Phase equilibria of rock forming ferromagnesian silicate in granitic systems. *American Journal of Science, 283,* 993 – 1033.

Nash, W.P., & Crecraft, H.R. (1985). Partition coefficients for trace elements in silicic magmas. *Geochim. Cosmochim. Acta. 49,* 2309 – 2322.

Nicolae, I., & Saccani, E. (2003). Petrology and Geochemistry of the late Jurassic calc-alkaline series associated to Middle Jurassic ophiolite in the South Apuseni Mountains (Romania). *Schweizerische und Petrographische Mitteilungen, 83,* 81 – 96.

Nyein, K.K. (2014). Petrology and Geochemistry of Langkawi Granites, North of Peninsular Malaysia. (Unpublished doctoral dissertation). University of Malaya.

Oliver G., Zaw, K., Hotson, Mark., Meffre, Sebastien., Manka, T., (2013). U–Pb zircon geochronology of Early Permian to Late Triassic rocks from Singapore and Johor: A plate tectonic reinterpretation, Gondwana Research, http://dx.doi.org/10.1016/j.gr.2013.03.019

Parry, W.T., & Downey, L.M. (1982). Geochemistry of hydrothermal chlorite replacing igneous biotite. *Clays and Clay Minerals, 30,* 81 – 90.

Parry, W.T., & Downey, L.M. (1982). Geochemistry of hydrothermal chlorite replacing igneous biotite. *Clays and Clay Minerals, 30,* 81 – 90.

Patino Douce, A.E. (1997). Generation of metaluminous A-type granites by low pressure melting of calc-alkaline granitoids. *Geology, 25,* 743 – 746.

Patino Douce, A.E., & Beard, J.S. (1995). Dehydration melting of biotite gneiss and quartz amphibolite from 3 to 15 kbar. *Journal of Petrology, 36,* 707 – 738.

Pearce, J.A. (1996). Sources and settings of granitic rocks.*19,* 120 – 125.

Pearce, J.A., & Gale, G.E. (1977). Identification of ore deposition environment from trace element geochemistry. *Geol. Soc. London Special Pub*. 7, 4 – 24.

Pearce, J.A., Harris N.W., & Tindle, A.G. (1984). Trace Element Discrimination Diagrams For The Tectonic Interpretation of Granitic Rocks. *J. Petrology, 25*, 956 – 983.

Pearce, J.A., & Norry M.J. (1979). Petrogenetic implication of Ti, Zr, Y and Nb variations in volcanic rocks. *Contribution. Mineral. Petrol, 69,* 33 – 47.

Peccerillo, A., & Taylor S.R. (1976). Geochemistry of Eocene calc – alkaline volcanic rocks from the Kastamonu area, Northern Turkey. *Contribution Mineral. Petrol 58,* 63 – 81.

Piccoli, P.M., Candela, P.A. & Williams, T.J. (1999). Constraints on Estimating HCl and Cl in the Magmatic Volatile Phase in Granites and Granite-Related Ore Systems: A Potential Tool for the Estimation of High- and Low-Cl Systems. Second International Symposium on Granites and Associated Mineralizations; Salvador, Brazil. *Published in a special issue of Lithos, 46*, 573-589.

Pichavant, M., Montel, J.M., & Richard, L.R. (1992). Apatite solubility in peraluminous liquids : Experimental data and an extension of the Harrison model. *Geochimica et Cosmochimica Acta, 56,* 3855 – 3861.

Rajah S.S. 1967 (MS). Geology and mineral resources of sheet 125 Johore. Proceedings of the Senior Officers Conference, 1966. *Geological Survery Dept. of W. Malaysia*, 41 – 47.

Ramli, M.S.I. (2011). General Geology of Hanson Quarry and Adjacent Area of kampong Belungkur, Pengerang. Johor Darul Takzim (pp.114).

Richardson, J.A. (1950). The Geology and mineral resources of the neighbourhood of Chegar Perah and Merapoh, Pahang, Malaya. Memoir Geological survey dept. Fed. Malaya (pp. 162).

Rogers, R., Karason, H., & Van Der Hilst, R. (2002). Epeirogenic uplift above a detached slab in norther Central America. *Geology, 204,* 1031 – 1034.

Rollinson, H.R. (1993). Using Geochemical Data : Evaluation, Presentation, Interpretation. (pp. 343). Prentice Hall., London.

Rozi Umor. (2009). Petrogenesis dan geokimia batuan igneus jalur tengah Semenanjung Malaysia. (Unpublished doctoral dissertation). University of Malaya, Kuala Lumpur.

Rudnick, R.L,. & Fountain, D.M. (1995). Nature and composition of the continental crust: a lower crust perspective. *Reviews of Geophysics, 33,* 267 – 309.

Rushmer,T. (1991). Partial melting of two amphibolites: Contrasting experimental results under fluid-absent conditions. *Contributions to Mineralogy and Petrology*, *107,* 41-59.

Ryall, P.J.C. (1982). Some thoughts on the crustal structure of Peninsular Malaysia – result of gravity traverse. *Geological Society of Malaysia Bulletin, 15,* 9 -18.

Saki, A. (2010). Mineralogy, geochemistry and geodynamic setting of the granitoids from NW Iran. *Geological Journal, 45,* 451 – 466.

Scrivenor J.B. (1917). The Geology of Malaya. MacMillan and Co. Ltd., London, 217.

Selby, D., & Nesbitt, B. E. (2000). Biotite Chemistry of the Casino Porphyry Cu-Au-Mo Mineralization, Yukon, Canada: Evaluation of Magmatic and Hydrothermal Fluid Chemistry. *Chemical Geology, 171,* 77-93.

Sevastjanova, I., Clements, B., Hall, R., Belousova, E.A., Griffin, W.L., & Pearson, N. (2011). Granitic magmatism, basement ages, and provenance indicators in the Malay Peninsula: Insights from detrital zircon U–Pb and Hf-isotope data. *Gondwana Research, 19,* 1024–1039.

Shand. (1942). Eruptive Rocks. John Wiley & Sons. (pp. 444).

Shellnutt, J.G., & Zhou, M.F. (2007). Permian peralkaline, peraluminous and metaluminous A-type granites in the Panxi district, Southwest China: their relationship to the Emeishan mantle plume. *Chemical Geology, 243,* 286 – 313.

Shen, X., Zhang H., Wang Q., Wyman D.A., & Yang, Y. (2011). Late Devonian – Early Permian A-type granites in the southern Altay Range, Northwest China: petrogenesis implications for tectonic setting "A_2 type" granites", 986 – 1007.

Sinclair, H. (1997). Flysch to molasse transition in peripheral foreland basins: The role of the passive margin versus slab breakoff. *Geology, 25,* 1123-1126.

Singh N., & Ghani, A.A. (2000). Sempah Volcanic Complex. *Geological Society of Malaysia Annual Geological Conference*, 67 – 72.

Sun S.S., & McDonough, W.F. (1989). Chemical and isotopic systematics of oceanic basalts : Implications for mantle composition and processes. *Geol. Soc. Lon, 42,* 313 – 345.

Sylvester, P.J. (1989). Post – collisional alkaline granites. *Journal of Geology, 97,* 261-280.

Taylor, S.R., & McLennan, S.M. (1985). The continental crust : its composition and evolution. Blackwell, Oxford.

Turner, S.P., Foden, J.D., & Morrison, R.S., (1992). Derivation of some A-type magmas by fractionation of basaltic magma : an example from the Pathaway Ridge, South Australia. *Lithos, 28,* 151 – 179.

Van de Zedde, D.M.A., & Wortel, M.J.R. (2001). Shallow slab detachment as a transient source of heat at mid-lithospheric depth. *Tectonics, 30,* 1095 – 1098.

Watkins, J., Clemens, J., & Treloar, P. (2007). Archaean TTGs as sources of younger granitic magmas: melting of sodic metatonalites at 0.6–1.2 GPa. *Contributions to Mineralogy and Petrology, 154,* 91–110.

Watkins, J., Clemens, J., & Treloar, P. (2007). Archaean TTGs as sources of younger granitic magmas: melting of sodic metatonalites at 0.6–1.2 GPa. *Contributions to Mineralogy and Petrology, 154,* 91–110.

Watson, E.B., & Harrison, M. (1983). Zircon Saturation Revisited : Temperature and Composition Effects In A Variety Of Crustal Magma Types. *Earth Planet Sci. Lett.*, 295 – 304.

Watson, E.B., & Harrison, T.M. (1984). Accessory minerals and the geochemical evolution of crustal magmatic systems: a summary and prospectus of experimental approaches. *Phys. Earth Planet. Int., 35,* 19-30.

Wedenpohl, K.H. (1995). The composition of the continental crust. *Geochimica et Cosmochimica Acta, 59,*1217 – 1232.

Whalen, J.B., & Currie, K.L. (1990). The Topsail igneous suite, western Newfoundland : fractionation and magma mixing in an 'anorogenic' A-type granite suite. In: Stein, H.J., Hannah, J.L. (eds) Ore – Bearing Granite Systems: Petrogenesis and Mineralizing processes. *Geological Society of America Special Paper, 246,* 287 – 299.

Whalen, J.B., Currie, K.L., & Chappell, B.W. (1987). A-type granites : geochemical characteristics, discrimination and petrogenesis. *Contrib. Mineral. Petrol, 95,* 407 – 419

Whalen, J.B., Jenner, G.A., Longstaffe, F.J., Robert, F., & Gariepy, C. (1996). Geochemical and Isotopic (O, Nd, Pb and Sr) Constraints on A-type Granite Petrogenesis Based on the Topsails Igneous Suite, Newfoundland Appalachians. *J. Petrology, 37,* 1463 – 1489.

Willbourn, E.S. (1917). The Pahang Volcanic Series. *Geological Magazine, 54,* 447-462.

Wilson M. (2007). Igneous Petrogenesis a Global Tectonic Approach. Springer (pp. 457).

Wilson, D.J., Christiansen, Eh.H., & TIngney, D.T. (1994). Geology and geochemistry of the Golden Butte Mine – A small Carlin-type gold deposit in eastern Nevada: BYU. *Geology Studies,* 40, 185 – 211.

Wong, I.F.T. (1960). The agglomerate of Bukit Kepayang, Pahang. (Unpubl. B.Sc. (Hons) thesis). Dept. of Geology University of Malaya, Kuala Lumpur.

Wood, B.J., & Banno, S. (1973). Garnet-orthopyroxene-clinopyroxene in simple and complex systems. *Contrib. Mineral. Petr., 42,* 109-124.

Wormald, R.J., & Price, R.C. (1988). Peralkaline granites near Temora, southern New South Wales, tectonic and petrological implications. *Australian J. Earth Sci., 35,* 209-221.

Zainal Ismail. (1984). Petrology and geochemistry of Santi area, Pengerang, South-east Johore. (Unpubl. B.Sc. (Hons) thesis). Dept. of Geology, University of Malaya, Kuala Lumpur.

Zhao, J.-X., Ellis, D.J., Kilpatrick, J.A., & McCulloch, M.T. (1997). Geochemical and Sr-Nd isotopic study of charnockites and related rocks in the northern Prince Charles Mountains, East Antarctica: implications for charnockite petrogenesis and proterozoic crustal evolution. *Precambrian Research*, 81(1), 37-66(30).

Zhao, X.F., Zhou, M.F., Li, J.W., & Wu, F.Y. (2008). Association of Neoproterozoic A- and I-type granites in South China: Implications for generation of A-type granites in a subduction-related environment. *Chemical Geology, 257*, 1 – 15.